Politecnico di Torino-Department of Energy (DENERG)

Doctoral Dissertation

Doctoral Program in Energetics (34th Cycle)

# Towards Climate Resilient and Energy Efficient Buildings:

## A Comparative Study on Energy Related Components, Adaptation Strategies, and Whole Building Performance

By

**Mamak Pourabdollahtootkaboni**

******

**Supervisor(s):**

Prof. Vincenzo Corrado, Supervisor

Prof. Ilaria Ballarini, Co-Supervisor

**Doctoral Examination Committee:**

Prof. Alfonso Capozzoli , Politecnico di Torino, Chair of the Evaluation Board

Prof. Giovanni Vincenzo Fracastoro , Politecnico di Torino

Prof. Mohamed Hamdy. Norwegian University of Science and Technology

Prof. Marco Manzan, Università degli Studi di Trieste, Ph.D. thesis referee

Prof. Anna Mavrogianni, University College London - UCL, Ph.D. thesis referee

Politecnico di Torino

2022

# Declaration

I hereby declare that the contents and organization of this dissertation constitute my own original work and do not compromise in any way the rights of third parties, including those relating to the security of personal data.

Mamak P.Tootkaboni

2022

* This dissertation is presented in partial fulfilment of the requirements for **Ph.D. degree** in the Graduate School of Politecnico di Torino (ScuDo).

# Acknowledgment

I want to thank my supervisors, Professor Vincenzo Corrado, and Professor Ilaria Ballarini, for providing guidance, feedback, and encouragement throughout the entire process of my research. I would also like to thank the reviewers of this dissertation, Professor Anna Mavrogianni, and Professor Marco Manzan, for taking the time and effort to review my thesis profoundly and help me develop this work.

# Abstract

Climate change is one of the greatest global challenges of our time, and its impacts have already been studied in a variety of research fields. Given that the building sector accounts for a considerable amount of worldwide energy consumption and it is the primary source of greenhouse gas emissions, its contribution to climate change is evident. Therefore, the crucial role of building energy performance in climate change mitigation is a primary concern of a large and growing body of literature. However, buildings are not merely the cause of climate change. Due to their long lifespans, they are also adversely affected by it in numerous ways, demonstrating the importance of fostering their adaption capacity and climate resilience. Up to now, less attention has been paid to the built environment's climate resilience and adaptation compared to its role in mitigating climate change. In addition, there is far too little research on analysing the Italian building stock toward this issue, and there is a need to perform quantitative analyses, particularly on a regional scale. Accordingly, this research attempts to analyse buildings' energy performance, optimization, and thermal comfort in a changing climate (long-term assessment) within a regional scale for Italian building stock. Several adaptation strategies regarding the building's condition and resilient cooling solutions are studied and comparatively analysed to measure their effect on buildings' energy performance and thermal comfort. To this aim, as a first step, future weather data generation methods are studied considering representative concentration pathway (RCP) 4.5 and 8.5 ($W/m^2$ ) scenarios introduced by the fifth assessment report of the Intergovernmental Panel on Climate Change. The reliability of these future weather data is assessed, and a weather data set is created for which the systemic errors and biases are also adjusted. Followingly, a preliminary analysis is carried

out to draw a clearer picture of the effects of climate change on the Italian built environment for typical and Nearly Zero Energy Buildings (NZEBs). Advanced solar shading/advanced glazing, cool envelop materials (CEMs), and ventilative cooling are the resilient cooling solutions that have been assessed. The results suggest that, depending on the building's condition, mechanical ventilative cooling and ultra-selective double-glazed windows have the greatest impact on reducing the effects of climate change. It has been discovered the combination of these solutions could help keep the trade-offs of energy efficiency. Finally, a global sensitivity analysis is performed to discover the contribution of variances of parameters regarding specific resilient cooling technologies and building conditions to variances of particular key performance indicators representing energy performance and thermal comfort of buildings. This sensitivity analysis is applied to a representative building in the climate zone of Rome -using the created future weather data- and has been performed for three time periods (2010s, 2050s, and 2090s). In brief, the results demonstrated the changes in the built environment energy performance and thermal comfort pattern. For the Italian residential building stock, the annual thermal energy need for space cooling will dramatically increase (up to 55%) while the annual thermal energy need for space heating will moderately decrease. Moreover, the risk of overheating increases significantly (up to 155%). Accordingly, annual electrical energy consumption (from the grid) for cooling and ventilation rises up to 70%. Such changes are highly dependent on the building typology and its state of refurbishment. It is seen that even the NZEBs do not meet the requirements in the future. In addition, the significant contribution of buildings' condition (level of insulation) and their typology is revealed to foster buildings' climate resilience and adaptation capacity.

# Contents

# List of Figures

# List of Tables

# 1. Introduction

## 1.1 Motivations

Recently, the issue of climate change and its associated impacts has received considerable attention in a wide range of disciplines. According to the fifth Assessment Report (AR5) of the Intergovernmental Panel on Climate Change (IPCC), if the emissions continue to rise, the global average temperature will be 2.6-4.8 degrees Celsius higher than the present by the end of the 21$^{st}$ century. Limiting this temperature rise is necessary for combating the worst and most serious impacts. Accordingly, the world members of the UN Framework Convention on Climate Change (UNFCCC) in 2010 agreed on limiting the temperature rise to a maximum of 2 °C above pre-industrial levels and considering the reduction of this maximum value to 1.5 °C in the near future. However, in the latest report of the Intergovernmental Panel on Climate Change (AR6), it is shown that despite the implementation of nationally determined contributions (NDCs), global greenhouse gas (GHG) emissions in 2030 are very likely to cause temperature rise more than 1.5 °C limit during the twenty-first century. Even supposing the immediate stop of the greenhouse gas emissions, the temperature increase will endure as a result of already present greenhouse gases in the atmosphere (IPCC, 2021).

This result comes from the provision of detailed projection scenarios performed by IPCC through analysing human activities' influence based on historic data. In more detail, historical cumulative carbon dioxide ($CO_2$) emissions recorded between 1850-2019 have been confirmed to cause an increase in global surface temperature, and based on these data, illustrative emissions scenarios for three 20-year time periods have been analysed to predict the changes in global surface temperature for near term (2021-2040), mid-term (2041-2060) and long-term (2081-2100). IPCC defines emission scenario as “a plausible representation of the future development of emissions of substances that are radiatively active (e.g., greenhouse gases (GHGs) or aerosols that absorb incoming solar radiation or outgoing infrared radiation), plus human-induced land cover changes that can be radiatively active via albedo changes, based on a coherent and internally consistent set of assumptions about driving forces (such as demographic and socio-economic development,

technological change, energy, and land use) and their key relationships" (IPCC: Mitigation of climate change, 2014; Oxford, 2007). These emissions scenarios help to predict the possible future climate in a scientific way. While these scenarios were also presented in the fifth assessment report of IPCC (IPCC: Mitigation of climate change, 2014), the sixth report considers a broader range of greenhouse gas (GHG), land use, and air pollutants.

The fifth assessment report introduced the representative concentration pathways (RCPs), according to which four different emissions and atmospheric composition pathways (2.6, 4.5, 6.0, and 8.5 $W/m^2$) were analysed. Each RCP projection is based on a set of economic, technological, and land-use assumptions besides many relevant mitigation scenarios in a way that the foreseen future is a function of actions referring to limiting greenhouse gas emissions. In addition, the RCPs are based on different pathways of radiative forcing as the effective change in the amount of solar energy received per second of sunlight per square meter of land ($W/m^2$). This quantity is a function of the concentration of greenhouse gases (e.g., $CO_2$, $CH_4$, $N_2O$), clouds, aerosols such as sulphate aerosols that reflect incoming sunlight, and changes to the land surface that alters its albedo or reflectivity. "In essence, radiative forcing is a measure of the increase in heating of the Earth's surface due to changes in the atmosphere or to the Earth's surface" (IPCC: Mitigation of climate change, 2014). As an example, for RCP8.5, which is the worst-case climate change scenario, the amount of radiative forcing that exceeds by 2100 equals 8.5 $W/m^2$. This scenario assumes a 'business-as-usual' in the years to come. According to this RCP, the concentrations of $CO_2$ in the atmosphere will become three to four times higher than pre-industrial levels. On the other hand, the aggressive mitigation scenario (RCP 2.6) is the best-case scenario, according to which the emissions will be halved by 2050, and the temperature is not likely to exceed 2 ° C more. As explained earlier, for this scenario, a 2.6 $W/m^2$ of radiative forcing is expected to be stabilized at around or after 2100. The following figure represents all four RCPs and their associated and predicted impacts on temperature rise.

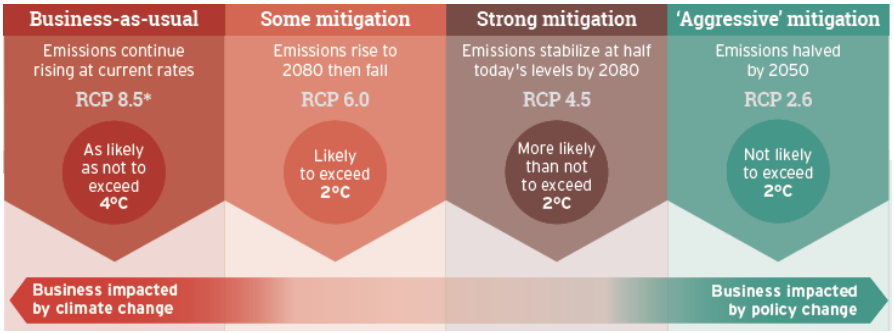


Figure 1: The four RCP (Representative Concentration Pathway) scenarios each project a certain amount of carbon to be emitted by 2100 - adapted from IPCC AR5 (Symon, 2013)

Afterward, the concept of Shared Socio-Economic Pathways (SSPs) was introduced by IPCC, and it has been applied in the sixth assessment report. The most significant difference in this new set of scenarios lies in consideration of mitigation and adaptation policies and socio-economic challenges within the framework. Shared Socio-Economic Pathways are categorized as sustainability (SSP1), middle-of-the-road development (SSP2), regional rivalry (SSP3), inequality (SSP4), and fossil-fuelled development (SSP5) (IPCC, 2021).

In addition, like the previous case of RCPs, for each SSP, the associated radiative forcing is specified following the assigned number representing the order of scenarios (SSP1-1.9, SSP1-2.6, SSP2-4.5, SSP3-7.0, and SSP5-8.5). Both the historical increases and the projected future of global surface temperature since 1850–1900 as a function of cumulative $CO_2$ emissions (Gt $CO_2$) for each of the five SSPs are presented in figure 2. As can be seen, the historical global warming is represented with the grey colour in the figure, and the global surface temperature projections are shown with different colours referring to each illustrative scenario line. The median estimate is represented as the central lines, and uncertainty ranges are shown as shaded areas.

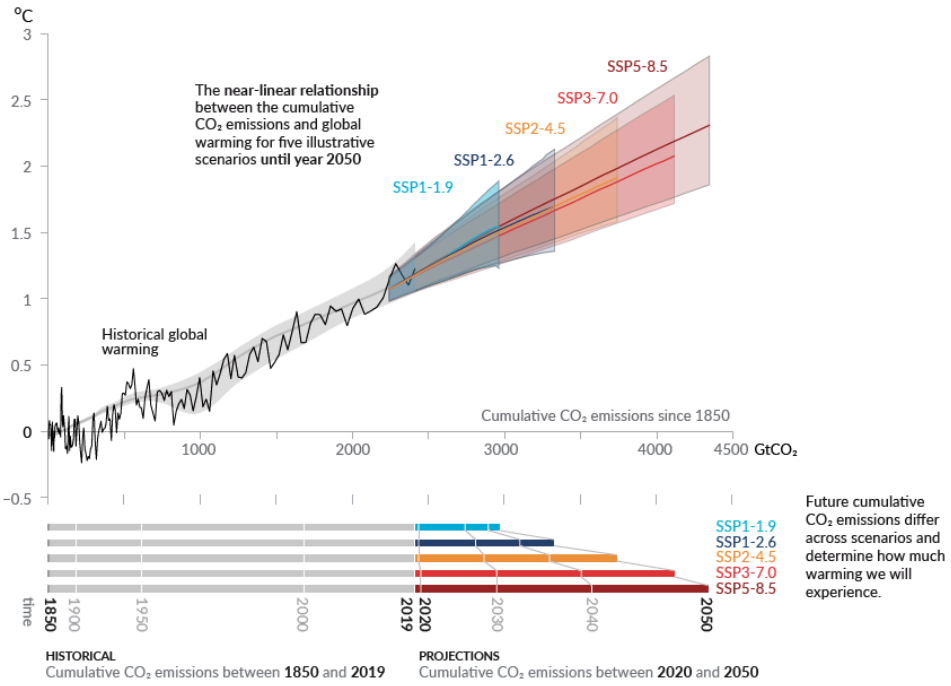


Figure 2: Global surface temperature increase since 1850–1900 (OC) as a function of cumulative $CO_2$ emissions ($GtCO_2$) – adopted from (IPCC, 2021)

The results show that even if the adaptation/mitigation requirements of SSP1-1.9 are met, until at least 2100, the temperature is likely to remain high above the last decade (IPCC, 2021). In addition, regardless of the scenario, until at least the mid-century, the global surface temperature is very likely to continue increasing, and it might exceed 1.5 °C and 2 °C during the 21$^{st}$ century unless a huge cut in greenhouse gas emissions is seen in the coming years and decades (IPCC, 2021).

The largest driver of climate change is the emission of greenhouse gases, of which more than 90% are carbon dioxide ($CO_2$) and methane. Considering that the building sector contributes to 32% of global energy consumption − as the main driver of GHG emissions − its impact on intensifying climate change is undeniable (Lucon et al., 2014). Accordingly, buildings can play a crucial role in the mitigation of climate change. Furthermore, buildings are not only responsible for climate change. Likewise, they are extremely affected by it in several ways considering their long-life span, and they need adaptation solutions as well. The negative impacts of global warming on buildings include both chronic stresses in the form of daily pressure -such as changes in the building energy consumption patterns- and acute shocks, such as a significant increase in the frequencies of extreme weather

events. Considering the latter, recent studies reveal that climate change has doubled the probability of the European heatwaves and longer heatwaves are more than 90% definite as the climate pattern has been disrupted (Symon, 2013). Heatwave is defined as a singular microclimate condition with temperatures over a specific percentile and characterized by more than three consequent hot days. This event is associated with drastic physiological impacts on human health. For instance, the August 2003 heatwave contributed to around 45,000 excess deaths across 12 European countries (Zuo et al., 2015). Some other impacts are the changes in building energy performance, thermal comfort conditions, and grid interactions (Chai et al., 2019).

The impacts of climate change on buildings − as mentioned earlier − do not only refer to acute shocks like heatwaves. These impacts also include long-term chronic stresses. Among all these impacts, one of the major challenges caused by climate change is building overheating, which leads to a significant rise in cooling energy consumption and, therefore, in energy shortage. The existing body of research on this issue is analysed in detail in section 1.3. Currently, countries worldwide have put in place policies and strategies to reduce the energy consumption of buildings in order to promote reductions of greenhouse gas emissions and energy utilization. It is possible to optimize building energy performance by using advanced technologies and energy retrofitting systems. Since 2007, the European Union (EU) has implemented a strict strategy aimed at lowering energy use and increasing global/overall energy savings. The Energy and Climate Policy Framework for 2030 (European Commission, 2014) sets forth ambitious EU commitments to reduce greenhouse gas emissions by at least 40% compared to 1990, to increase the share of renewable energy in final consumption, to increase the amount of renewable energy used in final consumption, to enhance energy efficiency, and to improve energy security, competitiveness, and sustainability. However, climate change would impact the functionality and habitability of buildings - as discussed above - and this effect will, in turn, cause the misuse of resource consumption. This effect needs to be adequately understood. The lack of such an understanding tarnished the existing energy efficiency and sustainability criteria. That’s where the resilience concept comes into play, and climate resilience here refers to the process of not only mitigation measures to support sustainable development and reduce the building's contribution to emissions but also adaptation scenarios in a way that future risks are taken into account. The present study informs these challenges and tries to investigate the climate resilience of buildings considering the impacts of

climate change on the built environment. In the following subsections of this chapter, initially, an overview of the definitions of resilience is given, then a review of literature is performed on the resilience of buildings to the impacts of climate change, and finally, the research questions and aims are presented.

## 1.2 Literature review on the concept of resilience related to building performance

We live in a world of increasing uncertainty and unpredictability coming from climate events, economic crises, demographic shocks, social inequity, and above all, climate change, which is responsible for intensifying lots of environmental threads. The existing state of flux and uncertainty resulted in the publicity and promotion of the resilience concept as a useful framework that can create tools to overcome future challenges. “It appears that resilience is replacing sustainability in everyday discourses in much the same way as the environment has been subsumed in the hegemonic imperatives of climate change” (Davoudi et al., 2012).

Among a wide range of academic disciplines − which currently adopt resilience thinking in their research − ecologists were the first to mainstream the concept. In 1973, in his seminal publication, C.S. Holling defined resilience as the capacity of a system to return to normality following a shock (Holling, 1973). According to this primitive definition, a system becomes more resilience in two ways, first by reducing the magnitude of the disturbance and second by enhancing the adaptive capacity in a way that the disturbance is absorbed before the system changes its structure (Holling, 1996). Later on, the concept started to become popular in other disciplines, including and not limited to engineering, psychology, social sciences, planning, etc. Accordingly, the definitions of resilience started to develop and vary based on the academic discipline.

The challenges driven by climate change made the resilience concept a central tool for fulfilling sustainable development goals (SDGs). Ensuring the sustainability and reliability of energy resources (goal 7), fostering the resilience of cities (goal 11), and especially, the urgent need to combat climate change impacts (goal 13) are some efforts to establish the importance of resilience thinking for future development. In addition to the necessity of mainstreaming the resilience concept, it is also suggested that the issue is urgent to be implemented. Limiting warming to less than 2 °C would thus require a rapid acceleration of mitigation efforts and

resilient solutions. Resilience here is defined as the “capacity of interconnected social, economic, and ecological systems to cope with a hazardous event, trend or disturbance, responding or reorganising in ways that maintain their essential function, identity and structure” (IPCC_AR6_WGIII, 2021). In addition, more specific definitions are also existing in the literature on the concept of climate-resilient development which is “the process of implementing greenhouse gas mitigation and adaptation measures to support sustainable development for all” (IPCC, 2021). Based on this definition, to mitigate the climate change impacts and to enhance resilience against them, it is necessary to maintain the adaptation capacity, reduce the exposure and vulnerability to the adverse effects, find innovative solutions and facilitate system transformations when needed.

To investigate the climate resilience of buildings to future uncertainties, it is necessary to further clarify the relevant definition of the term resilience and other related concepts in the field. In the relevant literature, the resilience of buildings against climate change impacts is usually defined based on abrupt climate events like heatwaves. This association is because building resilience usually refers to the capacity to cope with abrupt shocks or hazards. “Hazard is the potential occurrence of a natural or human-induced physical event or trend that may cause loss of life, injury, or other health impacts, as well as damage and loss to property, infrastructure, livelihoods, service provision, ecosystems, and environmental resources” (IPCC, 2021). This focus on heatwaves as climate hazards is essential since climate change is expected to increase the frequency and intensity of heatwaves, and it is necessary to make the existing and future buildings adaptable and resilient. In this context, resilience is defined as the capacity of systems (buildings, in this study) to withstand shocks (e.g., heatwaves), absorb the impacts, rapidly recover from them, and mitigate similar future scenarios (Chaudry et al., 2011; Keogh & Cody, 2012; Overbye et al., 2013; Skea, J. & Ekins, 2009).

Nevertheless, built environment climate resilience cannot be limited to capacity building against heatwaves and other abrupt events. It is also necessary to consider the chronic pressures caused by climate change impacts and investigate possible mitigation/adaptation scenarios. As an example, a substantial body of literature on climate change impacts demonstrates great changes in heating and cooling demands of buildings (Keogh & Cody, 2012; Wan et al., 2012) that are projected to be more challenging in hot summer and mild winter regions, when cooling demands are more critical (Li et al., 2012; Wan et al., 2012). If this increased demand for thermal

comfort is not addressed, it can have a negative impact on health, sleep quality, and job productivity, disproportionately affecting vulnerable groups and worsening energy poverty (Sun et al., 2020). In addition, "Closing the adaptation gap requires moving beyond short-term planning and ensuring timely and adequate implementation" (IPCC, 2022).

In case of either abrupt shocks -such as heatwaves- or chronic stresses -such as increased electricity demand- it is necessary to reduce the vulnerability of the buildings to make them more resilient. "Vulnerability is the propensity or predisposition to be adversely affected. Vulnerability encompasses a variety of concepts and elements, including sensitivity or susceptibility to harm and lack of capacity to cope and adapt" (IPCC, 2022). Thus, vulnerability is always associated with a coping capacity that is composed of exposure to drivers of change and adaption potential against the relevant challenges. Reducing exposure and thus reducing vulnerability is possible by removing the drivers of the unwanted changes or putting the desired system in places and settings where it is not adversely affected. Adaptation, in the case of this study, is "the process of adjustment to actual or expected climate and its effects." In addition to these two factors, A resilient pathway also considers the mitigation opportunity, which -in the case of climate change- is defined as "a human intervention to reduce the sources or enhance the sinks of greenhouse gases" (IPCC, 2022). The following table summarizes the terms which have been explained above and will be used in this study.

Table 1: Definitions of the term resilience and other correlated concepts

| ***Theme*** | ***Definition*** | ***Reference*** |
|---|---|---|
| **Adaptation** | "**Adaptation**: The process of adjustment to actual or expected climate and its effects. In human systems, adaptation seeks to moderate or avoid harm or exploit beneficial opportunities. In some natural systems, human intervention may facilitate adjustment to expected climate and its effects. {WGII, III}" | (IPCC, 2021)(IPCC: Mitigation of climate change, 2014), (IPCC: Mitigation of climate change, 2014) |

| | | |
|---|---|---|
| | "**Adaptive capacity**: The ability of systems, institutions, humans, and other organisms to adjust to potential damage, to take advantage of opportunities, or to respond to consequences {WGII, III}" | (IPCC, 2013),<br><br>(IPCC: Mitigation of climate change, 2014) |
| **Disaster** | "**Disaster:** Severe alterations in the normal functioning of a community or a society due to hazardous physical events interacting with vulnerable social conditions, leading to widespread adverse human, material, economic or environmental effects that require immediate emergency response to satisfy critical human needs and that may require external support for recovery. {WGII}" | (IPCC, 2013)<br><br>(IPCC, 2022) |
| | "**Hazard:** The potential occurrence of a natural or human-induced physical event or trend or physical impact that may cause loss of life, injury, or other health impacts, as well as damage and loss to property, infrastructure, livelihoods, service provision, ecosystems, and environmental resources. In this report, the term hazard usually refers to climate-related physical events or trends or their physical impacts. {WGII}" | (IPCC, 2013), (IPCC: Global and Sectoral Aspects, 2014)<br><br>(IPCC, 2022) |
| **Exposure** | "The presence of people, livelihoods, species or ecosystems, environmental functions, services, and resources, infrastructure, or economic, social, or cultural assets in places and settings that could be adversely affected. {WGII}" | (IPCC, 2013), (IPCC: Global and Sectoral Aspects, 2014) (IPCC, 2022) |
| **Global warming** | "Global warming refers to the gradual increase, observed or projected, in global surface temperature, as one of the | (IPCC, 2013), (IPCC: Mitigation of climate change, 2014) (IPCC, 2022) |

| | | |
|---|---|---|
| | consequences of radiative forcing caused by anthropogenic emissions. {WGIII}" | |
| **Mitigation** | "Mitigation (of climate change) A human intervention to reduce the sources or enhance the sinks of greenhouse gases (GHGs)." | (IPCC, 2013), (IPCC: Mitigation of climate change, 2014) (IPCC, 2022) |
| **Resilience** | "**Climate-resilient pathways:** Iterative processes for managing change within complex systems in order to reduce disruptions and enhance opportunities associated with climate change" | (IPCC, 2013) |
| | "The capacity of social, economic, and environmental systems to cope with a hazardous event or trend or disturbance, responding or reorganizing in ways that maintain their essential function, identity, and structure, while also maintaining the capacity for adaptation, learning, and transformation." | (IPCC, 2013), (IPCC: Global and Sectoral Aspects, 2014), (IPCC: Mitigation of climate change, 2014) |
| | "The ability of a system to preserve its functions in a risky and changing environment (WGII Section 2.5 and Sections 20.2 – 20.6; Folke et al., 2010; Gallopin, 2006)" | (IPCC: Mitigation of climate change, 2014) |
| | "Resilience refers to the ability of any urban system to withstand and recover quickly from all plausible shocks and stresses and maintain continuity of functions." | (UN-Habitat, 2017) |
| | "**Climate resilient development (CRD):** in the WGII Report refers to the process of implementing greenhouse gas mitigation and | (IPCC, 2022) |

| | | |
|---|---|---|
| | adaptation measures to support sustainable development for all." | |
| **Risk** | "The potential for consequences where something of value is at stake and where the outcome is uncertain, recognizing the diversity of values. Risk is often represented as probability or likelihood of occurrence of hazardous events or trends multiplied by the impacts if these events or trends occur. In this report, the term risk is often used to refer to the potential, when the outcome is uncertain, for adverse consequences on lives, livelihoods, health, ecosystems and species, economic, social, and cultural assets, services (including environmental services), and infrastructure. {WGII, III}" | (IPCC, 2013)<br><br>(IPCC: Global and Sectoral Aspects, 2014)<br><br>(IPCC: Mitigation of climate change, 2014)<br><br>(IPCC, 2022) |
| **Sustainability** | "**Sustainability**: A dynamic process that guarantees the persistence of natural and human systems in an equitable manner. {WGII, III}" | (IPCC, 2013), (IPCC: Mitigation of climate change, 2014) |
| | "**Sustainable development:** Development that meets the needs of the present without compromising the ability of future generations to meet their own needs (WCED, 1987). {WGII, III}" | (IPCC, 2013), (IPCC: Mitigation of climate change, 2014) |
| **Uncertainty** | "A state of incomplete knowledge that can result from a lack of information or from disagreement about what is known or even knowable. It may have many types of sources, from imprecision in the data to ambiguously defined concepts or terminology or uncertain projections of human behaviour. Uncertainty can therefore be represented by quantitative measures (e.g., a probability density function) or by | (IPCC, 2013) |

| | | |
|---|---|---|
| | qualitative statements (e.g., reflecting the judgment of a team of experts) (see Moss and Schneider, 2000; Manning et al., 2004; Mastrandrea et al., 2010). See also Confidence and Likelihood. {WGI, II, III}" | |
| | "A cognitive state of incomplete knowledge that can result from a lack of information or from disagreement about what is known or even knowable." | (IPCC: Mitigation of climate change, 2014) (IPCC, 2022) |
| **Vulnerability** | "The propensity or predisposition to be adversely affected. Vulnerability encompasses a variety of concepts and elements, including sensitivity or susceptibility to harm and lack of capacity to cope and adapt. {WGII}" | (IPCC, 2013) (IPCC: Global and Sectoral Aspects, 2014) (IPCC, 2022) |

In order to clarify the interconnection between the over mentioned themes -which are helpful for creating the methodological framework of this study- the following scheme is presented. According to this scheme, resilience consists of two interconnected components of risk and vulnerability. The reduction of both factors helps to foster the resilience of the system. In addition, for risk reduction, mitigation and risk management are the solutions, among which the mitigation of future risk is a strategy that this study aims to contribute to. Turning now to vulnerability reduction, the enhancement of adaptive capacity, and reducing exposure to risk are the components. The study aims to contribute to both of these two components of vulnerability reduction in case of the impacts of climate change on buildings.

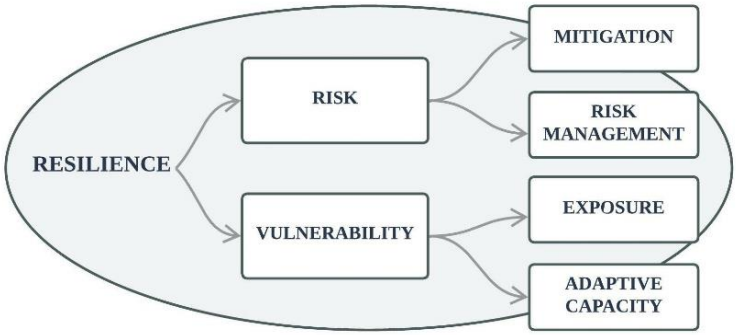


Figure 3: Schematic representation of resilience and its correlated concepts

As mentioned earlier, this thesis studies the challenges referring to the adverse impact of climate change on building energy performance. These adverse impacts include changes in the energy consumption pattern (especially cooling need), increased hours of discomfort, power outage, etc. In order to enhance the coping capacity and adaptation potential and reduce the vulnerability of buildings, it is necessary to first analyse the patterns of changes in each of the overmentioned factors based on the context of the study. In addition, to shed light on the concept of climate resilience for buildings -which builds up the theoretic background of the study-, it is essential to unpack the impacts of climate change on the built environment. In other words, prior to defining the climate resilience of buildings, it is necessary to answer, "resilience to what?" to adopt the proper definition of the concept. There is a growing body of literature that analyses the effect of climate change on building energy performance (BEP), which is summarized in the following paragraphs.

## 1.3 The effect of climate change on building energy performance and thermal comfort

There is an increasing body of literature that investigates the impacts of climate change on building energy performance. Wan et al. (Wan et al., 2012) estimated the changes in the energy use for heating and cooling of an office building in five major representative cities of China with different climates, using MIROC3.2-H for weather projection. The authors identified that the estimated increase in cooling energy use is up to 24.2% for the low forcing scenario and argue that there would be a shift towards more electricity demand. To determine the effect of climate

change on U.S building energy performance, Pengyuan Shen (P. Shen, 2017) used the morphing method for downscaling the global climate models and analysed residential and office buildings in four cities. He identified that there is a rise in cooling energy use and a decrease in heating energy use in both office and residential buildings for all the cities. However, the extent of variation is different, and Shen concluded that climate change is diminishing the inconsistency of energy use in residential buildings located in cold and hot regions in the U.S. In another article, Shen and Lukes (P. Shen & Lukes, 2015) measured the impact of climate change on the efficiency of a ground source heat pump, for office and residential buildings in the U.S., using TRNSYS and eQuest simulation software. They estimated that global warming decreases the efficiency of the ground source heat pump, in all the studied cities, due to the rise in inlet and outlet water temperature of the heat pump. However, this negative impact is not significant for office buildings. Berardi and Jafarpur (Berardi & Jafarpur, 2020) demonstrated the need to perform analysis of the future energy performance of buildings by assessing the heating and cooling demand of 16 ASHRAE building prototypes using future weather data of populated urban regions in Canada. They point out that would be an increase in cooling demand by up to 126% and a decrease in heating demand by up to 33%. It was also highlighted that a higher insulation layer, higher zone ratios, lower window-to-wall ratio, and smaller outdoor air supply can scale down the negative effect of climate change on building energy performance. In Argentina, Flores-Larsen et al. (Flores-Larsen et al., 2019) analysed a typical mid-income house for medium and long-term climate change using the A2 scenario of the global model HadCM3 for four different cities. The authors concluded that cooling loads increase by 360-790 % and heating loads decrease by up to 59% in 2080. They also argued the effect of present bioclimatic strategies on the future performance of buildings toward global warming. The same studies were carried out for countries with colder climates, like Nordic countries. Nik and Kalagasidis (Nik & Sasic Kalagasidis, 2013) discussed the future energy performance of residential building stock in Stockholm and its uncertainties by analysing 153 buildings for 12 climate scenarios and with three cooling solutions. The authors found out that the heating demand will decrease, and the cooling demand will increase. However, the variation in cooling demand is more sensitive to different climate scenarios, and in most cases, it can be covered by natural ventilation in the Swedish climate. Another example is the analysis of a residential single-family from the 1980s in Benevento (Italy) by De Masi et al. (2021) using medium and long-term climatic projections

(2050 s and 2080 s, respectively). The case study also employed a number of passive retrofit solutions. The installation of double-glazed low emissive windows and the insulation intervention were found to be ineffective because the findings also revealed a 56% decrease in heating energy requirements and a 62% increase in cooling requirements (2080 s). The morphing future climatic data for Stockholm City and Rome were used in a different study (J. Shen et al., 2020) to examine the adaptive designs for multifamily buildings in the changing climate. The cooling and dehumidification need in Rome would increase from 5.3% to 23.6%, while the heating and humidification needs would fall from 27% to 16%, leading to more failure of the majority of conventional adaptive design methods. Additionally, for buildings in Rome that rely solely on natural ventilation, overheating would be a growing concern for public health. The research was conducted on a neighbourhood in Bari (south Italy) as indicative of a typical construction typology of the late 1970s in Italy in order to quantify the influence of climate change on the energy consumption of the public housing building stock (Vurro et al., 2022). The CCWorldWeatherGen tool (CCWorldWeatherGen V.1.8 - University of Southampton Blogs, 2012)was used to create the climatic data for the years 2020, 2050, and 2080 using the morphing technique. The cooling energy consumed will rise by 37% in 2050 compared to 2020 and by 38% in 2080 compared to 2050.

There is also research being conducted on overheating risk. Peacock et al. (Peacock et al., 2010) investigated overheating risk in UK dwellings by studying occupant thermal discomfort indicator (CIBSE, 2006) and the number of ‘‘cooling nights’’ in a year. The authors considered near term period (by the year 2030) for their analysis and concluded that overheating appears mostly in the south of the UK, which can cause the cooling problem for a third of a year. This increase in cooling demand and overheating risk was also predicted for Mediterranean countries. Dino and Akgül (Dino et al., 2019) investigated the impact of climate change on a typical mid-rise residential building in four cities in Turkey, considering three space cooling scenarios. They concluded that the occupants would experience overheating risk, especially in naturally ventilated dwellings. As a result of current and future climate change, building stocks that are currently free running in the summer may quickly utilize air conditioning systems, which will have an effect on carbon emissions, grid performance, and socioeconomic and health inequalities.

For air-conditioned buildings, they found that the increase in the annual mean temperature increases the cooling load by up to 177%, varied for different cities.

Cartalis et al. (Cartalis et al., 2001) simulated climate change in 2030 in Greece. They pointed out the increase in cooling degree days and cooling demand, with various magnitudes in different cities, and discussed the importance of modification of energy management in the country. This change in the energy use pattern was also identified by Zachariadis and Hadjinicolaou for Cyprus (Zachariadis & Hadjinicolaou, 2014). An increase of 6% in the country's annual electricity demand was estimated. Besides, the authors also ran economic analysis and argued that the country might need to forsake up to two years of economic growth to cope with extra electricity needs. Pérez-Andreu et al. (Pérez-Andreu et al. 2018) analysed a typical Mediterranean residential building in Valencia (as the representative city for the Mediterranean climate) under various scenarios for the mid and the end of the 21st century. The authors concluded that the heating demand decreases while cooling demand and overheating risk increase considerably. Moreover, they discussed a range of passive improvement measures for the building (up to reaching nearly zero-energy building) and found out that the expected energy consumption changes are not going to happen after the major retrofit. Rodrigues and Fernandes (Rodrigues & Fernandes, 2020) performed a similar series of analyses but by considering 16 different Mediterranean cities. They demonstrated that the extent of the cooling demand increases varies for different locations and must be analysed further. The general conclusion they made is that the present ideal U-values will not exacerbate the risk of overheating for all the studied cities except one of them.

In addition, the studies on the impacts of climate change on buildings are not limited to the overmentioned articles. Several authors have analysed such impacts on the energy performance of energy-efficient buildings. As an example, Sameni et al. (Tabatabaei Sameni et al., 2015) analyse 25 flats over three cooling seasons in Coventry, UK. The sample buildings are built under the Passivhaus standard, which was first developed in Germany in the late 1980s as a model that minimizes space heating and cooling needs. These buildings mainly use passive design features such as insulation, airtightness, and solar orientation in addition to limited active elements -such as mechanical ventilation with heat recovery (MVHR)- to meet energy efficiency measures. Their analysis shows that the standard of Passivhaus dwellings in the UK may face overheating and thermal discomfort condition during cooling seasons. Therefore, they point out the necessity of identifying the buildings with a higher risk of overheating under both current and future climate conditions. A more recent study by Attia et al. (Attia et al., 2020) analysed a Belgian reference case of nearly zero-energy building (NZEB). This study measured the climate

change-related increases in overheating hours by the years 2050 and 2100 regarding static and adaptive comfort models. The results show a remarkable presence of overheating (up to +43,5% by the end of the century) in the sample buildings and the failure to overcome the risk of overheating by 2050. Another study was performed by Xiaoming Wang et al. (Wang et al., 2010), where the impacts of climate change on the heating and cooling energy need in residential buildings in Australia were analysed. The local climate was projected using nine General Circulation Models (GCMs) under three carbon emission scenarios. The study showed that in the newly constructed 5-star houses, the heating and cooling need is subject to a significant variation between 26% to 101% by 2050 and 48% to 350% by 2100. In addition, this study is applied to five different regional climates, from cold to hot and humid, and the overmentioned result is reached regardless of the region. The other relevant finding refers to fewer absolute changes while higher percentage changes in the total energy requirements for energy efficient (5-star) buildings. In specific Regions like Sydney, which has more H/C balanced temperate climate, this increase might reach 530% for a 7-star house. Accordingly, they suggest that the high sensitivity of energy efficient buildings to global warming must be addressed in their planning, considering the future energy requirements. A more recent study is done by D. D'Agostino et al. (D'Agostino et al., 2022) on Eight European climate zones of Stockholm, Milan, Vienna, Madrid, Paris, Munich, Lisbon, and Rome. The research analyses the energy balance and changes in the PV outputs of the Nearly Zero Energy Buildings (NZEBs), considering a future climate change scenario regarding the year 2060. The building simulations are derived for both baseline and cost-optimized residential buildings. They notice that the heating decreases by 38% to 57% while cooling increases by 99% to 380% in different cities. In addition, the productivity of PV in NZEB sample increases up to three-times regarding the requirements of the baseline building. They claim that considering climate change impacts, energy efficiency is an "effective hedge" since optimized NZEBs are more resilient against temperature extremes. Another study by Karimpour et al. (Karimpour et al. 2015), analysing a building with an energy efficient envelope in the mild temperature climate of Adelaide, Australia, shows that the cooling demand will be dominated by 2070 due to climate change and heating need reduces significantly. They conclude that the measures which help to reduce the cooling load of better-insulated buildings will become more critical in the future. Therefore, the current strategies -which excessively focus on heating- must be dramatically changed toward the cooling need. They also suggest some

solutions that help to overcome the overmentioned challenges, including using foil in roofs, more reflective roofs, and tiles for floor covering. In the Italian context, the energy performance of an NZEB multi-family residential building in Lecce, Italy, for 2020, 2050, and 2080 weather scenarios was calculated by Baglivo et al. (2022). The findings indicate that the NZEB verifications are not entirely met. In addition to an increase in cooling requirements of up to 75% from 2020 to 2080, all flats will see an increase of around 16% in the number of hours when the operative temperature is over 26 °C while the outdoor temperature rises by 11%. Another study examined the effects of climate change on a residential NZEB in Rome that was constructed in accordance with Italian law. The energy need for cooling and heating respectively increased up to 50.3% and decreased up to 185.8%. In the same vein, Summa et al. (Summa et al., 2020) study the virtuosity of NZEBs in the future by evaluating the changes in the yearly performance of a residential NZEB in Rome regarding future scenarios. The study compares the current energy consumption with the one of 2050 by performing hourly dynamic simulations. It is concluded that the reference building might meet an increase of 18% in annual power consumption by 2050 due to the protracted activation of the air conditioning system and enhanced peak power requirements. It was discovered that peak electricity demand was particularly concerning. It will be crucial in the future to effectively reduce the requirement for air conditioning by aiming for a resilient NZEB design.

## 1.4 Aims and research questions

In summary, the review of the reported literature verifies the increasing concern about the effect of climate change on the future energy performance of buildings especially referring to the cooling demand rise and overheating risk. However, as seen earlier in section 1.3, little research - mostly in recent years – has been conducted on analysing the Italian building stock toward this issue, so there is still a need to deepen these analyses. Although a paradigm shift in the BEP is likely to happen, there is a need to perform quantitative analysis on a regional scale. The aim of this Ph.D. research is to assess and foster the climate resilience of Italian building stock through a regional approach. This thesis intends to investigate and optimize energy performance and thermal comfort of buildings in a changing climate (long-term assessment) on the regional scale. Several factors in buildings - particularly regarding building conditions and considering cooling strategies- are effective in optimizing the energy performance and thermal comfort of buildings both at present and in the future. The contribution of these factors to the BEP varies due to future

climate changes, and in order to assess their climate resilience, it is crucial to be comparatively analysed in different periods of time. To this aim, a set of KPIs (hours of exceedance, thermal energy need for space cooling, electrical energy consumption from the grid for cooling) are selected to represent the present, and future performance of buildings/thermal comfort and the relative impact of several building's conditions (insulation level of envelops) and cooling strategies (advanced solar shading/advanced glazing, cool envelop materials, and ventilative cooling) on these KPIs are analysed. This comparative analysis is first performed quantitatively for a representative building in Rome in three different periods (2010s, 2050s, and 2090s). Furthermore, in order to broaden the study and more accurately analyse the relative contribution of each building's condition or cooling technology to the variation of KPIs, a variance-based sensitivity analysis (Sobol) is performed. Through this process, the variances of the KPIs are considered as model outputs and are decomposed into fractions which can be attributed to the parameters referring to the building's conditions and cooling strategies as model inputs.

The remaining part of the thesis proceeds as follows: First, in chapter 2, the framework of the research is presented by noting the collaboration with the project IEA-EBC Annex 80: Resilient cooling and defining the case studies. In chapter 3, information regarding future weather data generation is given, which is essential for analysing the future performance and thermal comfort of buildings. Within the relevant sub-sections, a literature review on weather data creation is provided, followed by an analysis of different future weather datasets, a reliability assessment of existing future weather data models, and finally, explaining methods for adjusting systemic errors and biases. Following the creation of future weather data, a preliminary analysis is carried out in chapter 4 in order to create a broad and clearer picture of the climate change impacts on typical Italian residential buildings. In chapter 5, the required methodological information on the resilient cooling technologies, the case study, and KPIs are provided, and both sets of analysis explained above are performed. Finally, the most significant results and conclusions of this thesis are explained.

# 2. Framework of the research

## 2.1 IEA-EBC Annex 80: Resilient cooling

This thesis is developed in synergy with the research activities of the IEA EBC Annex 80 on Resilient Cooling of Buildings (*IEA EBC Annex 80 - Resilient Cooling of Buildings*, n.d.), which is part of the Technology Collaboration Programme (TCP) Energy in Buildings and Communities (EBC) of the International Energy Agency (IEA). Officially the activities of the Annex started in July 2019 and continued until July 2022, besides a reporting phase of one year until the end of July 2023. The Annex mainly aims to support and mainstream low-energy and low-carbon cooling systems in order to foster the transition toward resilient built environments. The main challenges that the annex tries to tackle are cooling and overheating issues in buildings. Four groups of active and passive cooling technologies are addressed with different aims:

a) Reduce heat loads to people and indoor environments

b) Remove sensible heat from indoor environments

c) Enhance personal comfort apart from space cooling

d) Remove latent heat from indoor environments

The annex tries to obtain these objectives through coordinating a four-step approach: (A) systematic technology assessment, (B) specific R&D-actions, (C) real performance evaluations, and (D) support of policy actions. Within this framework, the Annex focuses on the following subtasks: Subtask A: Fundamentals, Subtask B: Solutions, Subtask C: Field studies, and Subtask D: Policy Actions.

This research takes advantage of and contributes to subtasks A, B, and D. Subtask A deals with definitions and provides evaluation criteria. More detailed, it analyses disciplines, disaster risk management strategies, and resilience measures to define resilience in terms of cooling for buildings. In addition, for the evaluation of

resilience, it introduces a set of key performance indicators (KPIs). These KPIs are provided through a multidimensional approach that considers economical and technical criteria, environmental impacts, cultural and social aspects, and ecological issues. The weather data task force was created within this subtask to agree on a common and scientifically robust methodology to produce sets of weather data of characteristic climate zones & representative cities. Subtask B analyses these indicators in terms of limitations and performance besides the implementation barriers and opportunities. It also supports integrating resilient cooling systems to measurement methods of energy performance and indoor comfort prediction. By developing and proposing new solutions, technologies, and applications, it aims to expand the current low carbon/energy cooling solutions. Finally, for improving resilient cooling and overheating protection solutions, this task supports specific R&D activities. The last subtask which is relevant to this thesis is subtask D which deals with policy actions. This task aims to identify international best practices and potential barriers by analysing a set of policies, including product labelling programmes, AC minimum energy performance standards (MEPs), building regulations, standards, and compliance requirements. The identification of best practices and potential barriers helps to provide a set of future policy recommendations in order to mainstream the resilient cooling systems on national, European, and international levels for the future.

## 2.2 Definition of case studies

For the purpose of analysing the future energy performance and thermal comfort of the Italian residential building stock, the buildings simulated in this research have been selected from the IEE-TABULA research project (Ballarini et al., 2014). TABULA was aimed at creating a harmonized definition of the residential building typology at the European level. Each participating country developed its national building typology and identified representative building types of the existing residential building stock. Each building type has average geometrical and thermo-physical features of the building stock cluster that it represents. In TABULA, each cluster is characterized by a specific climatic zone, building size, and construction period. The building typology can be effectively applied to develop bottom-up energy models by taking the advantage of scaling up the results of the representative building type to the building stock cluster. Consequently, the building typology approach can be used to predict the energy performance of building stocks (Ballarini & Corrado, 2017), to assess effective energy-saving potentials, and to

develop reliable refurbishment scenarios of the stock (Corrado & Ballarini, 2016a). Three building types of the Italian residential building typology have been selected: single-family house (SFH), multi-family house (MFH), and apartment block (AB), all belonging to the construction period 1946–1960. These buildings have been chosen as they present a higher energy-saving potential compared to buildings of other construction periods(Ballarini et al., 2015; Corrado & Ballarini, 2016b) For each part of the study, one or more of them are used based on the aim of analysis. The main geometric and thermo-physical features of the building types are shown in Table 2. The building sizes cover a significant range of shape factors ($A_{env}/V_{gr}$) and window-to-wall ratios (*WWR*).

Table 2: Data of the Italian residential building typology (construction period:1946–1960)

| | | Building type | | |
|---|---|---|---|---|
| | | Single-family house (SFH) | Multi-family house (MFH) | Apartment block (AB) |
| Thermal zones and boundary conditions:<br>conditioned space<br>unconditioned space<br>adjacent building<br>ground | | 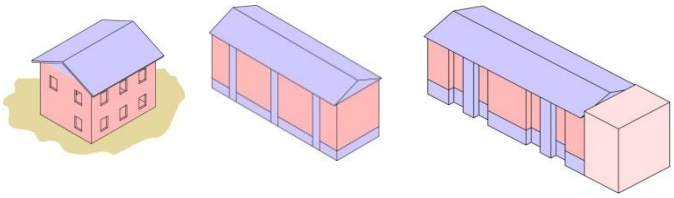 | | |
| Geometric parameters | Symbol | | | |
| *Gross conditioned volume* | $V_{gr}$ [$m^3$] | 584 | 3076 | 5949 |
| *Net floor area* | $A_{f,net}$ [$m^2$] | 162 | 827 | 1552 |

| | | | | |
|---|---|---|---|---|
| *Thermal envelope area* | $A_{env}$ [$m^2$] | 424 | 1576 | 2740 |
| *Shape factor* | $A_{env}/V_{gr}$ [$m^{-1}$] | 0.73 | 0.51 | 0.46 |
| *Window-to-Wall Ratio* | *WWR* [-] | 0.09 | 0.20 | 0.23 |
| *Number of floors* | - | 2 | 3 | 4 |
| *Number of units* | - | 1 | 12 | 24 |
| Thermo-physical parameters: | Symbol: | | | |
| *External wall thermal transmittance* | $U_{wl,ext}$ [$W \cdot m^{-2}K^{-1}$] | 1.48 | 1.48 | 1.15 |
| *Wall thermal transmittance to adjacent unconditioned space* | $U_{wl,unc}$ [$W \cdot m^{-2}K^{-1}$] | - | 1.70 | 2.32 |
| *Upper floor thermal transmittance* | $U_{fl,up}$ [$W \cdot m^{-2}K^{-1}$] | 1.65 | 1.65 | 1.65 |
| *Lower floor thermal transmittance* | $U_{fl,lw}$ [$W \cdot m^{-2}K^{-1}$] | 2.00 | 1.30 | 1.30 |
| *Windows thermal transmittance* | $U_w$ [$W \cdot m^{-2}K^{-1}$] | 4.90 | 4.90 | 4.90 |
| *Total solar energy transmittance of glazing for normal incidence angle* | $g_{gl,n}$ [-] | 0.85 | 0.85 | 0.85 |

The buildings have uninsulated envelope components, as the construction period predates the first Italian law on energy savings issued in 1976. For all stages of analysis performed in this thesis, the retrofitted state of the building has been considered accordingly. However, according to the annual report on the energy certification of buildings (Italian National Agency for New Technologies, Energy and Sustainable Economic Development & Italian Thermo Technical Committee, 2021), among the buildings analysed to get an energy performance certificate within the last four years, most of them were built before 1991, ( 41.8% for the period 1946–1960). The distribution by energy class of these cases confirms the prevalent presence of properties with lower performance (60-70%), with few cases in the best energy classes (around 3-4%).

The opaque external wall is solid brick masonry, while the horizontal envelope components are reinforced brick-concrete slabs. The transparent envelope components are single-glazing and wood-frame windows with exterior wooden Venetian blinds ($g_{gl+sh}$ = 0.35). The blind has a solar transmittance of 0.4 and solar reflectance of 0.12. The buildings have been simulated using the dynamic simulation engine Energy Plus (Version 9.0). The energy performance of the building types was assessed considering standard user behaviour. Hourly profiles of internal heat gains and ventilation airflow rates were set up under the Italian National Annex draft of EN 16798-1 technical standard (Italian National Annex of EN 16798-1 technical standard). An example of the hourly profile is shown in Figure 4 for the internal heat gains of each building type; the heat gains take into account occupants, electric lighting, and appliances and follow a typical residential hourly occupancy profile. The variability of the heat gains among the building types is due to a different occupancy density in the building unit, as specified in EN 16798-1.

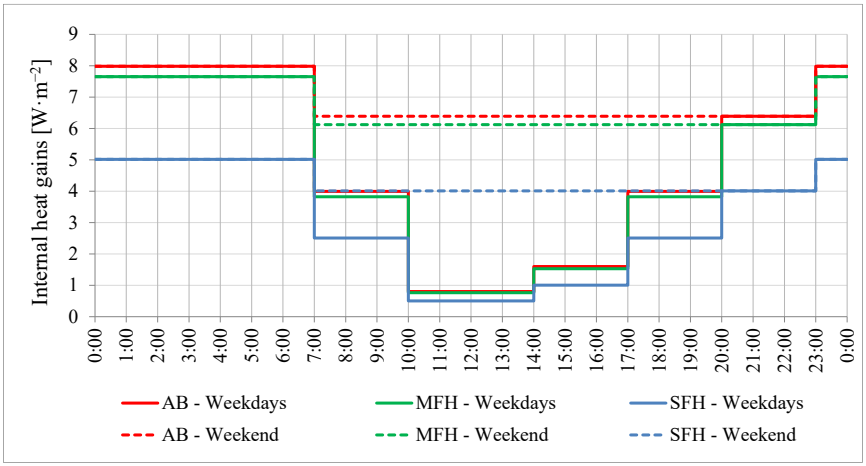


Figure 4: Hourly profile of the internal heat gains per unit of net floor area

The Italian most common technical building system technologies are considered for the base case studies: centralized gas standard boilers for heat generation and radiators as heat emitters. Space cooling is provided by an individual (per-apartment) direct expansion air conditioner (split systems). According to Italian standards (The Italian National Organization for Standardization, UNI/TS 11300-1: 2014), heating and cooling temperature set points were assumed equal to 20 °C and 26 °C, respectively. Moreover, the heating season and cooling period was assumed on the base of the climate zone. To carry out the energy simulation, the blinds are considered under operation if the beam *plus* diffuse solar irradiance incident on the window exceeds 300 W/m$^2$. Besides, mean monthly natural ventilation airflow rates equal to 0.30 h$^{-1}$ were applied.

# 3. Creation of future weather data for energy performance and thermal comfort assessment

## 3.1 Literature review on weather data creation

To investigate the future performance of a building in the context of climate change, building energy simulation (BES) is a vital support tool. BES needs a robust weather dataset that defines the external boundary conditions the building will face during its lifetime. Typically, a representative year of hourly weather data is required to represent the typical regional climate condition and to define the dynamic energy behaviour of the building. Several methodologies have been developed to create this one-year climate data from historical climate records (Herrera et al., 2005). The most commonly used methodology is the Typical meteorological year (TMY), which was introduced in 1978(Hall et al., 1978). TMY is a fictive year constructed of twelve representative typical months (Barnaby et al., 2011). Representative months are selected by comparing the distribution of each month with the long-term distribution of that month for the available climate dataset (the Finkelstein–Schafer statistics) (Finkelstein et al., 1971). The analysis of the present climate is based on the observation of climate variables and the application of statistical methods for understanding the current trends. On the other hand, the analysis of future climate is based on future scenarios and the projections of climate models.

Future scenarios are the input data used to provide initial conditions for General Circulation Models or Global Climate Models (GCMs), which are models for forecasting climate change. Global climate models are complicated numerical models that simulate the state and evolution of the atmosphere, including atmospheric circulation and energy exchanges in terms of radiation, heat, and moisture. They simulate the processes related to cloud formation and precipitation and take into account the interaction with the ocean and the land (Ramon et al.,

2019). To check if GCMs can simulate the evolution of the climate systems, they are validated against past climate conditions (Uppala et al., 2005). After verification and validation, GCMs are set to run by forcing greenhouse gas concentration scenarios as an initial condition. GCMs results have global or continental scale spatial resolution and long temporal resolution such as seasonal or annual periods. GCMs, provide climate information on a global scale with a typical spatial resolution of 150–600 km (Symon, 2013). Consequently, if they are used for building energy simulation, the climate change effect and related weather extremes at the local level will not be considered. In this case, the GCMs should be downscaled to applicable spatial (less than 100 km ) and temporal resolution (less than monthly value). There are two main approaches to downscale GCMs: dynamical and statistical downscaling. Several studies compared different methodologies that use these approaches for the generation of future weather data. Jentsch et al. indicate that weather variability is not generated in the statistically downscaled weather dataset, and this approach includes the effect of climate change independently between the variables (M. Jentsch et al., 2013). On the other hand, Dias et al. point out that the statistical downscaling approach has the advantage of reducing the computational time so that various climate change scenarios can be applied (Bravo Dias et al., 2020), besides providing enough information to study the performance of the building (Moazami et al., 2019). In light of these studies, there is still a need to deeply analyse different methodologies for future weather data generation. Statistical downscaling and dynamical downscaling are two main approaches; they are presented as follows.

Statistical downscaling develops and applies statistical relationships between regional or local climate variables and large-scale climate data using deterministic or stochastic approaches (Moazami et al., 2019). This downscaling approach is a computationally less demanding alternative that facilitates achieving various sets of results. The simplicity of this method—in comparison with dynamical downscaling—persuades many researchers to favor it. This method is mostly applied to GCM projections, while it may also be applied to Regional Climate Model (RCM) output as being a better representative of the local climate (Laflamme et al., 2016). In the two following paragraphs, major approaches for applying statistical downscaling are explained in more detail.

Stochastic weather generators are among the statistical models which fill in missing data and enable the production of long synthetic weather series indefinitely. This

becomes possible by simulating major properties of observed meteorological records, including daily means, variances, covariances, frequencies, extremes, etc. (Belcher et al., 2005). These models rely on statistical analysis of recorded climate data in which a few independent weather variables—such as solar irradiation—are adequate to derive all other relevant variables. The stochastic weather generation method has the advantage of enabling the integration of the distribution used for the climate change signal. In addition, it is accountable for potential changes in weather patterns and climate variability (Ramon et al., 2019). However, what appears to be a limitation of this method is the need for a large amount of data to train the model since distributions for generating future data are based on the baseline data given to the model (Belcher et al., 2005). The well-known tool that uses this method is Meteonorm(*Meteonorm Software V.7.3*, 2018). More details about this software and the way it becomes applied in this study will be explained in Section 2.2.1.

Morphing is the most common statistical downscaling method for the adjustment of time series toward the future. This method was first presented by Belcher et al. in 2005, assuming the current weather data as a baseline (Belcher et al., 2005). In order to transform this baseline to a future time series, monthly climate change signals given by a GCM, or RCM are used. There are three ways to morph data—shifting, scaling, or a combination of them—depending on the climate variable and expression of the climate change signal (absolute, relative):

• The Shift is applied according to Equation (1):

$$x_m = x_0 + \Delta x_m. \quad (1)$$

where $\Delta x_m$ is the absolute monthly mean change derived from a GCM or RCM predicted for a given variable ($x_0$), such as atmospheric pressure, for the month '$m$',

• The Stretch is applied according to Equation (2):

$$x_m = \alpha_m \cdot x_0. \quad (2)$$

where $\alpha_m$ is the relative monthly mean change derived from a GCM or RCM predicted for a given variable ($x_0$), such as wind speed, for the month '$m$',

• The combination of Shift and Stretch is applied when both absolute and relative monthly mean changes derived from a GCM or RCM are predicted for a given variable ($x_0$), such as dry-bulb temperature, for the month m, according to Equation (3):

$$x_m = x_0 + \Delta x_m + \alpha_m (x_0 - x_{0,m}) \quad (3)$$

where $x_{0,m}$ is the variable $x_0$ average over the month '*m'* for all the considered averaging years of future data provided by the climate models.

CCWorldWeatherGen (CCWorldWeatherGen V.1.8 - University of Southampton Blogs, 2012) and WeatherShift$^{TM}$ (WeatherShift,2020) are two available tools that use the morphing method to create future weather data. More details about these tools and their application in this study will be explained in Section 2.2.

Dynamical downscaling uses a nesting strategy to obtain climate information at a resolution of 2.5–100 km. To this aim, a Regional Climate Model (RCM) is used to derive local or regional climate information. This method simulates "atmospheric and land surface processes while accounting for high-resolution topographical data, land-sea contrasts, surface characteristics, and other components of the Earth system" (American Meteorological Society, 2013). The climate information generated by RCMs has much finer spatial resolution compared to GCMs. This allows RCMs to better represent the spatial and temporal variability of local climate and guarantee physically consistent datasets (Soares et al., 2012). However, a large amount of computational power and storage for data creation is one of the limitations of this method. Furthermore, the accuracy of the relevant GCM determines the overall quality of the output. In order to evaluate such uncertainties, different GCM–RCM pairings are combined, and a series of simulations are performed. ENSEMBLES (van der linden & Mitchell, 2009) and EURO-CORDEX (Jacob et al., 2014) projects are two of such efforts.

EURO-CORDEX—as the main reference framework for regional downscaling research—aims to facilitate the process of knowledge exchange and communication. Many sectors—e.g., the building sector, agriculture, heat and fire risk, and air quality—utilize EURO-CORDEX since it provides a consistent database of downscaled multi-year projections for various regions all over the world (Giorgi, 2019). In addition, by providing a better understanding of the regional and

local climate and its associated uncertainties, EURO-CORDEX evaluates and enhances different RCMs. CORDEX includes a large RCM database, and it is updated with new climate data from available domains all over the globe (World Research Climate Program (WRCP), n.d.). For European countries, the grid resolution provided by EURO-CORDEX projections equals 12.5 km. For the Middle East and North Africa, this quantity is 25 km, while the rest of the world has the grid resolution of 50 km. The time scales—on which the data in the multi-layer format are available—include monthly, daily, every six hours, every three hours, and hourly during the historical period from 1976 to 2005 and for the future period from 2006 to 2100. The data are available either for RCP 4.5 or RCP 8.5 scenarios, depending on the model (*EUROCORDEX: Cordex Archive Specifications*, n.d.). Although most of the available data on the platform are not bias-adjusted, a number of bias-adjusted data are available for some specific models and climate variables.

## 3.2 Application for Weather data creation

Four future weather datasets to be analysed in this work were generated for Rome using Meteonorm, CCWorldWeatherGen, and WeatherShift™ weather generator tools, and one RCM (GERICS-REMO-2015) from the EURO-CORDEX project. The weather datasets were developed for the 2001-2020 (2010s), 2041-2060 (2050s), and 2081-2100 (2090s) periods. The following paragraphs describe the applied methodology in detail.

By integrating the climate database with spatial interpolation of the principal weather variables and a stochastic weather generator, Meteonorm generates hourly weather data for any site in the world (Remund & Kunz, 1997). These data can be used as input for building performance simulation. Weather variables such as global irradiance on a horizontal plane at the ground level, dry-bulb temperature, dew-point temperature, and wind speed are provided by Meteonorm. This tool can also be used for climate change studies. GCMs under the IPCC fourth assessment report (AR4) (Pachauri & Reisinger, 2008) are used in this tool to generate future weather data for different emission scenarios (B1, A1B, and A2), with 10-year intervals from 2010 until 2100 (Remund et al., 2010). The Meteonorm version 7.2 was used in this study to generate weather data for the A2 emission scenario (pessimist scenarios) for the city of Rome.

The CCWorldWeatherGen is a Microsoft® Excel-based tool developed by the Sustainable Energy Research Group of Southampton University (M. Jentsch et al., 2013). It uses the Morphing methodology to create future weather datasets in Energy Plus Weather (EPW) format for different locations all over the world. The output data of the UK Met-office, the Hadley Centre Coupled Model 3 (HadCM3, n.d.) global climate model, forced with IPCC A2 emission scenarios, is used in this tool. The HadCM3 climate model was chosen since, by the time—in comparison with 29 other climate models—this model was the only one that had all necessary climate variables for the morphing procedure (M. F. Jentsch, n.d.). What HadCM3 provides as input for the Morphing procedure in CCWorldWeatherGen is the monthly value of relative changes regarding the period of 1961–1990. The Excel tool superimposes this input on the weather variables of the baseline weather data stored in an EPW file. The tool generates future weather data sets for 3-time slices: 2001-2020 (2010s), 2041-2060 (2050s), and 2081-2100 (2090s). Being a free online tool is an advantage that makes it widely used. However, due to possible differences in the reference time frame between HadCM3 and the EPW data, inaccuracy in the outputs of the tool may occur (M. F. Jentsch et al., 2008). In this study, the International Weather for Energy Calculation (IWEC) TMY file of Rome—downloaded from the Energy Plus database—was used to be morphed for the overmentioned time periods.

The WeatherShift ™ tool was developed upon morphing methodology by Arup and Argos Analytics for creating future weather data (WeatherShift). “The tool blends 14 of the more recently simulated GCMs[1] into cumulative distribution functions (CDF) (Pachauri & Reisinger, 2008). It is based on RCP 4.5 and 8.5 emission scenarios of the IPCC's fifth assessment report. Creating CDFs allows a percentile distribution (called warming percentile factor) and “smooths out” the inter-modal uncertainty and stochastic climate behaviour (Troup & Fannon, 2016).

The tool produces future weather data for time periods of 20 years, starting from 2011 and ending in 2100. The morphing method in this tool is applied to 8 climate variables of the reference TMY: the mean, maximum, and minimum daily

[1] BCC-CSM1.1, BCC-CSM1.1(m), CanESM2, CSIRO- Mk3.6.0, GFDL-CM3, GFDL-ESM2G, GFDL-ESM2M, GISS-E2-H, GISS-E2-R, HadGEM2-ES, IPSL-CM5A-LR, IPSL-CM5A-MR, IPSL-CM5B-LR, NorESM1-M

temperature, relative humidity, daily total solar irradiance, wind speed, atmospheric pressure, and precipitation. The future projections are relative to the baseline period of 1976-2005. In this study, the 50$^{th}$ percentile and the RCP 8.5 emission scenarios were selected to set the tool for generating future weather datasets of Rome. The IWEC-TMY was the baseline for this procedure.

The CORDEX platform provides a variety of climate models and socioeconomic projections, among which the selection of the proper one was the first step. Several conditions had to be met in order to reduce the available climate model options. First, the availability of weather variables for reassembling weather datasets input for energy simulations of buildings. Second, providing 3 hours minimum of temporal frequency and finally, 25 km as the minimum of spatial frequency.

So far, there are three GCM-RCM climate model combinations at the moment of the study that meet the above-mentioned criteria, which are Met Office Hadley Centre (MOHC) HadGEM2-ES/GERIC-REMO 2015, Max Planck Institute for Meteorology (MPI-M) MPI-ESM-LR/GERIC-REMO 2015, and Norwegian Climate Centre (NCC) NorESM1-M /GERIC-REMO 2015. For a holistic assessment, an ensemble-based approach must be followed. However, regarding limitations caused by computational cost, for either of these options, the dry-bulb temperature projections were compared to several other models, and the (MPI-M) MPI-ESM-LR/REMO combination was finally chosen for being the closest to the median temperature of all climate models projections according to figure 5. (Flato et al., 2013).

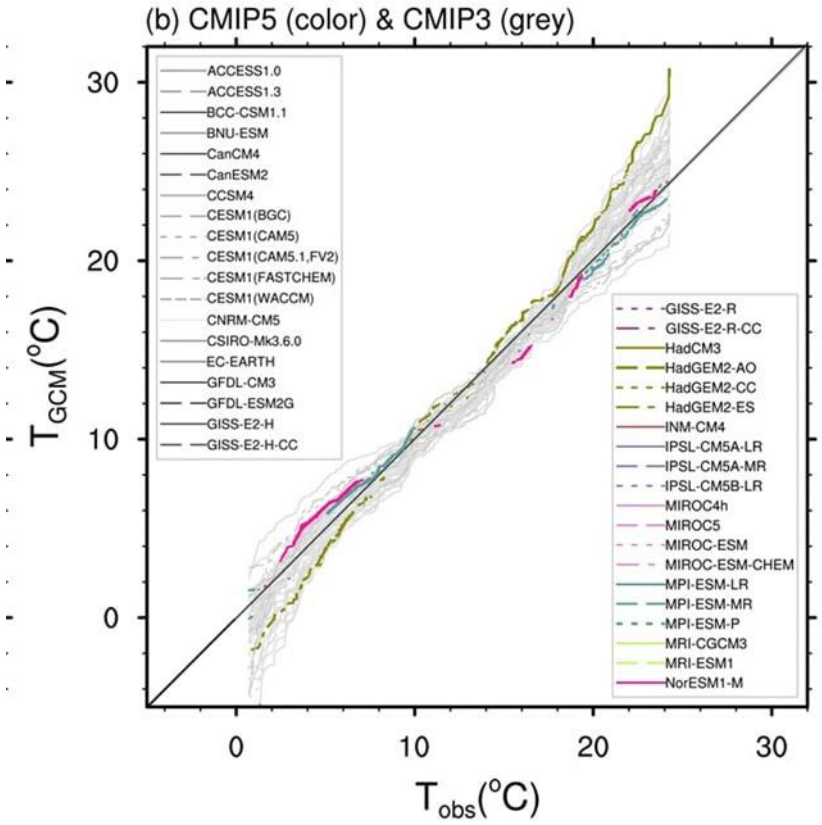


Figure 5: "Ranked modelled versus observed monthly mean temperature for the Mediterranean region for the 1961–2000 period" (IPCC, 2013b)

The data for this model was downloaded from the EURO-CORDEX entry point through the Earth System Grid Federation (ESGF) for the Europe domain on a 0.11 ° grid in polar coordinates (equivalent to a 12.5 km grid). These data are available in the NetCDF4 format, which is a file format for storing multidimensional scientific data. The extraction of the data for our case study (city of Rome) was performed through the Cordex Data Extractor software (CORDEX Data Extractor, n.d.), which allows finding the closest data point on the grid to the desired latitude and longitude. The extracted climate variables are near-surface air temperature, near-surface relative humidity, surface air pressure, surface downwelling shortwave radiation, and near-surface wind speed. RCP 8.5 scenario was adapted to extract these data for 2010s (2001-2020), 2050s (2041-2060), and 2090s (2081-2100) periods.

For splitting the direct and diffuse components of global solar irradiation, the Boland–Ridley model (Boland et al., 2008) is applied in this study. The method is a robust and straightforward predictor model that needs a few input data. It is reliable as the Italian Standardization body has adopted it to split the global solar irradiance for creating national climatic data (UNI 10349-1:2016). In addition, the model was validated in a later study (Ridley et al., 2010).

Boland–Ridley determines a logistic function (sigmoid function) for the diffuse fraction of global solar radiation on a horizontal surface based on the clearness index, which is the ratio of the global solar radiation to the extra-terrestrial solar radiation all on a horizontal plane. The latter can be easily calculated using the solar elevation and the extra-atmospheric solar irradiance received on a theoretical surface orthogonal to the sun's rays and at the earth's mean distance from the sun (depending on the earth's orbital angle). By having this fraction, the direct and diffuse components can be calculated.

Following this, for the generation of the weather data for building energy simulation, direct normal solar irradiance (Kasten, 1996) is required. This value equals the division of the solar irradiation direct component to the cosine of the solar zenith angle. Calculation of direct-normal solar radiation can yield unphysical results when the direct-horizontal solar radiation and the cosine of the solar zenith angle are both small because the sun is low. In this case, a threshold is introduced by applying a physical model(Remund et al., 2003) that considers the Rayleigh optical depth (in the function of the mass of air) and the Linke Turbidity (TL) (Remund & Bern, 2010), which accounts for scattering and absorption by both atmospheric aerosols and atmospheric gases.

Typical meteorological years (TMYs) are created using the international standard EN ISO 15927-4 (CEN, 2005) method. The procedure is applicable for assessing the climate change impact on the long-term mean energy loads of buildings. It is not suitable for constructing extreme or semi-extreme meteorological data. TMYs are constructed from ’12’ representative months (typical months) from multi-year records. For selecting the ‘typical months,’ two sets of parameters are taken into account: Primary parameters, including dry-bulb air temperature, global solar irradiance, and relative humidity (or air absolute humidity, water vapour pressure, or dew point temperature) and secondary parameters, including wind speed. The Finkelstein–Schafer statistic ($F_s$) (Finkelstein & Biometrika, 1971) is calculated for

all the primary climatic parameters for each month and year of the data set. $F_s$ is a goodness-to-fit statistic that proved to be more potent than conventional alternatives. It is the sum of the differences between two cumulative distribution functions: the first relating to a specific year and the second regarding the multi-year dataset. By ranking the $F_s$ in increasing order for each primary parameter and calculating the total ranking (the sum of the primary parameter's ranks) for each year, for each calendar month, three months (with the lowest total ranking) are selected. The month with the lowest deviation in wind speed (secondary parameter) is selected as the "typical" month to be included in the typical year. This method is applied to three sets of 20-year RCM data (2010s, 2050s, and 2090s) to generate a TMY for present and future typical meteorological years (F-TMY) for 2050s and 2090s. These TMYs were then converted to EnergyPlus weather files (.EPW) for use in building energy simulations. The EnergyPlus auxiliary program "weather converter" tool(EnergyPlus Version 9.6.0 /Auxiliary Programs. 2021) is used for this purpose.

## 3.3 Reliability assessment of existing future weather data models

This section aims to contribute to evaluating the suitability and robustness of different future weather data for analysing the future performance of reference buildings both in terms of thermal comfort and energy performance. It represents a comparative study of four future weather datasets explained in section 3.2, considering IWEC-TMY as the present weather dataset. The study investigates the impact of each type of these future weather data on building energy performance and thermal comfort predictions. It evaluates the heating and cooling demand, the global/overall energy performance in the presence of heating and cooling systems, and the overheating risk in a free-floating regime. SFH and AB were selected from the representative of the existing residential building stock in Italy (explained in section 2.2) since these two building sizes present a significantly different shape factor—0.73 $m^{-1}$ for the SFH and 0.46 $m^{-1}$ for the AB—and window-to-wall ratio: 0.09 for the SFH and 0.23 for the AB. As a generation subsystem type for this analysis, a reversible heat pump has been chosen, considering continuous operation. The analysis was carried out for Rome, as it is one of the representative cities of Mediterranean hot summer climates according to the Köppen classification (Köppen, 1884). Representative Concentration Pathways 8.5 (business as usual)

(Symon, 2013) have been applied in this study for the mid-century period from 2041 to 2060 (2050s). This period was used for the analysis, since GCMs uncertainties due to internal climate variability, climate model, and future scenarios increase significantly over time (Hawkins & Sutton, 2009, 2011). A schematic representation of different future weather data reliability assessment is presented in figure 6.

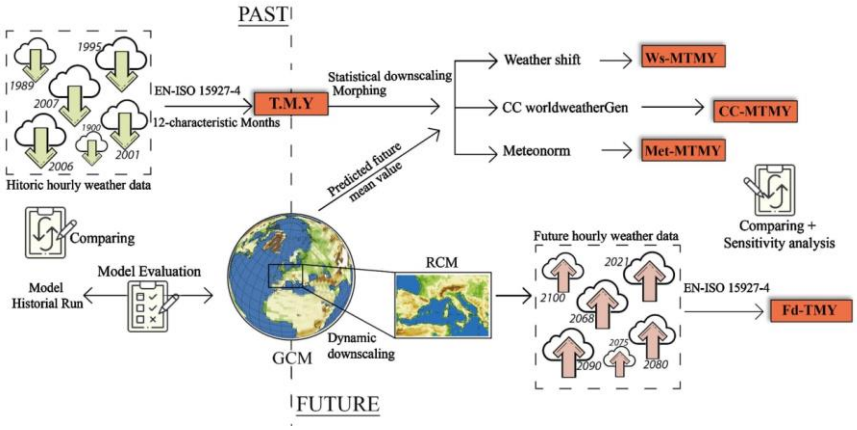


Figure 6: Graphic representation of different future weather data reliability assessment

### 3.3.1 Energy performance assessment

The building energy performance was assessed by means of a detailed dynamic simulation model using EnergyPlus (version 9.0) with an hourly time step. The results are discussed in terms of annual thermal energy need for space heating and space cooling ($EP_{H/C,nd}$) and electrical energy demand per unit of area ($E_{el}/A_{f,net}$). The latest indicator ($E_{el}/A_{f,net}$) was calculated according to Equation (4):

$$E_{el}/A_{f,net} = \frac{EP_{H,nd}}{\eta_{H,u} \cdot \eta_{H,g}} + \frac{EP_{C,nd}}{\eta_{C,u} \cdot \eta_{C,g}} \quad (4)$$

where $EP_{H/C,nd}$ is the annual thermal energy need for space heating/cooling, $\eta_{H/C,u}$ is the mean seasonal efficiency of the heating/cooling utilization (including emission, control, and distribution) subsystems, and $\eta_{H/C,g}$ is the mean seasonal efficiency of the heating/cooling generation subsystem.

The reference mean seasonal efficiency values of the utilization subsystems were assumed in compliance with the Italian Interministerial Decree of June 26th, 2015 (Italian Republic, Interministerial Decree of June 26th, 2015). As a reversible heat pump has been selected as a generation subsystem type to carry out the analysis, a future value of the mean seasonal generation efficiency was adopted to take into account the increase of the ambient temperature due to climate change. The mean seasonal efficiency of the heating generation subsystem was calculated assuming proportionality between the maximum theoretical mean coefficient of performance at present and its future value over different temperatures, as in Equation (5):

$$\eta_{H,g} \sim \frac{\sum_{\text{heating season}} \Phi_H}{\sum_{\text{heating season}} \left( \Phi_H \cdot \frac{T_{cond,out} - T_{evap,in}}{T_{cond,out}} \right)} \quad (5)$$

where $\Phi_H$ is the hourly thermal energy load for heating, $T_{cond,out}$ is the condenser outlet temperature (hot water), and $T_{evap,in}$ is the evaporator inlet air temperature.

In the same way, proportionality between the maximum theoretical mean energy-efficiency ratio and its future value over different temperatures has been assumed, as in Equation (6):

$$\eta_{C,g} \sim \frac{\sum_{\text{cooling season}} \Phi_C}{\sum_{\text{cooling season}} \left( \Phi_C \cdot \frac{T_{cond,in} - T_{evap,out}}{T_{evap,out}} \right)} \quad (6)$$

where $\Phi_C$ is the hourly thermal energy load for cooling, $T_{evap,out}$ is the evaporator outlet temperature (chilled water), and $T_{cond,in}$ is the condenser inlet air temperature.

### 3.3.2 Thermal comfort assessment

The thermal comfort was assessed in accordance with the EN 16798-1 standard (European Committee for Standardization, 2005). The adaptive comfort model was adopted to predict how the pattern of outside weather conditions affects the indoor thermal sensation of the user in free-floating condition. In this model, the optimal operative temperature ($\theta_{o,c}$, in °C) is calculated as in Equation (7):

$$\theta_{o,c} = 0.33 \cdot \theta_{r,m} + 18.8 \quad (7)$$

where $\theta_{r,m}$ is the outdoor running mean temperature (in °C), which is calculated as in Equation (8):

$$\theta_{r,m} = (1-\alpha) \cdot \{\theta_{ed-1} + \alpha \cdot \theta_{ed-2} + \alpha^2 \cdot \theta_{ed-3}\} \quad (8)$$

where α is a constant between 0 and 1 (recommended value is 0,8), $\theta_{ed-1}$ is the daily mean outdoor air temperature for the previous day, and $\theta_{ed-i}$ is daily mean outdoor air temperature for the *i*-th previous day.

In this research, a medium level of occupant expectation ( the second category of indoor environmental quality, as defined in (European Committee for Standardization, 2005)) was applied, in which the range of comfort is between $\theta_{o,c}$ +3 °C (highest limit) and $\theta_{o,c}$ − 4 °C (lowest limit). In addition, the hours of exceedance (*HE*) were calculated as an indicator to quantify indoor overheating. The *HE* indicator is equal to the number of hours during the cooling period in which the operative temperature of the zone is greater than the upper limit temperature of the thermal comfort range.

### 3.3.3 Results and discussion

The aim of this part of the research is to analyse different types of future weather datasets by comparing their relative impact on building energy performance predictions. In the first set of results, boxplots of the outdoor dry-bulb temperature and the global horizontal solar irradiance during daily hours, which are the weather key variables in building energy simulation, are plotted (Figures 7 and 8). Boxplots show a pattern of increase in both variables due to climate change. All future weather files show almost similar mean values higher than the present weather file. Nevertheless, F-TMY—which is derived from a dynamical downscaling method—shows lower dispersion compared to other future files (statistically downscaling methods).

Followingly, Figures 9 and 10 present net thermal energy needs for heating and cooling normalized by the conditioned floor area for the single-family house and apartment block for present and different future weather data to assess the building

energy performance of the case studies. The heating energy demand for the single-family house (SFH) dominates over the cooling demand. In addition, SFH also has higher energy demand for heating compared to the apartment block (AB). This is due to the higher shape factor (S/V) ratio, which entails that heat transfer by transmission is the most relevant term of the energy balance, and outdoor temperature is the main driving force. Consequently, the decrease of $EP_{H,nd}$ in the values of $EP_{H,nd}$ and $EP_{C,nd}$. It appears that the heating need is slightly dominant in the present, but it will be overtaken by cooling in the future. For all future weather data except F-TMY, the relative change of $EP_{H,nd}$ is in the range of 30 % to 34 % for both buildings, while the relative change of $EP_{C,nd}$ is above 160 % for SFH and above 100 % for AB. This unevenness in relative variation is mainly related to the different magnitudes of the present energy need, in which more contribution refers to cooling need. As regards F-TMY, lower values of $EP_{H,nd,}$ and $EP_{C,nd}$ are shown compared to the other future weather data, meaning that $EP_{H,nd}$ will decrease more and $EP_{C,nd}$ will increase less. This trend is strictly dependent on the lower dispersion of temperature values for F-TMY compared to the other future weather datasets. Comparing the four sets of weather data, WeatherShift$^{TM}$ (WS), Meteonorm (MET), and CCWorldWeatehrGen (CCW) show almost similar variations in $EP_{H,nd}$ and $EP_{C,nd}$, while the F-TMY presents a significantly different variation in the two indicated parameters. This comes from the fact that WS, MET, and CCW are all statistically downscaled weather datasets, and F-TMY is a dynamically downscaled weather dataset. In order to better present this trend, the box plots of thermal energy load for heating in the month of January and for cooling in the month of August are shown in Figures 11-14. The figures indicate that for both SFH and AB, the mean values for the month of January are almost the same for all future weather files, while the deviation of F-TMY is lower than the three other files. On the other hand, for the month of August, the mean values of WS, MET, and CCW is significantly higher than F-TMY. The reason lies in the fact that the dynamically downscaled weather data, in comparison with the statistical ones, better represents the temporal variability of climate, which leads to a more consistent dataset. As another outcome of the inconsistency in the statistical downscaled weather files, figures 12 and 14 demonstrate the overestimation of the data in the thermal energy load for cooling in August.

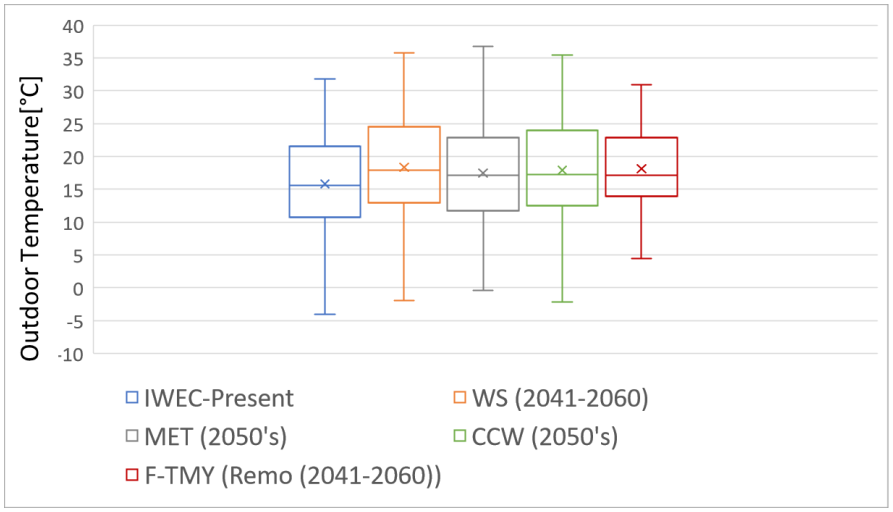


Figure 7: Boxplots of the outdoor dry-bulb temperature for IWEC (Present), WeatherShift™ (WS), Meteonorm (MET), CCWorldWeatehr-Gen (CCW), and F-TMY. All future weather files are for 2050s, considering Representative Concentration Pathway (RCP) 8.5.

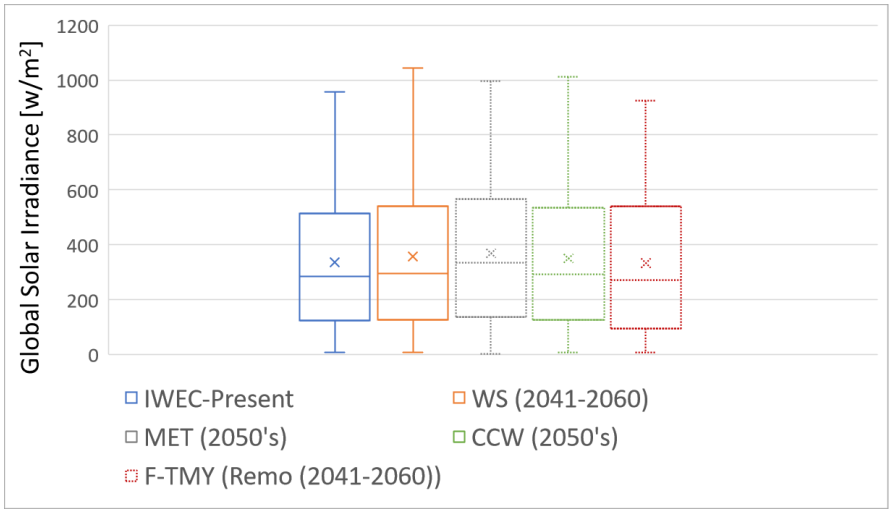


Figure 8: Boxplots of the global solar irradiance for IWEC (Present), WeatherShift™ (WS), Meteonorm (MET), CCWorldWeatehr-Gen (CCW), and F-TMY. All future weather files are for 2050s, considering Representative Concentration Pathway (RCP) 8.5.

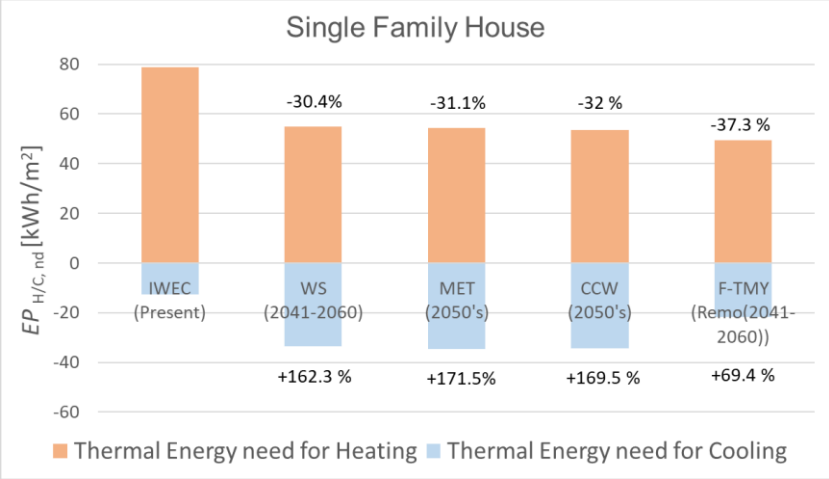


Figure 9: Net thermal energy needs for heating and cooling normalized by the conditioned floor area for the single-family house for IWEC (Present), WeatherShift™ (WS), Meteonorm (MET), CCWorldWeatehr-Gen (CCW), and F-TMY. All future weather files are for 2050s considering RCP 8.5.

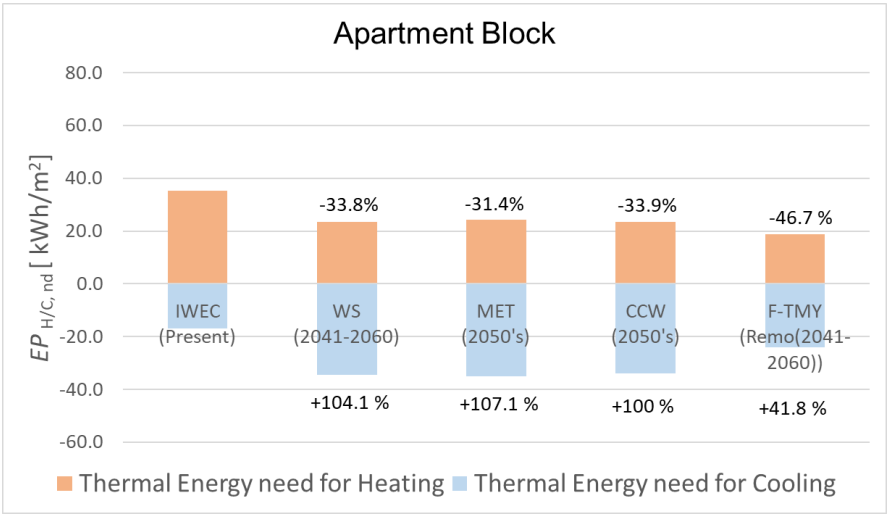


Figure 10:Net thermal energy needs for heating and cooling normalized by the conditioned floor area for the apartment block for IWEC (Present), WeatherShift™ (WS), Meteonorm (MET), CCWorldWeatehr-Gen (CCW), and F-TMY. All future weather files are for 2050s considering RCP 8.5.

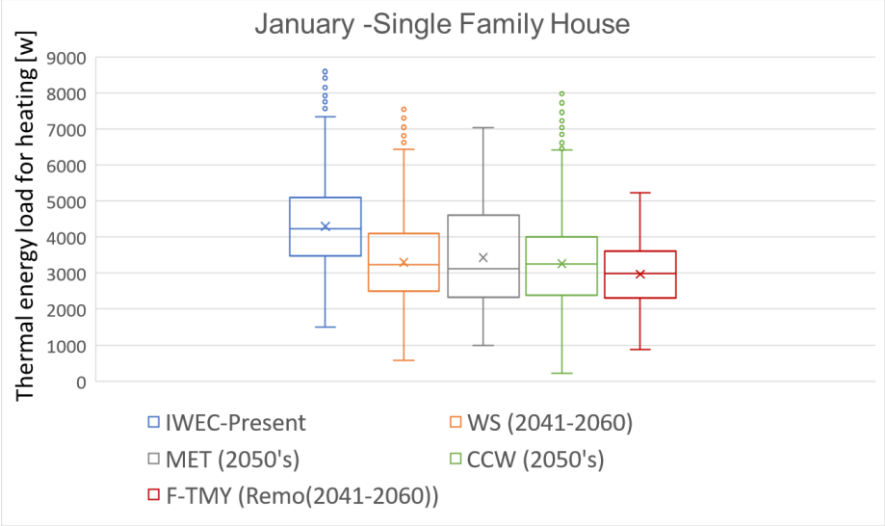


Figure 11: Boxplots of heating loads in January for the single-family house for IWEC (Present), WeatherShift™ (WS), Meteonorm (MET), CCWorldWeatehr-Gen (CCW), and F-TMY. All future weather files are for 2050s considering RCP 8.5.

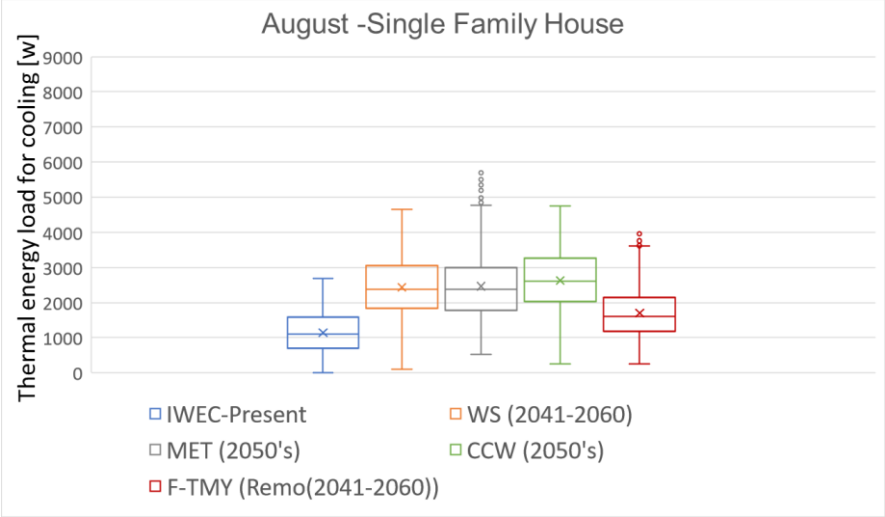


Figure 12: Boxplots of cooling loads in August for the single-family house for IWEC (Present), WeatherShift™ (WS), Meteonorm (MET), CCWorldWeatehr-Gen (CCW), and F-TMY. All future weather files are for 2050s considering RCP 8.5.

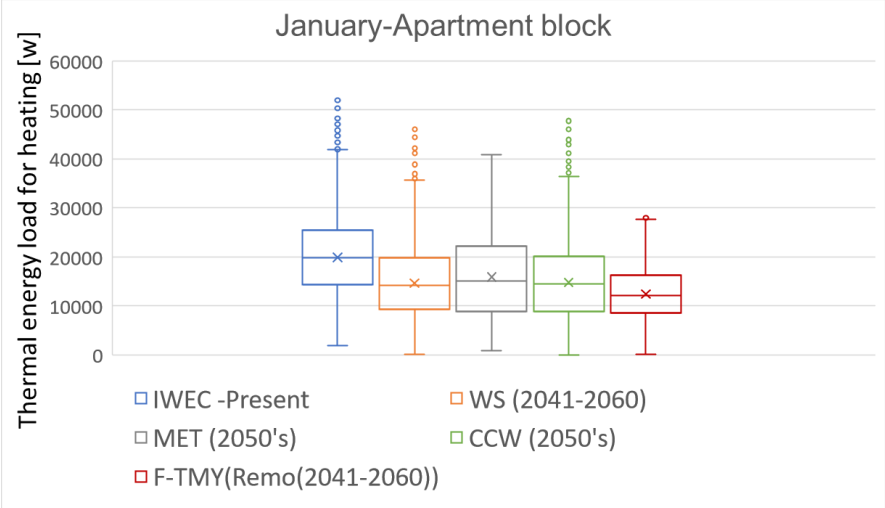


Figure 13: Boxplots of heating loads in January for the apartment block for IWEC (Present), WeatherShift™ (WS), Meteonorm (MET), CCWorldWeatehr-Gen (CCW), and F-TMY. All future weather files are for 2050s considering RCP 8.5.

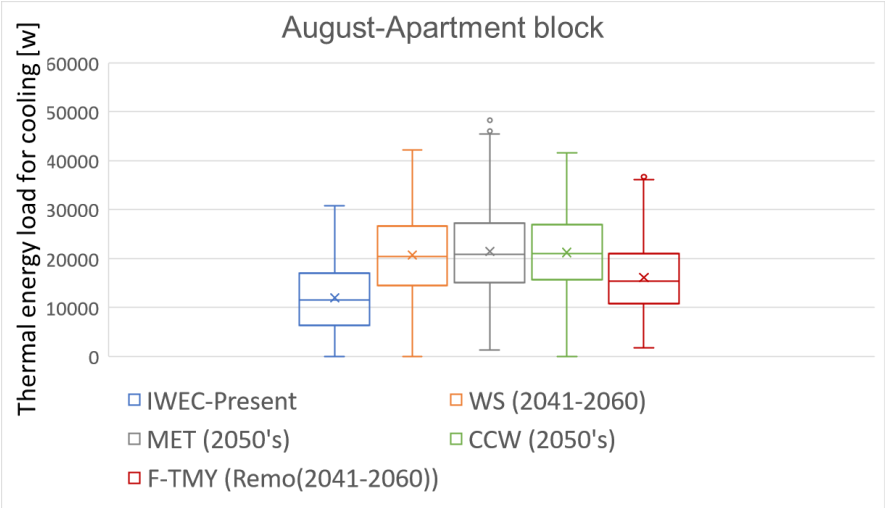


Figure 14: Boxplots of cooling load in August for the apartment block for IWEC (Present), WeatherShift™ (WS), Meteonorm (MET), CCWorldWeatehr-Gen (CCW), and F-TMY. All future weather files are for 2050s considering RCP 8.5.

The adaptive comfort analysis in the free-floating condition of SFH and AB for IWEC (Present), WeatherShift$^{TM}$ (WS), Meteonorm (MET), CCWorldWeatehrGen (CCW), and F-TMY is presented in Figures 15 and 16. The graphs show the distribution of hours of the cooling period (April 16$^{th}$ until October 14$^{th}$: 4368 hours) in three ranges: Comfort, warm discomfort, and cold discomfort. The discrepancy between F-TMY and other future weather data is pointed out. The percentage of warm discomfort hours for the WS, MET and CCW is almost the same and equals around 40 % for SFH and 90 % for AB. For the F-TMY, the percentage of warm discomfort hours is less for both cases (29 % for SFH and 72 % for AB). This discrepancy can be found in Figures 17 and 18, where boxplots of the last floor operative temperature of SFH and AB in August for present and different future weather data are presented. In this case, despite having similar dispersions, the mean values of the last floor operative temperature of F-TMY are significantly lower than the mean value of the other three future weather datasets for both SFH and AB. This is strongly dependent on the lower dispersion of temperature values for F-TMY.

If we now turn to the comparison of the two building types, occupants in AB will experience overheating much more often than the occupants in SFH because of a reduced potentiality of exploiting the heat transfer in AB through the envelope for ejecting heat produced by internal and solar sources. This is due to the lower S/V value and larger window-to-wall ratio (WWR) of the AB compared to SFH. In addition, hours of exceedance (HE) for all the weather datasets for SFH and AB are presented in Table 3. It is observed that the absolute change of the increase in the HE for statistically downscaled future weather datasets is almost the same, while for dynamically downscaled future weather, data are significantly lower.

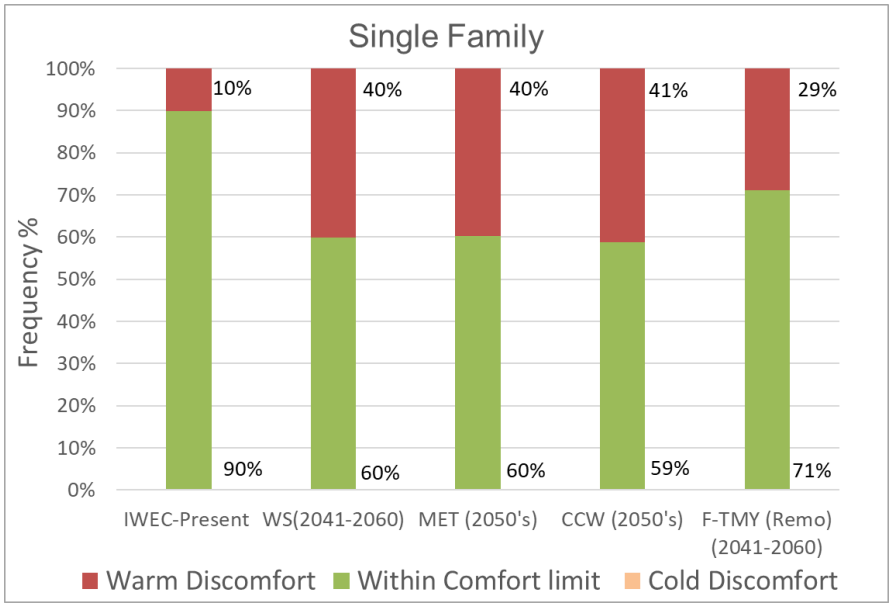


Figure 15: Adaptive comfort analysis for the single-family house for IWEC (Present), WeatherShift™ (WS), Meteonorm (MET), CCWorldWeatehr-Gen (CCW), and F-TMY. All future weather files are for 2050s considering RCP 8.5.

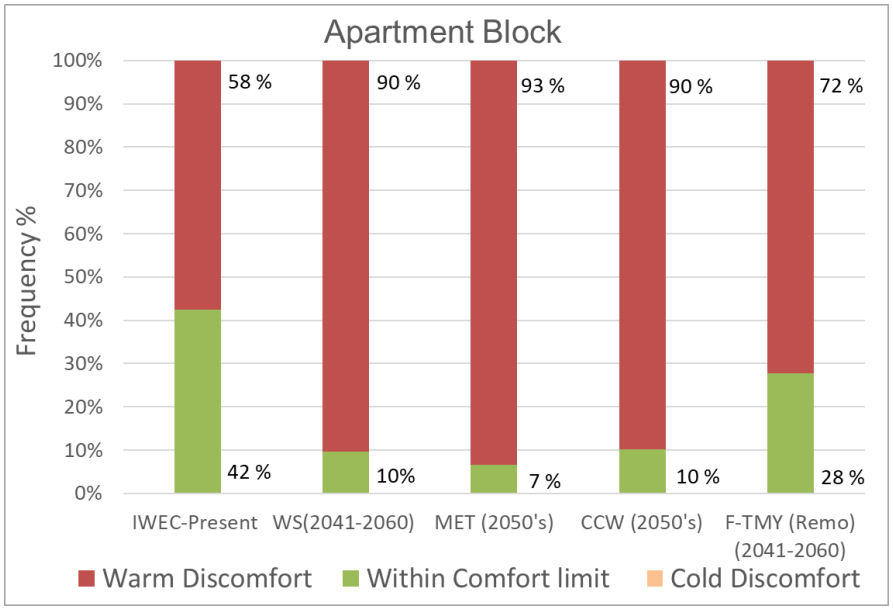


Figure 16: Adaptive comfort analysis for the apartment block for IWEC (Present), WeatherShift™ (WS), Meteonorm (MET), CCWorldWeatehr-Gen (CCW), and F-TMY. All future weather files are for 2050s considering RCP 8.5.

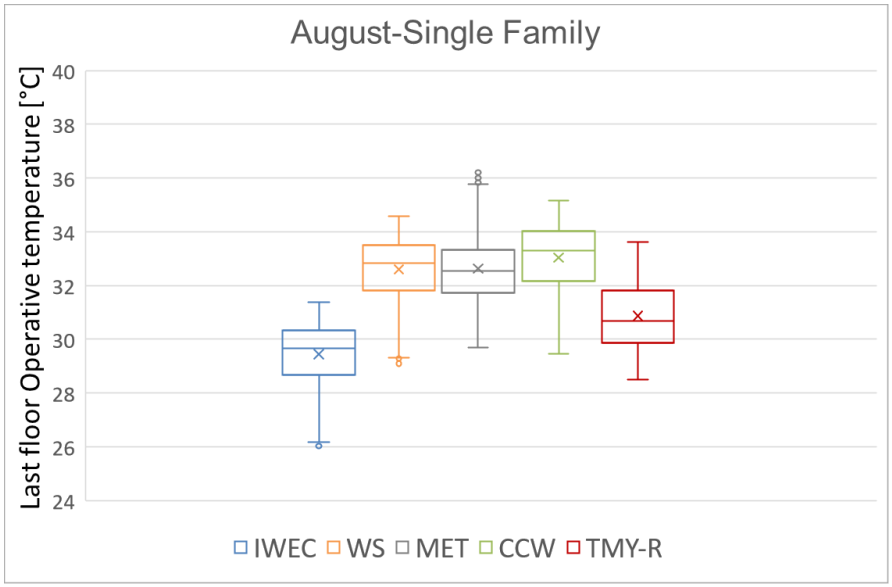


Figure 17: Boxplot of last floor operative temperature of the single-family house in August, for IWEC (Present), WeatherShift™ (WS), Meteonorm (MET), CCWorldWeatehr-Gen (CCW), and F-TMY. All future weather files are for 2050s considering RCP 8.5.

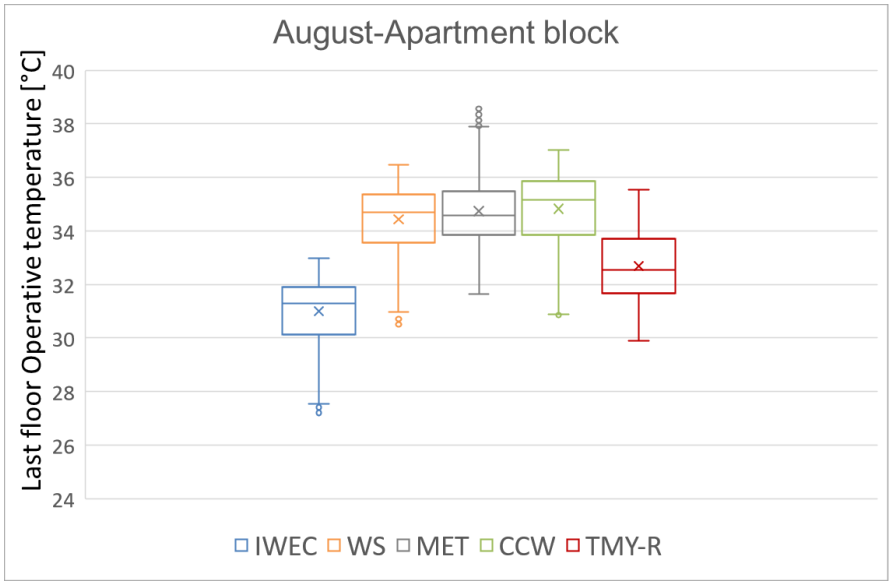


Figure 18: Boxplot of last floor operative temperature of the apartment block in August, for IWEC (Present), WeatherShift™ (WS), Meteonorm (MET), CCWorldWeatehr-Gen (CCW), and F-TMY. All future weather files are for 2050s considering RCP 8.5.

In addition, Table 3 also summarizes the values of the electrical energy demand per unit of area ($E_{el}/A_{f,net}$). The $E_{el}/A_{f,net}$ increases in SFH and AB similarly for WS, MET, and CCW, while the absolute change is not significantly high. On the other hand, $E_{el}/A_{f,net}$ slightly decreases for F-TMY in both cases. The reason can be explained below: as mentioned before, a future value for the mean seasonal efficiency of the heating ($\eta_{H,g}$) and the cooling ($\eta_{C,g}$) generation subsystem was adopted to consider the increase of ambient temperature due to climate change. The mean seasonal efficiency increases for the heating and decreases for the cooling for all the future weather datasets. However, due to the lower discrepancy of the temperature values for F-TMY compared to other future weather datasets, the increase for $\eta_{H,g}$ in the dynamically downscaled model is more, while the decrease in the $\eta_{C,g}$ is less. Consequently, according to Equation (4), the reduction in the energy for winter conditioning outweighs the cooling demand in the case of F-TMY. Finally, if the variation of $E_{el}/A_{f,net}$ for SFH and AB are compared, the absolute changes are lower for SFH, which comes from its higher S/V value that skews the energy usage of it more toward the heating regime.

Table 3: Electrical energy demand per unit of area and hours of exceedance for a single-family house (SFH) and apartment block (AB), for IWEC (Present), WeatherShift™ (WS), Meteonorm (MET), CCWorldWeatehr-Gen (CCW), and F-TMY. All future weather files are for 2050

| | | **IWEC** | **WS** | | **MET** | | **CCW** | | **TMY-R** | |
|---|---|---|---|---|---|---|---|---|---|---|
| | | | | *Absolute change* | | *Absolute change* | | *Absolute change* | | *Absolute change* |
| **SFH** | $E_{el}/A_{f,net}$ [kWh /m²] | 38.7 | 40.7 | *2* | 41.5 | *2.8* | 40.5 | *1.8* | 29.8 | *-8.9* |
| | *HE*[h] | 222 | 887 | *665* | 877 | *655* | 910 | *688* | 638 | *416* |
| **AB** | $E_{el}/A_{f,net}$ [kWh /m²] | 22.9 | 29 | *6.1* | 29.5 | *6.6* | 28.1 | *5.2* | 19.4 | *-3.5* |
| | *HE*[h] | 1273 | 1995 | *722* | 2060 | *787* | 1984 | *711* | 1596 | *323* |

Statistical and dynamical are the two main approaches to downscale global climate models for creating weather datasets to be used in building energy simulations. Considering there are different methodologies that use these approaches, evaluating their suitability and robustness is vital. This chapter set out to compare WeatherShift$^{TM}$, Meteonorm, and CCWorldWeatherGen—which are common weather generator tools applying statistical downscaling—in addition to a TMY created using a high-quality regional climate models database (from Euro-CORDEX) that applies the dynamical downscaling. All future weather files are for the 2050s considering RCP 8.5. Two representative buildings of the Italian residential building stock, including a single-family house (SFH) and an apartment block (AB), were selected to perform the analysis.

The results of this investigation show that different statistically downscaled future weather datasets created by weather generators predict the future energy performance and comfort analysis of the buildings quite similarly compared to the dynamical one. This is demonstrated by almost the same values in the mean outdoor dry-bulb temperature, relative changes of thermal energy need for heating and cooling normalized by the conditioned floor area, mean value of thermal energy load for heating and cooling, the hours of discomfort, and the absolute changes in the electrical energy demand per unit of area. However, when it comes to the dynamically downscaled weather data, the above-mentioned parameters follow a different pattern. According to the boxplots, these parameters show less dispersion and fewer outliers for dynamically downscaled weather data. Consequently, it was verified that dynamical downscaling, by better representing the spatial and temporal variability of local climate, provides physically consistent datasets.

The other significant result of this study is reached by comparing different building types. In more detail, the observed discrepancy between the future predictions of statistical and dynamical downscaling is affected not only by using different approaches for creating future weather datasets but also by building type. As an example, the thermal energy need for cooling in SFH for statistically downscaled datasets increases by around 170 %, and for the dynamical one, it increases by around 70%. On the other hand, in AB, this parameter increases 100 % for statistically downscaled data and around 40 % for the dynamical one. This inequality in relative variation comes from the different magnitudes of the present energy need for different building types. For buildings with a higher shape factor

(SFH), the heating energy demand dominates the cooling energy demand, which also makes them more sensitive to climate change.

Overall, this chapter has provided a deeper insight into analysing the effect of climate change on the future energy performance of buildings by considering different future weather datasets and building types. Firstly, it was shown that the climate change impact magnitude is not equal for different case studies so that in a changing climate, performing a regional and localized analysis becomes vital. In addition, the results demonstrated that the morphing method—regardless of its way of application—can provide adequate information to perform comparative analysis on long-term changes in energy building performance. However, the existing inconsistency within this method may lead to high prediction errors. In this case, the dynamical downscaling method is found to be more reliable when the aim is to develop, assess, and communicate resilient solutions to withstand as well as prevent the future impacts of climate change on building energy performance. Further studies are suggested to be carried out to consider model uncertainties of RCMs by following an ensemble-based approach. In addition, it is important to bear in mind that RCMs have been run not only for the future but also for the historical period. So, they can be compared with the real data, and the biases associated with the climate model data can be adjusted to reduce uncertainties and increase their physical consistency. This possibility does not exist for statistical downscaling method tools, as they are based on transforming the actual real data; it is possible to say they are often “black-box” tools.

## 3.4 Bias Adjustment

Making decisions and planning adaptation scenarios to enhance climate change resilience requires precise future climate projections, which rely on the accuracy of our global and regional climate models. Climate models -despite ongoing advancements- are subjected to systemic errors and biases. In this study, particularly for analysing the resilience of cooling technologies in chapter 5, the chosen GCM-RCM climate model combination ((MPI-M) MPI-ESM-LR/REMO ) has been bias adjusted. Quantile delta mapping (QDM) and Multivariate Bias Correction with N-dimensional Probability Density Function Transform (MBCn) are used to bias-correct climatic variables. QDM is a univariate bias correction algorithm that explicitly preserves climate models’ relative changes in simulated precipitation quantiles based on the quantile delta change/ perturbation and

detrended quantile mapping methods. Basically, these techniques are quantile mapping variations on the classic "delta change" on climate model projections models (Olsson et al., 2009). In this technique, for addressing systematic distributional biases in relation to observations in a historical baseline era, all projected future quantiles from a model are first detrended, and then quantile mapping is applied to the detrended series. The projected trends in the modelled quantiles are then reintroduced over the bias-corrected outputs following detrending and quantile mapping, ensuring that the bias correction had no impact on the underlying climate model's sensitivity to change (A. Cannon et al., 2015).

QDM, together with the majority of bias correction techniques used in climatology, are utilized in a univariate context. To consider how different climate variables might interact, Multivariate Bias Corrections (MBCn) using the N-dimensional Probability Density Function Transform method can be applied (A. J. Cannon, 2018). This method transfers all features of an observed continuous multivariate distribution to the matching multivariate distribution of variables from a climate model. In other words, for climate models, this method provides a multivariate generalization of quantile mapping in which the variable's quantile changes for the historical and projection periods are preserved.

The final result of this method is multivariate version of quantile mapping, which transfers the statistical properties of an observed continuous multivariate distribution to the equivalent multivariate distribution of simulated variables. According to Cannon et al. (2015), MBCn is not constrained to correcting a specific measure of joint dependence, such as Pearson or Spearman rank correlation, and it does not make strong stationarity assumptions about the temporal sequencing of climate models, in contrast to other multivariate bias correction algorithms, such as those by Bürger et al. (2011), Vrac and Friederichs (2015) Mehrotra and Sharma (2016), and Cannon (A. Cannon, 2016).

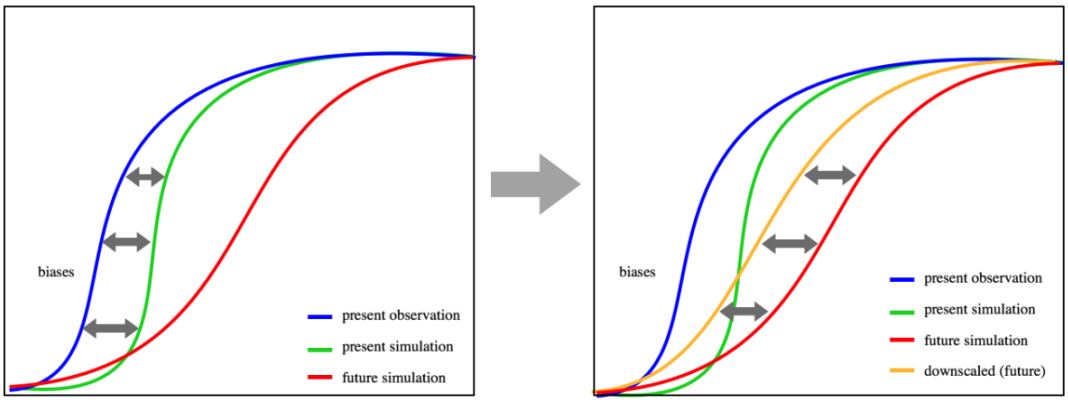


Figure 19: Representation of Statistical Downscaling using Quantile Mapping adopted from (Statistical Downscaling | Regional Climate Model Evaluation System-California Institute of Technology)

For applying the bias adjustment to the data, initially, the QDM approach is used to correct each of the climate variables. Then, using an iterative reshuffling procedure, the dependence structure of the climatic variables is adjusted. The climate data is rotated in all iterations by multiplying the data by random orthogonal matrices. Finally, using the inverse random matrices, the data are re-correlated. Except for global solar irradiation, the MBCn is used to bias-correct all variables of climate data. For global solar irradiation, QDM is applied. The reason is that the diurnal structure of global solar irradiation will break if MBCn is performed, and this is due to the reshuffling of marginally corrected global solar irradiation values in this method. As a result, this deficiency results in unrealistic values for either global or direct/diffused solar irradiation. Since it is aimed to keep the month-to-month variability of bias-corrected climate data, both calibrating the MBCn/QDM and predicting bias-corrected values are performed for each month of the year. For the calibration of bias-correction methods, all years for which observational data are available are taken into account.

### 3.4.1 Technical validation

Here, by comparing the observational data and the bias-corrected one over the period of validation, the bias correction is applied for the city of Rome. The relevant time period refers to the overlapping period of observational and contemporary one (2008-2017). In this way, for validation of the bias correction, the whole length of the available observational data is utilized. After being validated, it is seen that for both QDM and MBCn methods, the RCM simulations biases are significantly

reduced. These results are presented in table 4 and Figures 20 and 21. In table 4, for the observational and time-period, data referring to the mean climate statistics, raw RCM, and bias-corrected RCM are presented. The findings demonstrate a considerable bias in the projected temperature, solar irradiation, wind speed, and relative humidity from RCMs. This bias is diminished by the use of the bias-correction step. As it is clear from Figures 20 and 21, the bias correction not only minimizes bias throughout the average climate features but also effectively corrects bias entire distribution of climate variables. As can be observed, the bias-correction process properly modifies the PDFs of raw RCM to mimic the PDFs of observations. This underlines the efficiency of the bias-correction process in reproducing realistic estimates of a range of climate variables taken into account in this study, not only for temperature but also for more complex variables like wind speed.

Table 4: Mean temperature, solar irradiance, wind speed, and relative humidity in Rome over the validation time-period

| | | **Temperature** | | | **Solar irradiance** | | | **Wind speed** | | | **Relative humidity** | | |
|---|---|---|---|---|---|---|---|---|---|---|---|---|---|
| | | **°C** | | | **W/m²** | | | **m/s** | | | **%** | | |
| **CZ** | **City** | *OBS* | *RCM (raw)* | *RCM (bc)* | *OBS* | *RCM (raw)* | *RCM (bc)* | *OBS* | *RCM (raw)* | *RCM (bc)* | *OBS* | *RCM (raw)* | *RCM (bc)* |
| **3A** | Rome | 16.3 | 16.5 | 16.3 | 187.8 | 161.8 | 187.8 | 3.6 | 2.7 | 3.6 | 72.5 | 70.7 | 72.5 |

Table 5 shows values of mean temperatures, solar radiation, wind speed, and relative humidity for the city of Rome over the 20-year datasets of the 2010s, 2050s, and 2090s and three typical meteorological years (TMY) generated from them after bias adjustment. An increase in the temperature is revealed by comparing the contemporary period (2010s) with the two future periods (2050s and 2090s). On the other hand, global solar irradiation shows a decrease which can be the consequence of two factors: first, higher reflectance of solar radiation from increasing aerosol concentrations and sometimes increasing cloudiness, and second, increases in the

annual number of precipitation/rain events. In general, the projected changes in climate variables in the future TMYs are consistent with those resulting from the comparison of the 20-year datasets. This means that the statistically based TMYs are indeed representative of the climate projections over a significant period of time (i.e., 20 years). Therefore, they are suitable for assessing the impact of climate change on building energy loads.

Table 5: Mean temperatures, solar irradiance, wind speed, and relative humidity in Rome over 2010s, 2050s, and 2090s time periods obtained from multi-year bias-corrected RCM data and in the three TMYs weather files created from them.

| | **Temperature** | | | **Solar irradiance** | | | **Wind speed** | | | **Relative humidity** | | |
|---|---|---|---|---|---|---|---|---|---|---|---|---|
| | **°C** | | | **W/m²** | | | **m/s** | | | **%** | | |
| | *2010s* | *2050s* | *2090s* | *2010s* | *2050s* | *2090s* | *2010s* | *2050s* | *2090s* | *2010s* | *2050s* | *2090s* |
| **20-year data** | 16.0 | 16.9 | 19.5 | 187.6 | 185.7 | 183.7 | 3.6 | 3.5 | 3.4 | 72.1 | 75.0 | 71.4 |
| **TMY** | 16.2 | 17.0 | 19.5 | 189.4 | 187.6 | 182.2 | 3.6 | 3.4 | 3.2 | 71.8 | 73.5 | 71.6 |

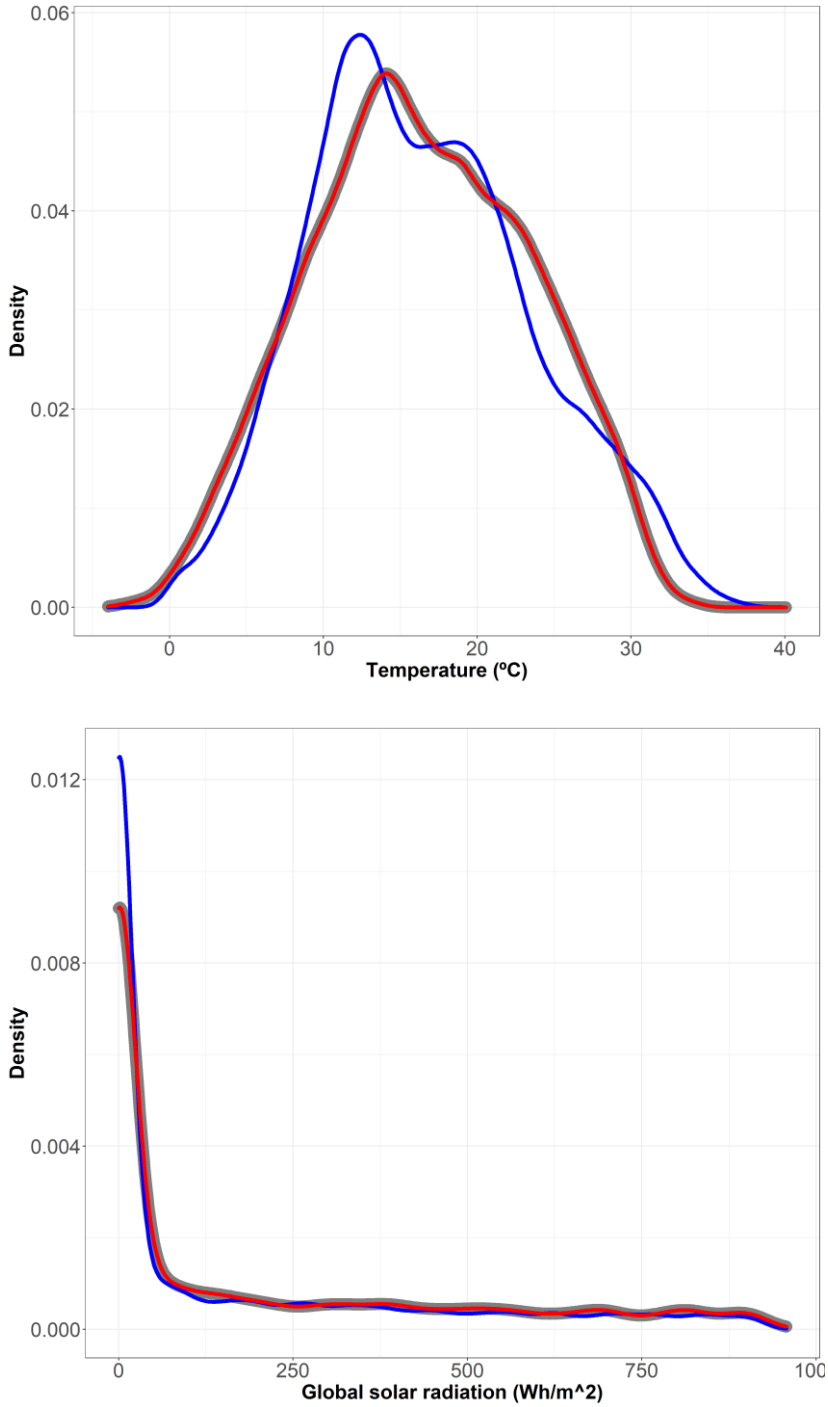


Figure 20: Probability density functions of temperature and solar irradiation at Rome from observations (grey), raw RCM (blue), and bias-corrected RCM (red) datasets over the validation period

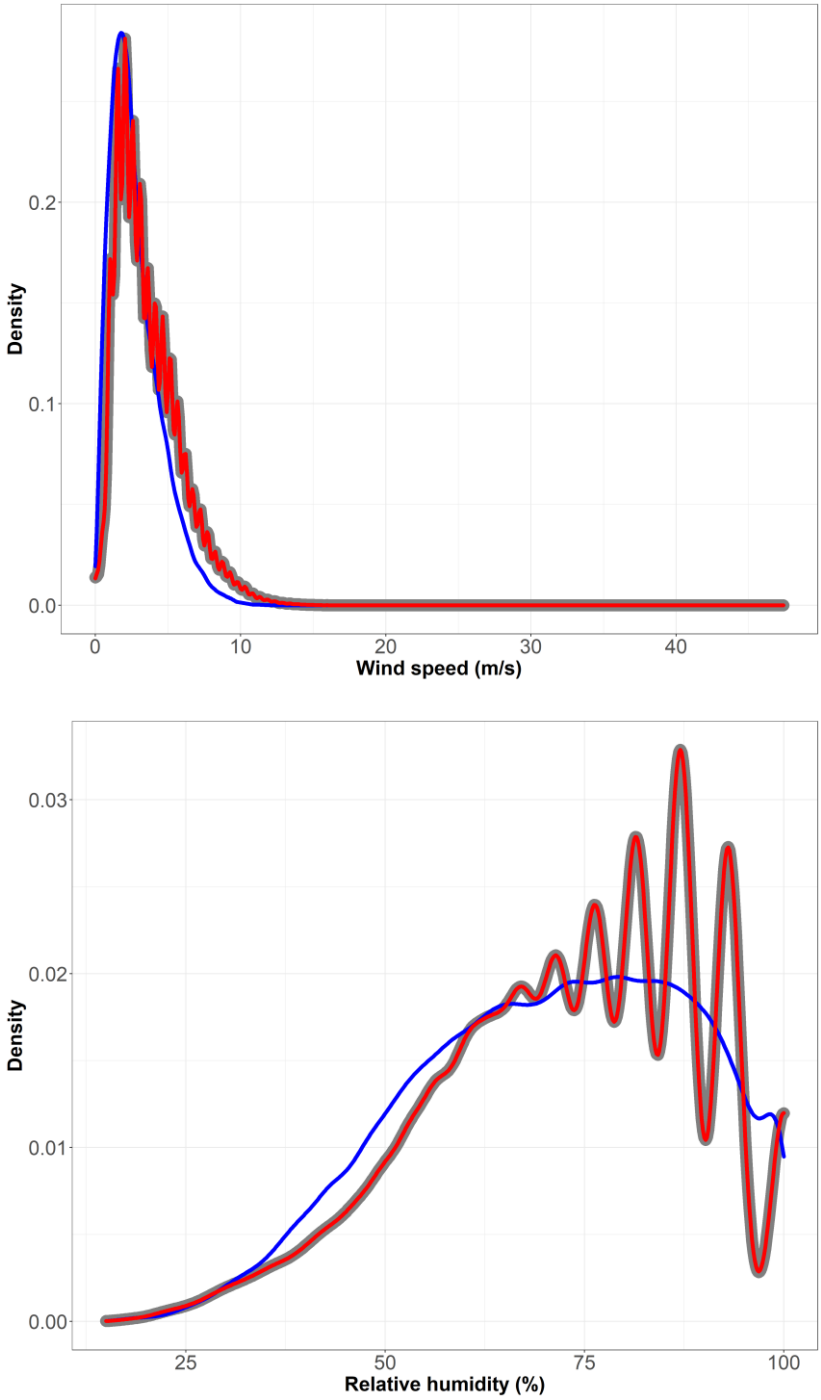


Figure 21: Probability density functions of wind speed and relative humidity at Rome from observations (grey), raw RCM (blue), and bias-corrected RCM (red) datasets over the validation period

# 4. Effect of climate change on the built environment

## 4.1 Analysis of Italian residential building stock

As a first step, to draw a clearer picture and to form a general overview of the future performance of Italian residential buildings, it is decided to perform a preliminary comparative analysis using the Morphing method. As discussed in section 3.3.3, this method can offer sufficient data to do a comparative analysis of long-term changes in energy-building performance. This part of the study uses the WeatherShift ™ tool to carry out analysis of Italian building stock for Milan. This city is chosen in this step, as it is one of the representative cities of the Italian middle climatic zone ($2100 < HDD \leq 3000$), which includes 4250 Italian municipalities on a total amount of 8100 (Italian Republic, Interministerial Decree of June 26th, 2015).

Herein four weather data sets were generated: referring to a near-term period (NT) from 2026 till 2045 and a long-term period (LT) from 2080 till 2099, considering RCP 4.5 and RCP 8.5 and the median (50 %) warming percentile. The Milan International Weather for Energy Calculation (IWEC) was used as the base scenario (Huang et al., 2014). In Table 6, the annual average of climate variables (dry bulb temperature, $T$, solar irradiance on horizontal plane, $SI_{hor}$, and relative humidity, $RH$) for four developed future weather data are presented. As shown, the dry bulb temperature is more likely to change compared with other variables, and LT-RCP 8.5 scenario is associated with the most significant variation. It is important to indicate that wind speed has not been morphed by the WeatherShift™ tool.

Table 6: Annual average value of Milan climate variables for different scenarios

| | Base | NT-RCP 4.5 | | NT-RCP 8.5 | | LT-RCP 4.5 | | LT-RCP 8.5 | |
|---|---|---|---|---|---|---|---|---|---|
| | | | Relative change | | Relative change | | Relative change | | Relative change |
| $T$ [°C] | 11.8 | 13.3 | 12.7 % | 13.7 | 16.1% | 14.3 | 21.2% | 16.6 | 40.7% |
| $SI_{hor}$ [W m$^{-2}$] | 147 | 154 | 4.7% | 156 | 5.6% | 155 | 5.6% | 171 | 16% |
| $RH$ [%] | 75 | 73.1 | −2.5% | 73.1 | −2.5% | 72.8 | −2.9% | 70.8 | −5.6% |

Subsequently, Heating Degree Days (HDD) and Cooling Degree Days (CDD) have been calculated for different scenarios. HDD and CDD reflect the heating and cooling energy demand for a building. In this calculation, base 18 °C heating and cooling degree days have been considered (ASHRAE, 2017). Figure 22 presents the monthly HDDs and CDDs for Milan base and future scenarios. It can be seen that HDDs increase, CDDs decrease, while changes in CDDs are more severe. However, degree days give a primary insight into changes in BEP, and for more deep analysis, BEP simulations must be run.

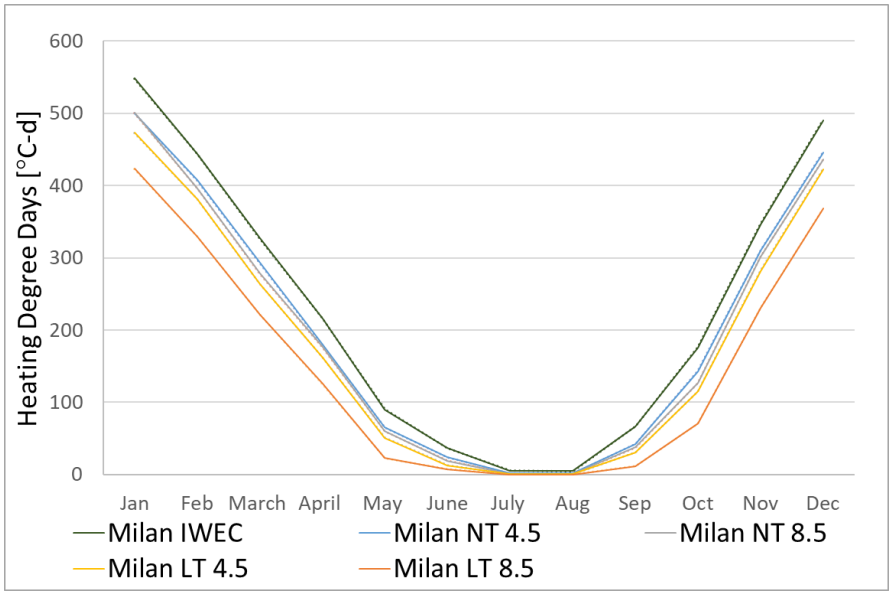


(a)

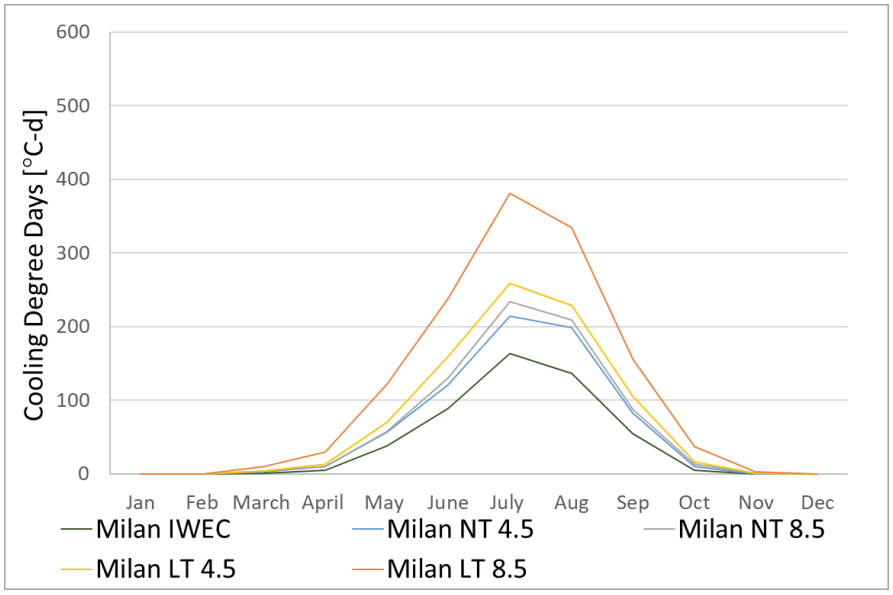


(b)

Figure 22: Monthly heating (a) and cooling (b) degree days for Milan under different scenarios.

For the purpose of analysing the future performance of Italian residential building stock, all the building types described in section 2.2 have been selected and simulated in the present chapter: single-family house (SFH), multi-family house (MFH), and apartment block (AB), all belonging to the climatic zone of Milan (zone E, 2100 < HDD ≤ 3000).

To assess the impact of climate changes in case of refurbished buildings, an insulated fabric of the existing buildings has been assumed. The insulation level of the envelope components was set to match the *U*-values of the reference building currently adopted to verify compliance with the nearly zero-energy building (NZEB) requirements in Italy. For each envelope component, in accordance with the Italian Interministerial Decree of June 26th, 2015 (Italian Republic, Interministerial Decree of June 26th, 2015), the *U*-values of the reference building are listed in Table 7 for the climatic zone of Milan. Whereas the replacement of the existing windows has been assumed, no modification of the solar shading devices has been considered because of the high performance of the wooden Venetian blind and the new window ($g_{gl+sh}$ = 0.12).

Table 7: Thermal transmittance values of the building envelope components assumed for the refurbished buildings in Milan (Italian Republic, Interministerial Decree of June 26th, 2015)

| **Building envelope component** | ***U*-value [W·m$^{-2}$K$^{-1}$]** |
|---|---|
| External wall | 0.26 |
| Upper floor (roof) | 0.22 |
| Bottom floor | 0.26 |
| Windows | 1.40 |

Since the energy efficiency increase due to the refurbishment actions that would occur in the future might differ from that hypothesized in the present work, the assumption to adopt the current reference *U*-values of the Italian NZEB can be considered a reasonable starting point to carry out the analysis.

The simulation engine, user behaviour, profiles of internal gains, and the operation of blinds are the same as explained in section 2.2. The heating period was set between October 15$^{th}$ till April 15$^{th}$ as indicated in UNI/TS 11300-1 for climatic zone E and fixed by the Italian energy regulations. The cooling mode is assumed to be available from April 16$^{th}$ till October 14$^{th}$ since the results show the cooling system is only active in the months of June, July, and August.

### 4.1.1 Energy performance assessment

The investigation of the climate change effect on building performance in the future is done based on the comparison of different indexes. The BEP was evaluated for all the scenarios by comparing the annual net energy need for space heating and space cooling of the building normalized by the net conditioned floor area ($EP_{H,nd}$ and $EP_{C,nd}$). Besides, the global/overall energy performance ($EP_{gl}$), expressed as the ratio of the annual non-renewable primary energy for space heating and space cooling to the net conditioned floor area, was calculated and analysed for different scenarios according to equation 9. The Italian most common technical building system technologies are considered in this study: centralized gas standard boilers for heat generation, and radiators as heat emitters, while space cooling is provided by individual direct expansion air conditioners (split systems).

$$EP_{gl} = \frac{EP_{H,nd} \cdot f_{P,nren,gas}}{\eta_{H,u} \cdot \eta_{H,g}} + \frac{EP_{C,nd} \cdot f_{P,nren,el}}{\eta_{C,u} \cdot \eta_{C,g}} \quad (9)$$

where, $EP_{H/C,nd}$ is the annual energy need for space heating/cooling, $f_{P,nren,gas/el}$ is the non-renewable primary energy conversion factor for natural gas (1.05) and electricity (1.95) respectively, $\eta_{H/C,u}$ is the mean seasonal efficiency of the heating/cooling utilization (including emission, control, and distribution) subsystems, which is equal to 0.81 for heating and 0.83 for cooling, and $\eta_{H/C,g}$ is the mean seasonal efficiency of the heating and the cooling generation subsystem. The reference mean seasonal efficiency values of the thermal subsystems were assumed in compliance with the Italian Interministerial Decree of June 26$^{th}$, 2015 (Italian Republic, Interministerial Decree of June 26th, 2015). The mean seasonal

efficiency of the heating generation was considered equal to the reference value (0.95), while the current mean seasonal efficiency of the cooling generation subsystem was assumed equal to the reference value of 2.5. As regards the future mean seasonal efficiency ratio of the cooling generation subsystem, it was obtained by assuming proportionality between the efficiency energy ratio (*EER*) of the chiller and its maximum theoretical efficiency ($EER_{\mathrm{Carnot}}$) over different temperatures, according to EN 16798-13 (CEN. EN 16798-13, 2017). The future seasonal mean seasonal efficiency ratio of the cooling generation subsystem is calculated as follows:

$$\eta_{\mathrm{C,g,future}} = \eta_{\mathrm{C,g,ref}} \cdot \frac{\sum_{\substack{\text{current}\\ \text{cooling}\\ \text{season}}} \left( \Phi_{\mathrm{C},j} \frac{T_{\mathrm{cond,in},j} - T_{\mathrm{evap,out}}}{T_{\mathrm{evap,out}}} \right)}{\sum_{\substack{\text{current}\\ \text{cooling}\\ \text{season}}} \Phi_{\mathrm{C},j}} \cdot \frac{\sum_{\substack{\text{future}\\ \text{cooling}\\ \text{season}}} \Phi_{\mathrm{C},j}}{\sum_{\substack{\text{future}\\ \text{cooling}\\ \text{season}}} \left( \Phi_{\mathrm{C},j} \frac{T_{\mathrm{cond,in},j} - T_{\mathrm{evap,out}}}{T_{\mathrm{evap,out}}} \right)} \quad (10)$$

where $\eta_{\mathrm{C,g,ref}}$, is the reference value of the cooling generation subsystem efficiency (equal to 2.5), $\Phi_{\mathrm{C},j}$ is the hourly thermal energy load for cooling at time *j*, $T_{\mathrm{evap,out}}$ is the evaporator air outlet temperature (equal to 280 K), and $T_{\mathrm{cond,in},j}$ is the condenser air inlet temperature at time *j*.

### 4.1.2 Thermal comfort assessment

For analysing the thermal comfort and overheating risk, the adaptive comfort model of EN 16798-1:2019, was implemented in free-floating condition. The main driving force behind the adaptive approach is the pattern of outside weather conditions and exposure to them. This allows the prediction of likely comfort temperatures or ranges of comfort temperature, from the outdoor running mean temperature, to capture the occupant's thermal sensation in a situation where they can be in comfort by taking adaptive adjustments (Italian National Annex of the EN 16798-1 technical standard). In this model, the optimal operative temperature ($\theta_{\mathrm{o,c}}$, in ° C) is calculated as mentioned earlier in equation 7. For assessing whether the building is overheated or not, the hours of exceedance (*HE*) indicator was calculated. *HE* is equal to the number of hours during the cooling period in which the operative temperature of the zone is greater than the upper limit temperature.

### 4.1.3 Results and discussion

The results obtained from the simulations of the selected building types are shown in Figures 23 to 31 and in Tables 7 and 8.

Figures 23 a to 25 a, which refer to the buildings before refurbishment, indicate that the thermal energy need for heating ($EP_{H,nd}$) decreases up to 29 % for SFH and up to 31% for MFH and AB. On the opposite, when the thermal energy need for cooling ($EP_{C,nd}$) is compared to the base scenario, increases up to 255 % for SFH, 180% for MFH, and 174% for AB, are obtained. As regards the refurbished buildings, which are represented through Figures 23 b to 25 b, the thermal energy need for heating ($EP_{H,nd}$) decreases up to 36 % for SFH and up to 38 % for MFH and AB. On the contrary, the thermal energy need for cooling ($EP_{C,nd}$) increases till 117% for SFH, 101% for MFH, and 111% for AB. The comparison between the thermal energy needs for heating and cooling before and after refurbishment shows that the relative variations of $EP_{H,nd}$ due to climate change increase after refurbishment for the same building while changes of $EP_{C,nd}$ decrease. This is due to the positive effect of the insulation when a cooling system is considered.

In addition, the thermal energy need for cooling in SFH − especially before refurbishment of the building − is found to be more sensitive to climate change. This result is due to the fact that SFH has a higher shape factor in comparison with MFH and AB, which means it has a larger surface area in proportion to its volume and will be more sensitive to the warming weather. It is also important to indicate that relative changes in cooling demand for either existing or refurbished buildings in all case studies are more dramatic in comparison with variation in their heating demand, and this can be associated with their lower cooling energy use in the present days.

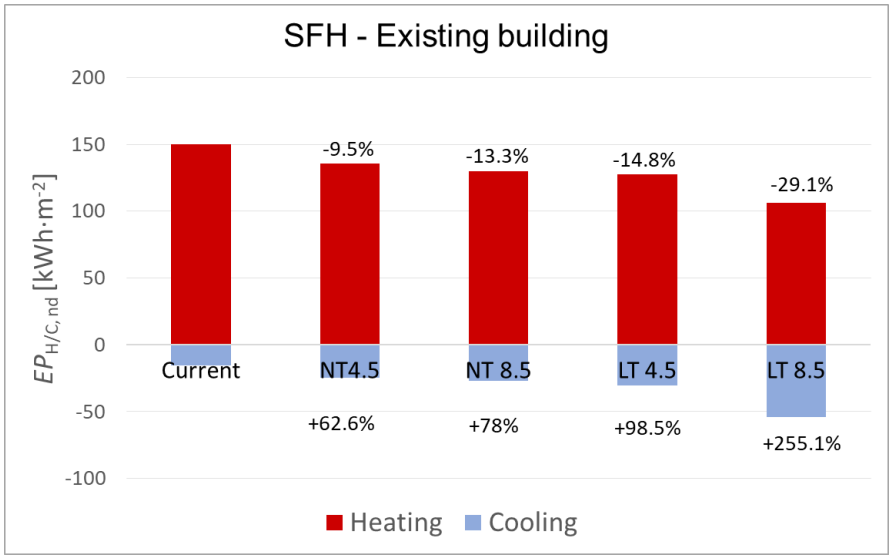


(a)

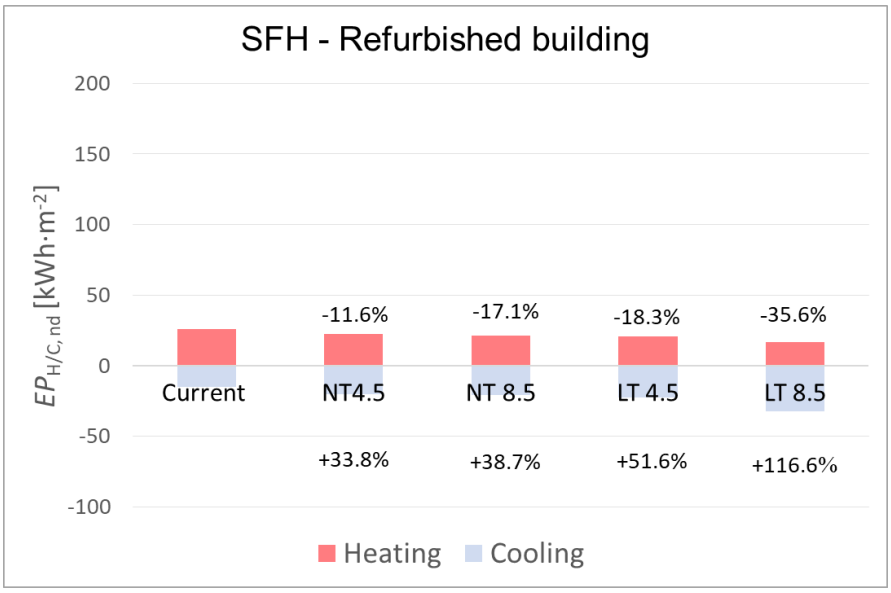


(b)

Figure 23: Thermal energy need for heating and cooling normalized by the conditioned floor area for single-family house (SFH) existing building (a) and after refurbishment (b) under different future scenarios in Milan.

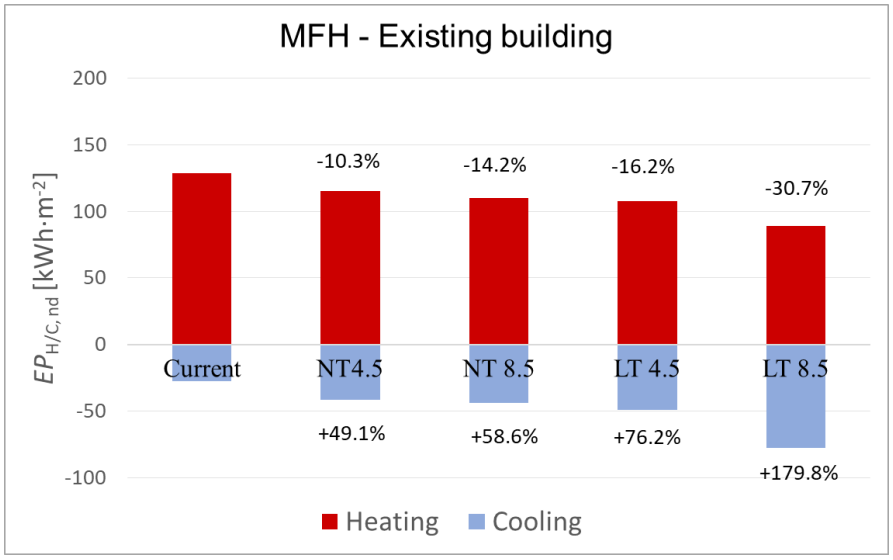


(a)

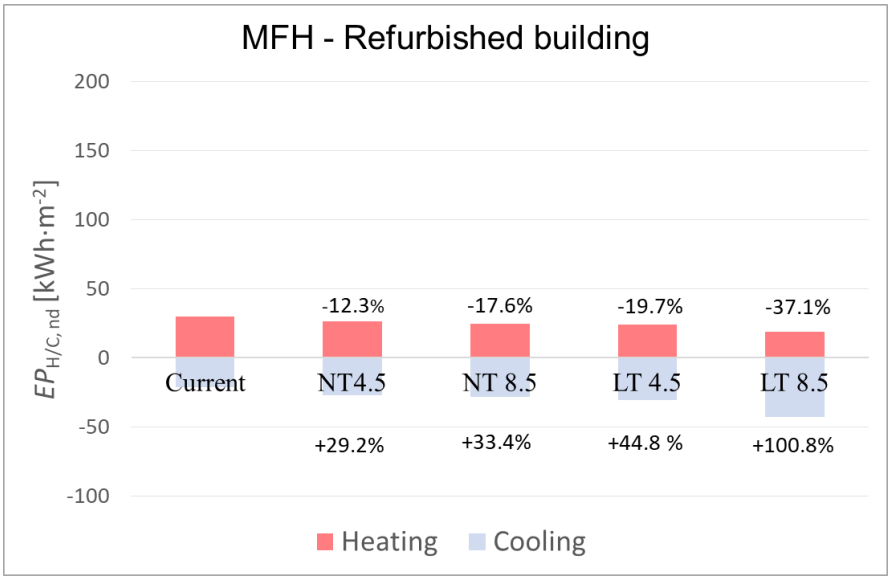


(b)

Figure 24: Thermal energy need for heating and cooling normalized by the conditioned floor area for multi-family house (MFH) existing building (a) and after refurbishment (b) under different future scenarios in Milan

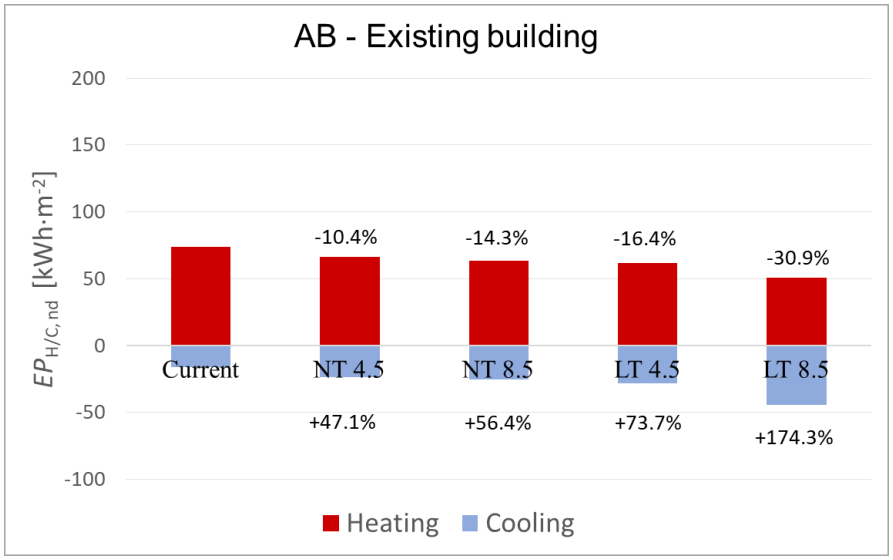


(a)

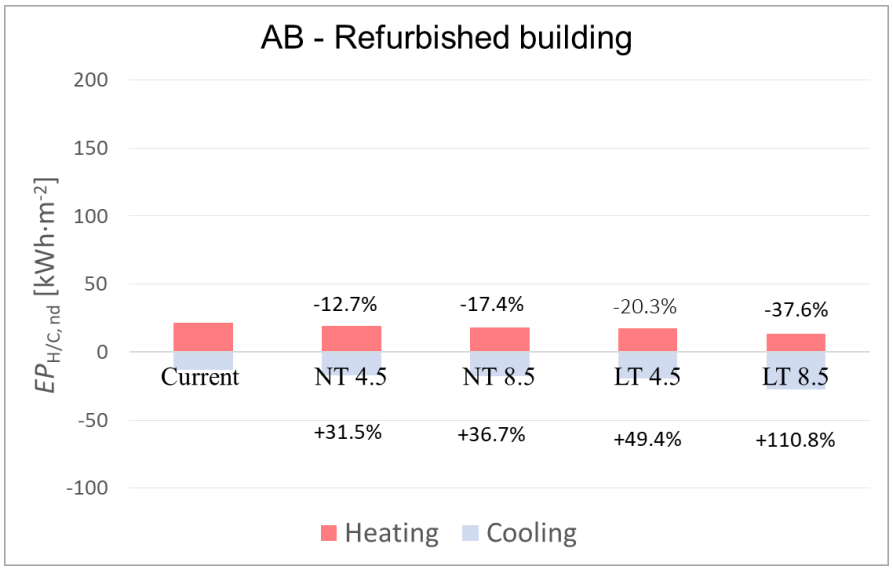


(b)

Figure 25: Thermal energy need for heating and cooling normalized by the conditioned floor area for apartment block (AB) existing building (a) and after refurbishment (b) under different future scenarios in Milan

Figures 26 to 28 present the breakdown of the adaptive comfort analysis. The graphs show the distribution of hours of the cooling period (April 16$^{th}$ till October 14$^{th}$ - 4368 hours) in three ranges: Comfort, warm discomfort, and cold discomfort. Figures 26 a to 28 a refer to the buildings before refurbishment, and Figures 26 b to 28 b represent buildings after refurbishment. Results report that for all analysed cases before refurbishment, occupants will experience overheating up to 50 % of the time by the mid-century (NT) and up to 80% of the time by the end of the century (LT). The overheating hours after refurbishment for the same building types reach 79 % of the time by the mid-century (NT) and 92 % of the time by the end of the century (LT). It is apparent that for all the scenarios and case studies, the period of warm discomfort increases due to climate change. This issue is more significant for buildings after refurbishment due to the negative effect of insulation that causes heat trap in the buildings in a free-floating regime. It is important to note these results do not take into account the effect of ventilative cooling because the standard ventilation flow rate is considered (0.30 $h^{-1}$). This trend can also be revealed in Figures 29 to 31, which present the hourly operative temperature on the upper floor of the analysed buildings in free-floating condition for the second week of May under different future scenarios. By comparing the hourly temperature profile after refurbishment (Figures 29 b to 31b) and existing buildings (Figures 29 a to 31a), although the changes in temperature are steadier after refurbishment, its average value is higher. In addition, MFH and AB are found to be more sensitive to overheating risk, and the reason is that MFH and AB buildings have larger windows in comparison to SFH, as their *WWR* is higher (see also Table 2). Likewise, this issue can be seen in the hourly temperature profiles (Figures 29 to 31). As an example, for the worst-case scenario (LT 8.5) after refurbishment, temperatures of the upper floor reach up to 31 °C for MFH and AB while they reach up to 29 °C for SFH. Besides, hours of exceedance (*HE*) for all the scenarios are presented in Tables 7 and 8. It can be seen that although *HE* increases after refurbishment, as mentioned earlier, the relative change in *HE* due to climate change for buildings will be less compared to buildings before refurbishment.

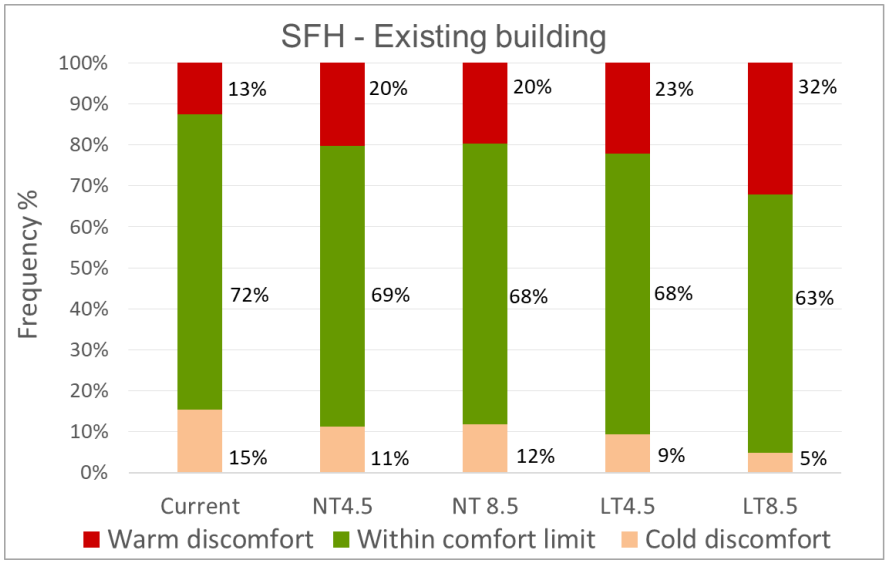


(a)

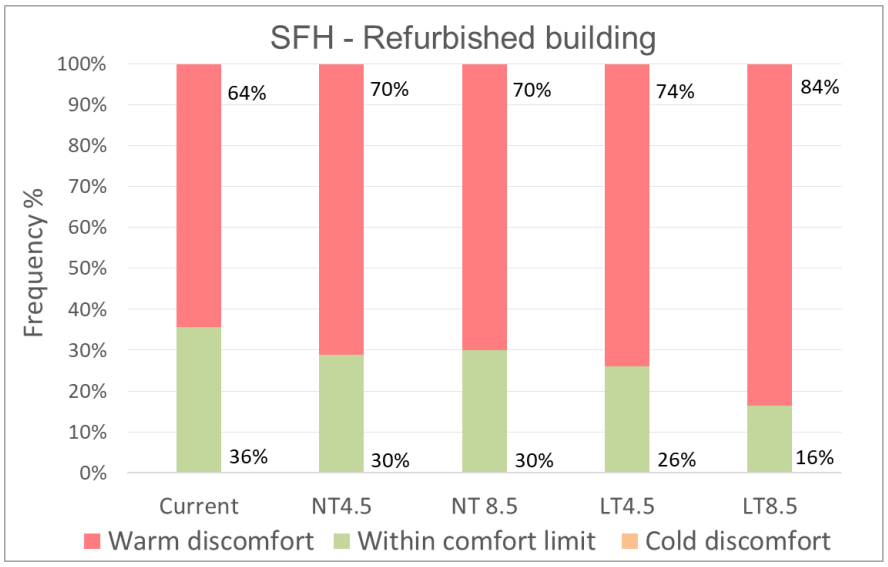


(b)

Figure 26 : Adaptive comfort analysis for single-family house (SFH) existing building (a) and after refurbishment (b) under different future scenarios in Milan

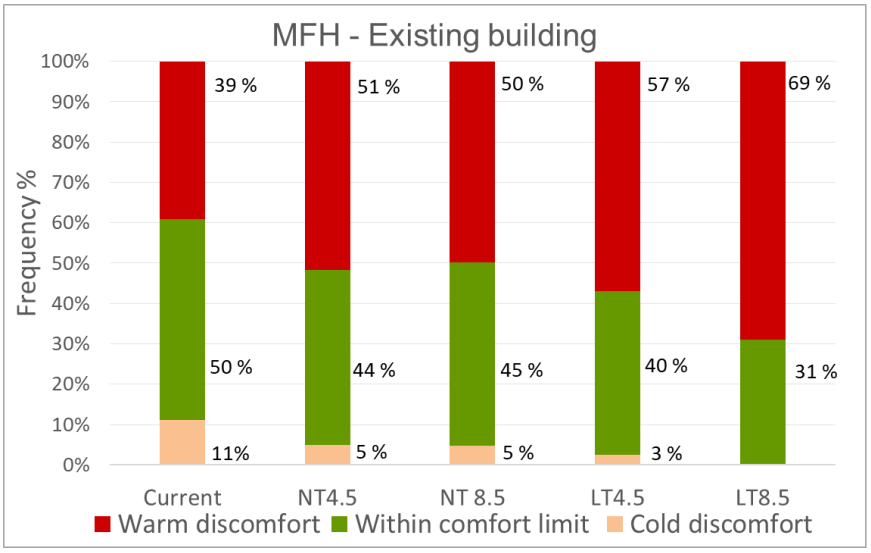


(a)

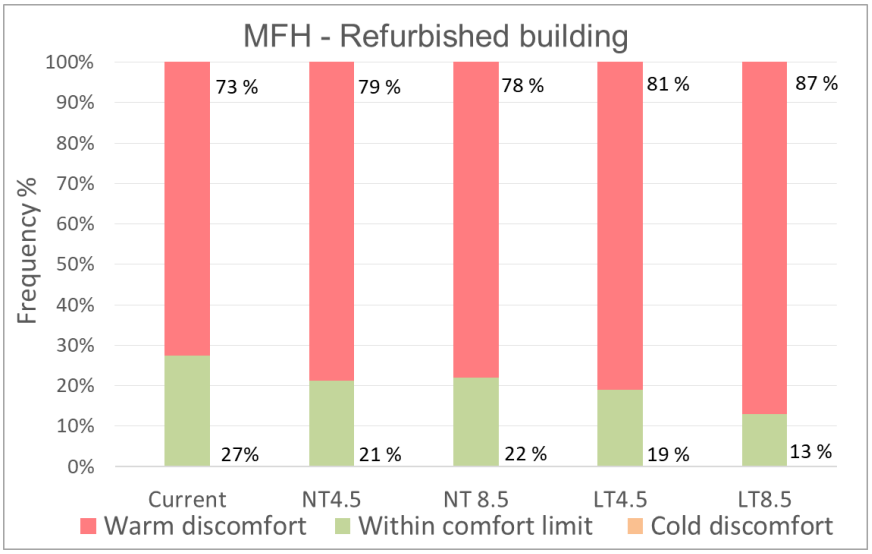


(b)

Figure 27: Adaptive comfort analysis for multi-family house (MFH) existing building (a) and after refurbishment (b) under different future scenarios in Milan

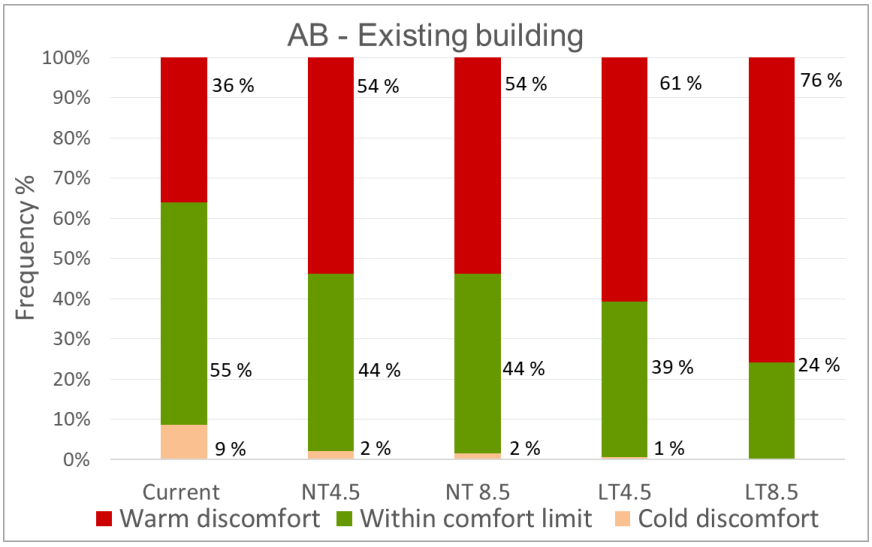


(a)

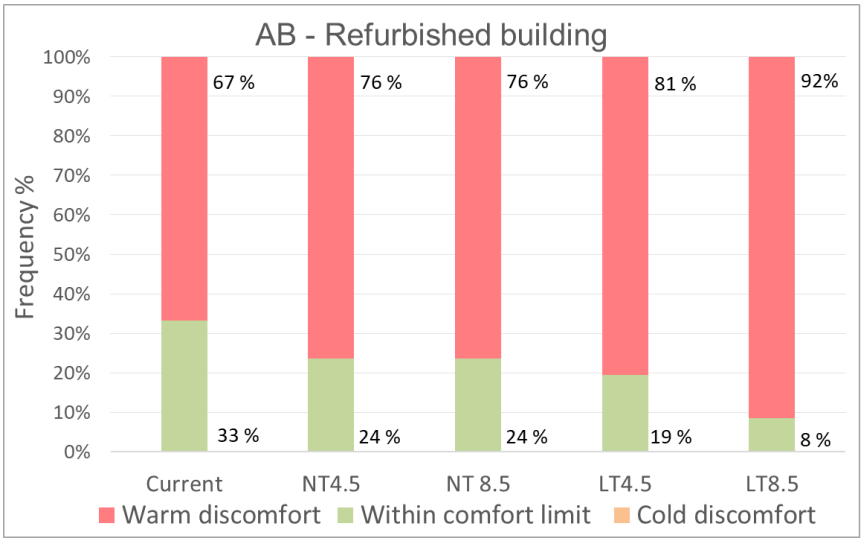


(b)

Figure 28: Adaptive comfort analysis for apartment block (AB) existing building (a) and after refurbishment (b) under different future scenarios in Milan

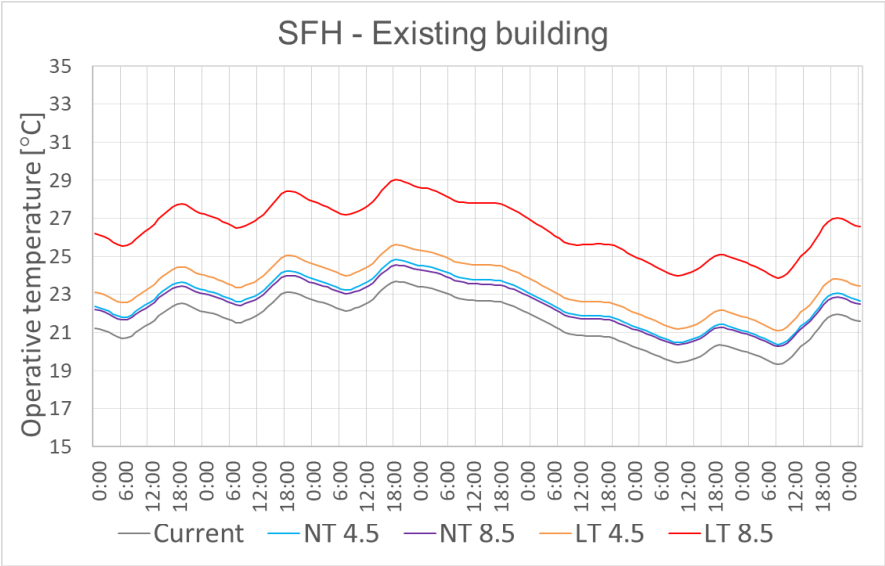


(a)

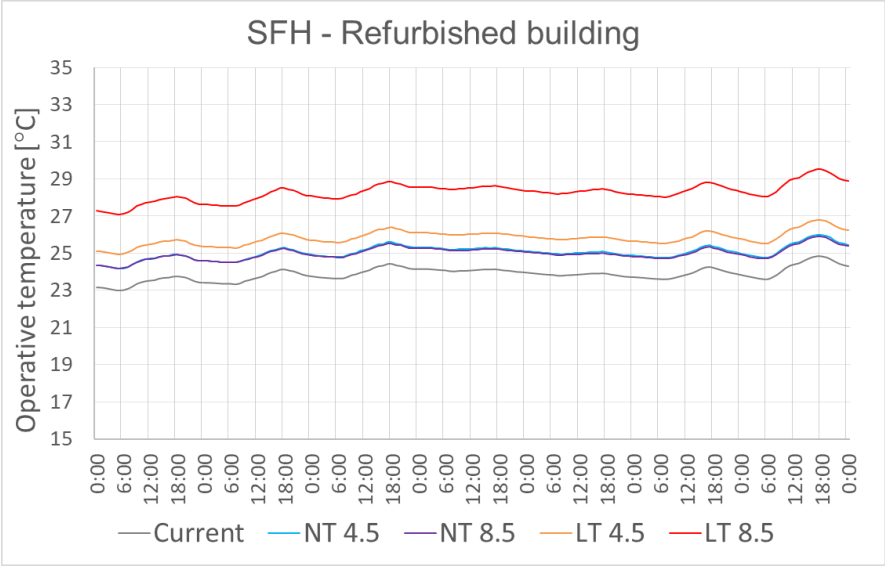


(b)

Figure 29: Hourly operative temperature in the upper floor of single-family house (SFH) existing building (a) and after refurbishment (b) for the second week of May under different future scenarios in Milan.

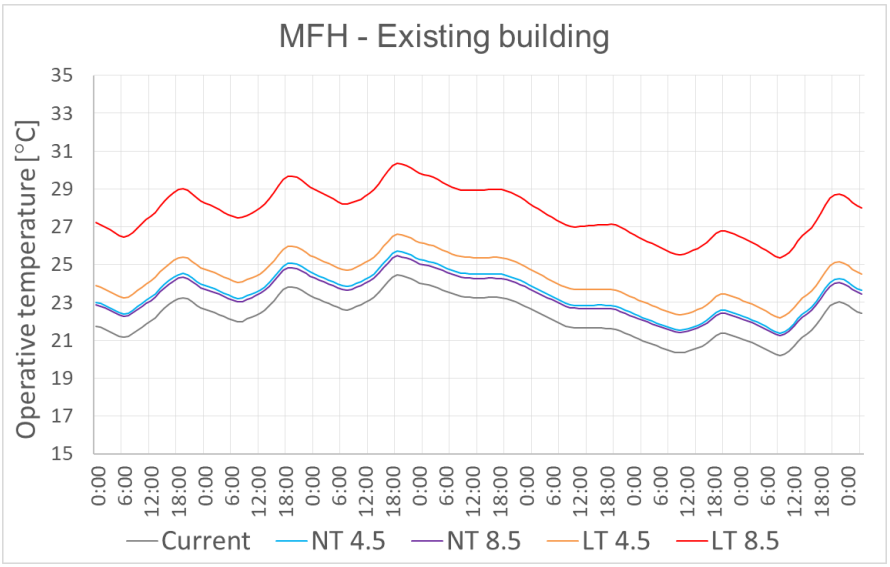


(a)

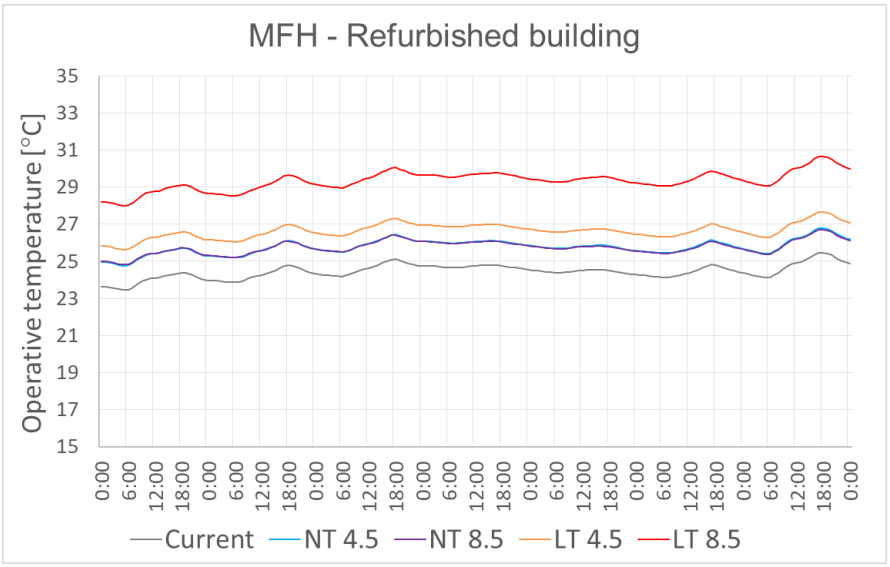


(b)

Figure 30: Hourly operative temperature in the upper floor of multi-family house (MFH) existing building (a) and after refurbishment (b) for the second week of May under different future scenarios in Milan.

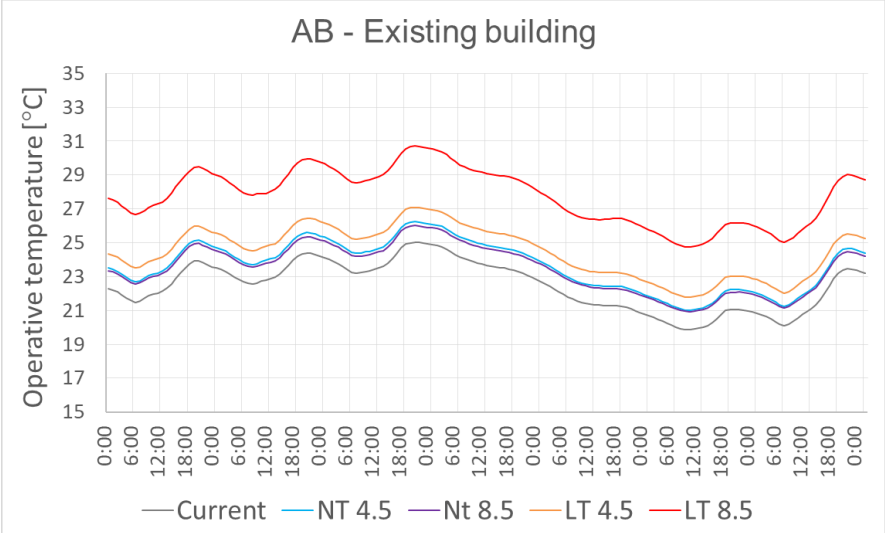


(a)

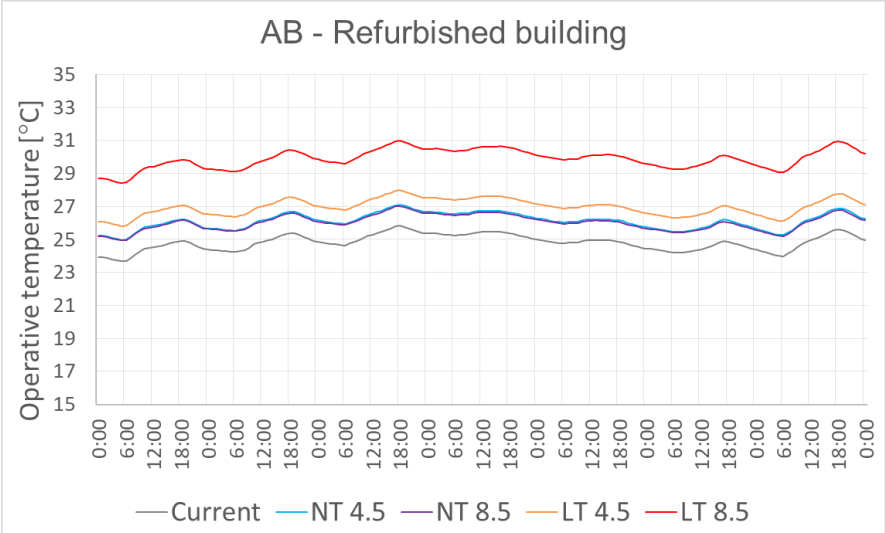


(b)

Figure 31: Hourly operative temperature in the upper floor of apartment block (AB) existing building (a) and after refurbishment (b) for the second week of May under different future scenarios in Milan.

Tables 8 and 9 also provide the results of the global/overall energy performance calculation. The analysis of this factor is crucial for the interpretation of the energy usage of case studies under the impact of global warming. Before the refurbishment, the $EP_{gl}$ increases for MFH and AB in all scenarios. However, the degree of change is not so significant, except for the pessimistic scenario (LT.8.5). This illustrates that the reduction in the energy for winter conditioning outweighs the cooling demand, which results in a slight alteration of the final total energy for the building.

The reason is that the analysis has been done for a city in the Italian middle climatic zone, having HDDs from 2100 to 3000, in which the energy usage of the building is more biased towards heating. Besides, it is also important to consider that electricity has a higher primary energy factor than natural gas. Nonetheless, the $EP_{gl}$ for SFH in all scenarios decreases except the LT.8.5. This is associated with the higher shape factor of SFH, which skews the energy usage of it more toward the heating regime. It results in a very limited decrease in the total primary energy.

After refurbishment, the $EP_{gl}$ increases for all the building types in all scenarios, and the degree of change is significant. Besides, the relative changes of $EP_{gl}$ for refurbished buildings are higher compared to existing buildings. As an example, in the pessimistic scenario (LT.8.5), the relative change of $EP_{gl}$ for SFH before refurbishment is equal to 9.1%, while after refurbishment, it reaches 70%. The reason is that the heating demand is not dominant anymore for any case study after the refurbishment. In other words, these results show that the effect of refurbishment on $EP_{gl}$ will reduce due to climate change. Even though the effect of the renovation is reduced by Climate Change, comparing the absolute values shows that there is still an improvement over the existing building.

Table 8: Global/overall energy performance and hours of exceedance for SFH, MFH, and AB, existing buildings under different scenarios in Milan.

| | | Base | NT-RCP 4.5 | | NT-RCP 8.5 | | LT-RCP 4.5 | | LT-RCP 8.5 | |
|---|---|---|---|---|---|---|---|---|---|---|
| | | | | Relative change | | Relative change | | Relative change | | Relative change |
| SFH | $EP_{gl}$ [kWh·m$^{-2}$] | 219 | 213 | *-2.5%* | 210 | *-3.9%* | 214 | *-2.4%* | 239 | *9.1%* |
| | *HE* [h] | 550 | 884 | *60.6%* | 884 | *60.6%* | 965 | *75.2%* | 1405 | *155.3%* |
| MFH | $EP_{gl}$ [kWh·m$^{-2}$] | 202 | 205 | *1.7%* | 204 | *1.4%* | 211 | *4.9%* | 258 | *28%* |
| | *HE* [h] | 1709 | 2228 | *30.4%* | 2184 | *27.8%* | 2490 | *45.7%* | 3014 | *76.4%* |
| AB | $EP_{gl}$ [kWh·m$^{-2}$] | 116 | 118 | *1.5%* | 117 | *1.2%* | 121 | *4.5%* | 147 | *26.9%* |
| | *HE* [h] | 1571 | 2346 | *49.3%* | 2346 | *49.3%* | 2650 | *68.7%* | 3315 | *111%* |

Table 9: Global/overall energy performance and hours of exceedance for SFH, MFH, and AB, after refurbishment under different scenarios in Milan.

| | | Base | NT-RCP 4.5 | | NT-RCP 8.5 | | LT-RCP 4.5 | | LT-RCP 8.5 | |
|---|---|---|---|---|---|---|---|---|---|---|
| | | | | Relative change | | Relative change | | Relative change | | Relative change |
| SFH | $EP_{gl}$ [kWh·m$^{-2}$] | 49.1 | 54.8 | *11.6%* | 55.5 | *13.1%* | 59.9 | *22%* | 83.6 | *70.2%* |
| | *HE* [h] | 2808 | 3057 | *8.8%* | 3057 | *8.8%* | 3232 | *15.1%* | 3652 | *30%* |
| MFH | $EP_{gl}$ [kWh·m$^{-2}$] | 60.9 | 68.8 | *13%* | 70.1 | *15.2%* | 75.7 | *24.3%* | 107.2 | *76.1%* |
| | *HE* [h] | 3172 | 3442 | *8.5%* | 3442 | *8.5%* | 3538 | *11.5%* | 3798 | *19.7%* |
| AB | $EP_{gl}$ [kWh·m$^{-2}$] | 42 | 46 | *9.6%* | 46.7 | *11.2%* | 49.8 | *18.6%* | 68.1 | *62.6%* |
| | *HE* [h] | 2917 | 3338 | *14.4%* | 3338 | *14.4%* | 3518 | *20.6%* | 3997 | *37%* |

Overall, comparing $EP_{H,nd}$, $EP_{C,nd}$, $EP_{gl}$, and *HE* of all building types for the near-term period scenarios presents a slight difference between RCP 4.5 and 8.5, while changes become more significant considering the long-term period. This finding represents that the effect of climate change on the Italian residential buildings from 2026 till 2045 does not alter a lot whether the $CO_2$ emission level stabilized or continues to grow. As an example, warm discomfort hours for all the case studies are almost the same in both NT scenarios and thermal energy need for cooling differs up to 2 kWh/m$^2$. Although climate change exacerbates the performance of

the buildings even in the NT period, the impact of reducing the emission levels will be significant for the long-term period assessment.

Finally, in order to generalize the results for different building types and insulation levels, a new parameter was introduced to express the outdoor temperature sensitivity of the building, expressed as the ratio of the overall transmission heat transfer coefficient ($H_{tr}$) to the gross conditioned volume ($V_{gr}$). $H_{tr}$ is calculated according to the EN ISO 13789 standard (CEN. EN ISO 13789, 2017), as in Equation (11):

$$H_{tr} = H_D + H_g + H_U + H_A = \sum_i b_i \cdot A_i \cdot U_i + \sum_k b_k \cdot l_k \cdot \psi_k \quad (11)$$

where, $H_D$ is the direct heat transfer coefficient between the heated or cooled space and the exterior through the building envelope, $H_g$ is the steady-state ground heat transfer coefficient, $H_U$ is the transmission heat transfer coefficient through unconditioned spaces, and $H_A$ is the transmission heat transfer coefficient to adjacent buildings. For each $i$-th component, $b_i$ is the adjustment factor for the temperature difference, $A_i$ is the area, and $U_i$ is the thermal transmittance. For each $k$-th linear thermal bridge, $b_k$ is the adjustment factor for the temperature difference, $l_k$ is the length of the linear thermal bridge, and $\psi_k$ is the linear thermal transmittance.

In Figure 32, the relation between $EP_{H,nd}$ , $EP_{C,nd}$, and $EP_{gl}$ versus $H_{tr}/V$ is presented. As can be seen from the trend lines, all three energy performance indicators increase when $H_{tr}/V$ grows. This trend is significantly slighter for $EP_{C,nd}$ as the refurbishment in this study is applied by merely increasing the insulation level of the envelope, which makes it less effective on thermal energy need for cooling. In Figures 33 and 34, the relation between the variation of all three energy performance indicators versus $H_{tr}/V$ for NT (2021-2040) and LT (2081-2099) periods based on the RCP 8.5 scenario is presented. RCP 8.5 scenario is selected as there is evidence that it is already late for more optimistic scenarios, so RCP 8.5 is the most probable scenario. Results show a decrease in $EP_{H,nd}$ and an increase in $EP_{C,nd}$ in both time periods. These changes are slighter in NT (2021-2040) period and greater in LT (2081-2099) period, expectedly. In addition, $EP_{gl}$ decreases with the slightest variation in both

time periods. In other words, the sensitivity of $EP_{gl}$ variations to the outdoor temperature after climate change is less than the other two indicators' variations.

A general consideration is that the $EP_{gl}$ variation after climate change mainly depends on the outdoor temperature sensitivity of the building and on the heating-to-cooling need ratio that, in turn, is a function of the outdoor temperature sensitivity. Consistently with this consideration, the performed analysis confirms that the $EP_{gl}$ is not biased toward heating after refurbishment. In addition, the most striking result to emerge is that after refurbishment, the effect of building typology on the energy performance, and also its variations due to climate change, will significantly decrease.

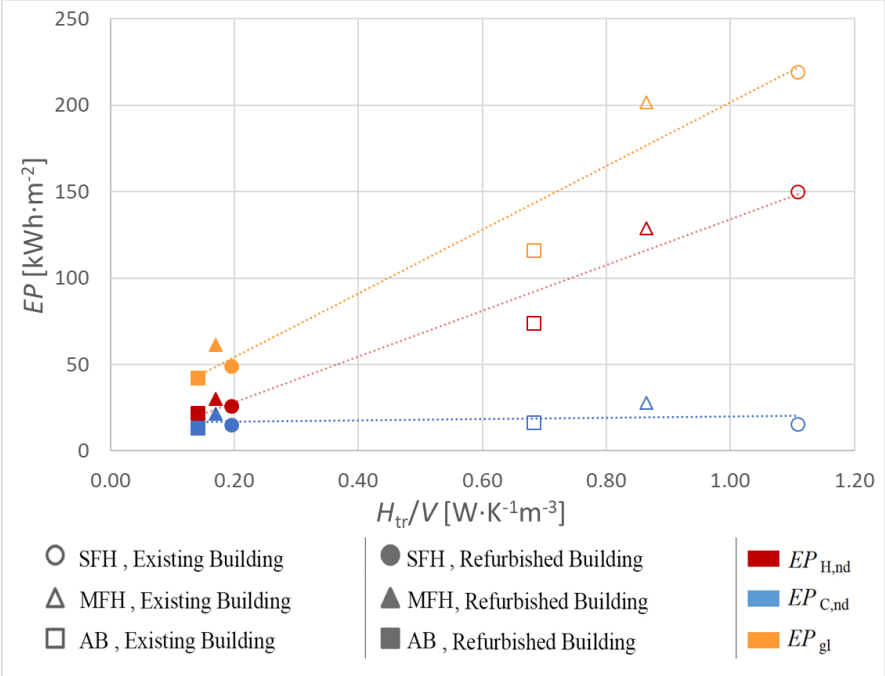


Figure 32: Energy Performance (*EP*) vs. $H_{tr}$/V

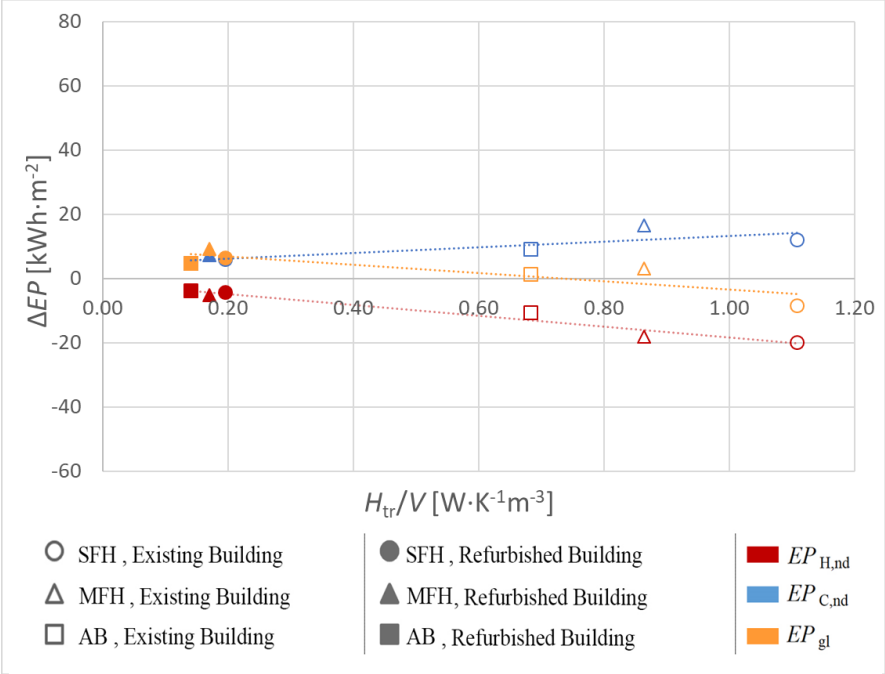


Figure 33: *EP* variation vs. $H_{tr}$/V for NT (2021-2040) RCP 8.5 scenario

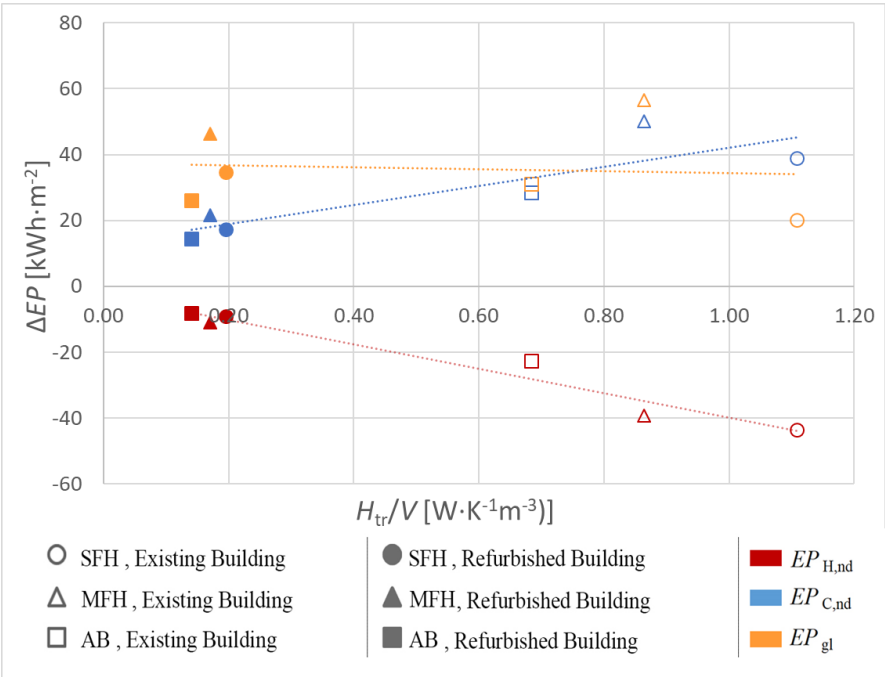


Figure 34: *EP* variation vs. $H_{tr}$/V for LT (2081-2099) RCP 8.5 scenario

This study sets out to analyse the impacts of climate change on Italian residential buildings' performance. While the changes in energy need pattern are well studied, the impacts of future scenarios on the Italian building stock on a regional scale are neglected. To fill this gap, three representative building types of the existing residential building stock were simulated under two future scenarios (RCP 4.5 and RCP 8.5) for the city of Milan (representative of the Middle Climatic zone). In addition, the effect of adding insulation level of the envelopes in all these conditions is analysed to incorporate the influence that the refurbishment has on the future performance of buildings, especially considering the measures that are commonly applied in the country. This analysis lays the foundation for future actions toward the resiliency of the built environment. To quantify and better present the impact of climate change, even considering the significant long-life span of buildings in Italy, both near-term (2026-2045) and long-term (2080-2099) periods were assessed.

For different residential building types, the results clearly show that there is a drastic rise in cooling energy use and a moderate decrease in heating energy use, as expected. The cooling and heating demand is demonstrated to change from 47.1 % (AB) to 255 % (SFH) and from −9.5 % (SFH) to −31 % (AB), respectively in existing buildings. For refurbished buildings, the changes in the cooling demand vary between 29 % (MFH) to 117 % (SFH), and in the heating demand varies between −12 % (SFH) to −38 % (AB). In addition, the overheating risk for existing buildings increases significantly as the warm discomfort hours raise between almost 30 % (MFH) to 155 % (SFH). After refurbishment, this increase varies between 8.5 % (MFH) to 37 % (AB). Likewise, it is shown that the global/overall energy performance for different scenarios changes from −3.9 % (SFH) to 28 % (MFH) for the existing and between 9.6 % (AB) to 76 % (MFH) for refurbished buildings. It was also concluded that buildings with higher shape factor are more sensitive to climate change, and this sensitivity is reduced by applying refurbishment. However, it is crucial to point out that the effect of refurbishment − despite being always positive − reduces in the future compared to the current situation. This illustrates the need to consider climate change for re-identifying refurbishment actions. Besides, it was confirmed that the effect of different scenarios on Italian residential buildings is more severe in the long term. Therefore, the climate change impact magnitude is not equal for different future weather scenarios and case studies, so in a changing climate, it becomes absolutely necessary to perform a regional and

localized analysis. These findings point out the urgent need to establish building adaptation measures for climate change.

In the next section, in order to reach a more holistic overview, the impact of climate change on energy performance and thermal comfort of a nearly zero-energy building is analysed. This analysis is applied to two other climate zones of Italy (Mediterranean Zone: Rome and Palermo) in addition to Milan.

## 4.2 Analysis of nearly zero energy buildings (NZEBs)

Energy efficient buildings like NZEBs - as efforts to reduce the contribution of the building sector on climate change – are also impacted by climate change like all building types in the same ways mentioned in sections 1.3 and 4.1. In the following, the associated energy performance requirements, and the key targets of NZEBs are explained in more detail.

According to Directive 2010/31/EU of the European Parliament (2010), 'nearly zero-energy building' means a building that has a very high energy performance. The nearly zero or very low amount of energy required should be covered to a very significant extent by energy from renewable sources, including energy from renewable sources produced on-site or nearby. As reported by the international standards, four classes of requirements are proposed for NZEBs: a) energy needs (building fabric), b) total (renewable + non-renewable) primary energy use, c) non-renewable primary energy use (without compensation between energy carriers), and d) non-renewable primary energy use (with compensation between energy carriers) (European Committee for Standardisation, 2017). In addition, it is desirable that indicators for partial EP requirements related to fabric and HVAC systems features are added in order to avoid performance unbalance between different systems and components of the building.

According to the Italian legislation, three main energy performance requirements are provided, namely the annual energy needs for space heating ($EP_{H,nd}$) and space cooling ($EP_{C,nd}$), and the overall annual total primary energy ($EP_{gl,tot}$), including space heating, space cooling, domestic hot water, mechanical ventilation, lighting, and transportation (the last two energy services only for non-residential buildings). The reference values of the performance indicators are obtained through the notional reference-building approach (European Committee for Standardisation,

2017b). Strict requirements are also provided for renewable energy ratio, namely for domestic hot water ($RER_W$) and for heating, cooling, and domestic hot water ($RER_{H+C+W}$), respectively.

The electrical energy produced by the PV system is allocated to different services (heating, cooling, DHW) according to their respective demands. The surplus energy, which includes exported energy and energy for non-EP uses (e.g., electrical appliances), is calculated on a monthly basis and is not accounted for in the EP assessment. Finally, partial requirements related to fabric include the envelope average U-value, the ratio of the envelope effective solar area to the floor area, and the thermal and solar properties of single envelope components. Specific requirements on the efficiency of generators and of other HVAC equipment are also provided.

The performance of NZEBs in the future has not yet been investigated sufficiently. The climate is changing, and compliance with NZEB requirements may not be a guarantee of energy performance and indoor environmental quality. Considering the long-life span of buildings, the performance of NZEBs should be analysed using future weather data to ensure energy efficiency, sustainability, and climate resilience over time.

This chapter investigates the effects of climate changes on the energy performance of a nearly zero-energy building in different climatic zones in Italy: Milan (2404 HDD), Rome (1415 HDD), and Palermo (751 HDD). The analysis is carried out by analysing the NZEB requirements under different scenarios. “Representative Concentration Pathways (RCPs)” 8.5 (business as usual) of emission, and concentration scenarios, according to the fifth assessment report of the Intergovernmental Panel on Climate Change (Symon, 2013), have been applied in this study. Dynamically downscaled future hourly weather data from the regional climate models ((MPI-M) MPI-ESM-LR/GERIC-REMO) are used in this work to create future typical meteorological year (TMY). The weather data was not bias adjusted in this step, as finding observational data for all three cities was impossible. Energy simulations are carried out using EnergyPlus for the mid-term (from 2041 to 2060) and long-term (from 2081 to 2100) periods. In Figure 35, the box plots of outdoor air-dry bulb temperatures for Milan, Rome, and Palermo TMYs in 2020, 2050, and 2090, are presented.

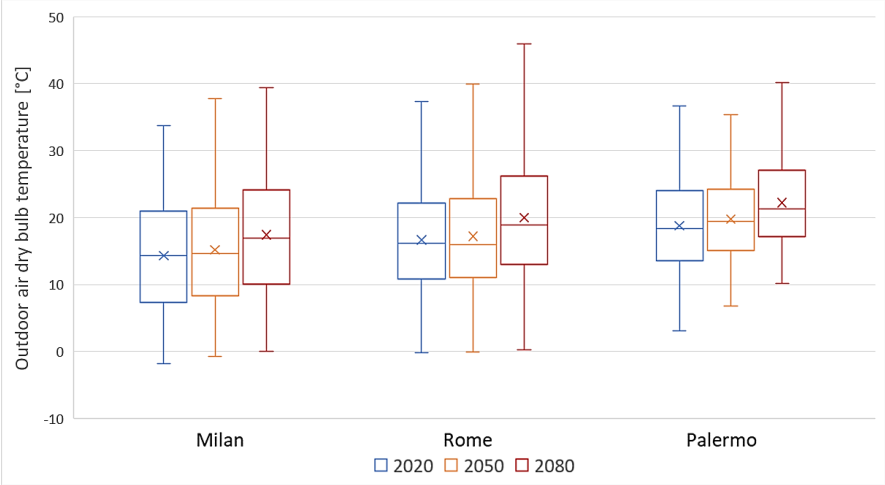


Figure 35: Box plot of outdoor air-dry bulb temperature for Milan, Rome, and Palermo in 2010, 2050 and 2080

The analysis has been carried out assuming as a case study the "Vivaldi House" (Figure 36), described in the EN 12831:2003 standard (European Committee for Standardisation, 2003). The "Vivaldi House" is a residential building with one conditioned story above ground and an unconditioned basement. The attic and the staircase are unconditioned too. The basement hosts the cellar and the garage and a conditioned hobby room. The West-oriented building facade is in adherence to another residential building. The conditioned story is 0.5 m above ground; part of the story is on a ventilated suspended floor. The main geometric data of the conditioned space are listed in Table 10.

The building is assumed to be located in three different Italian climatic zones, Milan, Rome, and Palermo. The technologies adopted in the case study represent the most widespread passive solutions in Italy. The opaque envelope components are thermally insulated on the external side. The transparent envelope components are Low-E triple-glazing windows for the building in Milan, Low-E double-glazing windows for the building in Rome, and uncoated double-glazing windows for the building in Palermo, to meet the thermal transmittance in accordance with the decree stated later. The South- and East-oriented windows are equipped with external movable solar shading devices.

With the aim to verify the NZEB requirements in Italy, the thermal transmittance of the envelope components was set in accordance with the reference building, as

defined in the Inter.D. of June 26th, 2015 (Italian Republic, Interministerial Decree of June 26th, 2015). The thermal transmittance values are listed in Table 11 for each climatic zone.

The parameters of the solar shading devices were set such that the total solar energy transmittance value of the glazing *plus* shading system is equal to 0.35, in agreement with the Italian reference building approach (Italian Republic, Interministerial Decree of June 26th, 2015).

Table 10: Geometric data of the case study

| Quantity | Value | Unit |
|---|---|---|
| Conditioned gross volume, $V_g$ | 396 | [$m^3$] |
| Conditioned net volume, $V_n$ | 278 | [$m^3$] |
| Conditioned net floor area, $A_{f,net}$ | 103 | [$m^2$] |
| Compactness ratio, $A_{envelope}/V_g$ | 0.99 | [$m^{-1}$] |
| Windows area, $A_{win}$ | 15.2 | [$m^2$] |
| Window-to-wall ratio, *WWR* | 0.15 | [-] |

Figure 36: Geometric model of the case study

Table 11: Thermal transmittance of the building envelope components of the NZEB in the analysed climatic zones

| Component | U-value [$W \cdot m^{-2}K^{-1}$] | | |
|---|---|---|---|
| | Milan | Rome | Palermo |
| External wall | 0.26 | 0.29 | 0.43 |
| Roof | 0.22 | 0.26 | 0.35 |
| Floor | 0.26 | 0.29 | 0.44 |
| Window | 1.40 | 1.80 | 3.00 |

Space heating and space cooling are provided through fan coil units. In design conditions, the supply water temperature is set to 55 ° C and 7 ° C for heating and cooling, respectively. The return water temperature is set to 40 ° C for heating and 12 ° C for cooling. The emission system is characterized by a continuous operation of the heating and cooling systems, considering 20 ° C and 26 ° C temperature set-points, respectively.

Heat (for space heating and domestic hot water) and cold are provided by an electrical reversible air-to-water heat pump with a multi-stage compressor. The

sizing of the heat pump is based on the heating peak load for Milan and on the cooling peak load for Rome and Palermo. In the heating mode, the design inlet air dry bulb temperature is 7 ° C and the outlet water temperature is 55 ° C. For Milan and Rome, the rated *COP* is equal to 2.90, and the rated heating power is equal to 5.5 kW. For Palermo, the rated *COP* is equal to 2.90, and the rated heating power is equal to 4 kW. In the cooling mode, the inlet air dry bulb temperature is 35 ° C and the outlet water temperature is 7 ° C. For Milan, the *EER* is equal to 3.33, and the rated cooling power is equal to 6.5 kW. For Rome and Palermo, the EER is equal to 2.9, and the nominal power for cooling is equal to 9 kW.

The domestic hot water delivery is set to 40 °C. To meet the need for domestic hot water, a 100-l hot water storage tank at a temperature of 55 °C is considered.

The efficiency of the heating/cooling/DHW utilization (including emission, control, and distribution) subsystems was assumed equal to 0.81 in compliance with the Italian Inter.D. of June 26$^{th}$, 2015 (Italian Republic, Interministerial Decree of June 26$^{th}$, 2015).

The photovoltaic system (235 W peak power) with crystalline silicon modules installed on the South-oriented roof pitch was considered as well. The Eckstein (1990) model for crystalline PV modules was employed, in which the electricity production (current voltage) of the circuit is a function of the module temperature. Besides, the cell temperature of modules is computed based on an energy balance relative to NOCT (Nominal Operating Cell Temperature) conditions (Duffie & Beckman, 1991).

For the simulation, a standard user behaviour was assumed for the quantification of the internal heat gains and the airflow rates by natural ventilation, according to the Italian National Annex of EN 16798-1 (Italian Thermomechanical Committee, 2020).

### 4.2.1 Energy performance assessment

The building energy performance indicators assessed in this part are the annual energy needs for space heating and space cooling ($EP_{H,nd}$ and $EP_{C,nd}$, respectively), the overall annual total primary energy ($EP_{gl,tot}$), which includes space heating, space cooling and domestic hot water, the mean seasonal coefficient of performance

($COP_m$) and the mean seasonal energy efficiency ratio ($EER_m$) of the heat generators, and the renewable energy ratio (*RER*), under different climate change scenarios. The indicators refer to the NZEB requirements, as defined by the Italian energy regulations.

The performance indicators are calculated and assessed through detailed dynamic simulation using EnergyPlus. The primary energy conversion factors of the energy carriers applied in this study are those provided by the Italian Interministerial Decree (Inter.D.) of June 26th, 2015 (Italian Republic, Interministerial Decree of June 26th, 2015). Specifically, the total primary energy conversion factor of electricity from the grid amounts to 2.42, split into non-renewable (1.95) and renewable (0.47) parts.

### 4.2.2 Results and Discussion

A set of comparative analysis is performed on different NZEB requirements in three Italian climate zones for the mid-term (2050s) and long-term (2090s) period for the selected case study. The aim is to assess the impact of climate change on the future performance of NZEBs.

The annual energy needs for space heating and space cooling ($EP_{H,nd}$ and $EP_{C,nd}$, respectively) are represented in Figure 37. The results show decreases in $EP_{H,nd}$ from 7.1 % up to 99.3 % for all the cities and for both time periods compared to 2020 as the reference case. On the other hand, $EP_{C,nd}$, increases from 4.5 % to 94.1 %. A closer analysis of these data shows that the NZEB compliance of annual energy needs for space cooling is not met in the future for either cities or time periods. However, the magnitude of the variation is not equal in different scenarios. As an example, the maximum increase in the cooling demand (94.1 %) is expected to occur in 2090s in Rome, while the maximum decrease in heating demand (99.3%) is likely to happen in Palermo by the same period. It is also important to indicate that NZEBs in Milan are the least sensitive to climate change, which is due to buildings' lower cooling energy use at present.

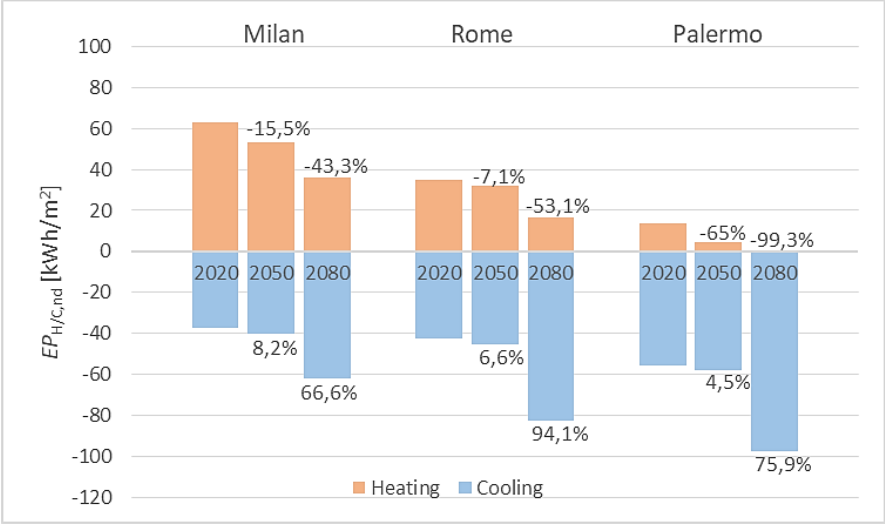


Figure 37: The annual energy needs for space heating and space cooling for Milan, Rome, and Palermo in 2010, 2050 and 2080

The overall annual total primary energy ($EP_{gl,tot}$) is presented in the last set of columns in Figures 38, 39, and 40 for all cities. In addition, the splits of $EP_{gl,tot}$ for heating (H), domestic hot water (W), and cooling (C) are shown in the previous columns of the same Figures. It can be noticed that $EP_H$ decreases, $EP_w$ remains constant, and $EP_C$ increases, regardless of the time period or the climatic zone. If we now turn into $EP_{gl,tot}$, it is seen that in 2050s, it decreases for Milan and Palermo, while it increases for Rome. This is due to a higher reduction of annual energy need for heating in 2050 for Milan and Palermo. On the other hand, in 2090s $EP_{gl,tot}$ decreases for Milan and increases for Rome and Palermo. The change in Milan is slight (−1.9 %), while for Rome and Palermo, this change is more significant (36.3 % and 45.6 %, respectively). This is due to the fact that for Milan − unlike the two other cities − the energy for winter conditioning outweighs the cooling demand, which results in a slight alteration of the final total energy for the building in the future. It can be concluded that in 2090s, the NZEB compliance of $EP_{gl,tot}$ was not met for Rome and Palermo, while in 2050s, it was not met only in the case of Rome.

In Figures 38-40, the share of either non-renewable ($EP_{nren}$) or renewable ($EP_{ren}$) primary energy is also presented. The relative changes in these values are noted in Table 12 as well. $EP_{nren}$ decreases for Milan and increases for Rome and Palermo for both periods. This might be associated with the dominance of the cooling energy need in Rome and Palermo, which leads to an increase in the electrical energy

demand from the grid. $EP_{ren}$ in 2050s decreases for Milan and Palermo (4.2 % and 8.8 %, respectively) and slightly increases for Rome (1.2 %). On the other hand, in 2090s, $EP_{ren}$ increases for all cities. It can be suggested that by the end of the century, the exploitation of renewable energy will increase due to climate change.

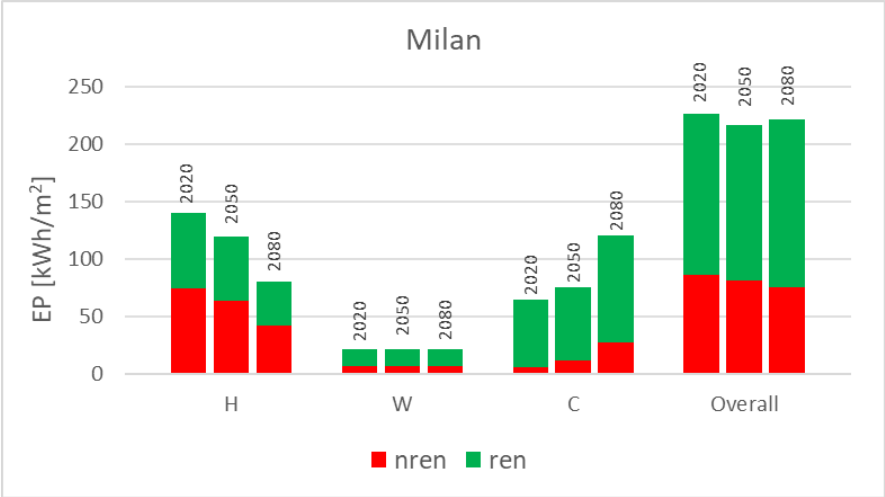


Figure 38: Annual primary energy for heating (H), domestic hot water (W), cooling (C), and overall, of the building in Milan, in 2010, 2050 and 2080

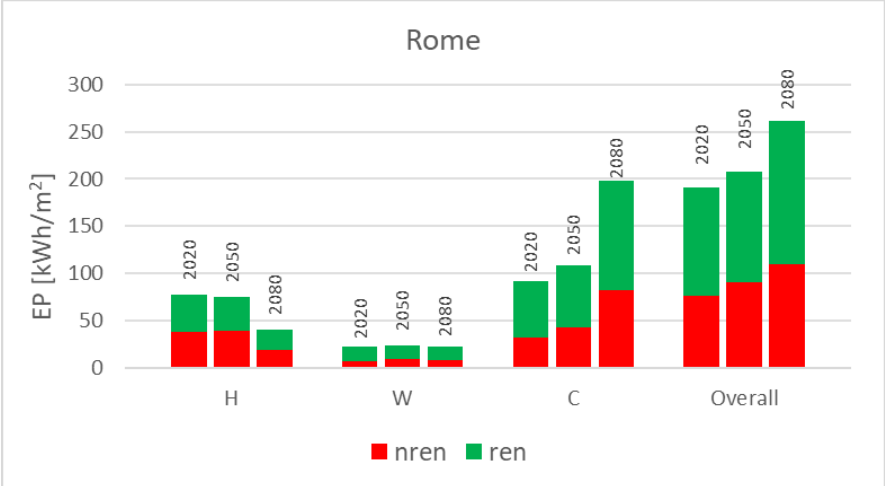


Figure 39: Figure 5: Annual primary energy for heating (H), domestic hot water (W), cooling (C), and overall, of the building in Rome, in 2010, 2050 and 2080

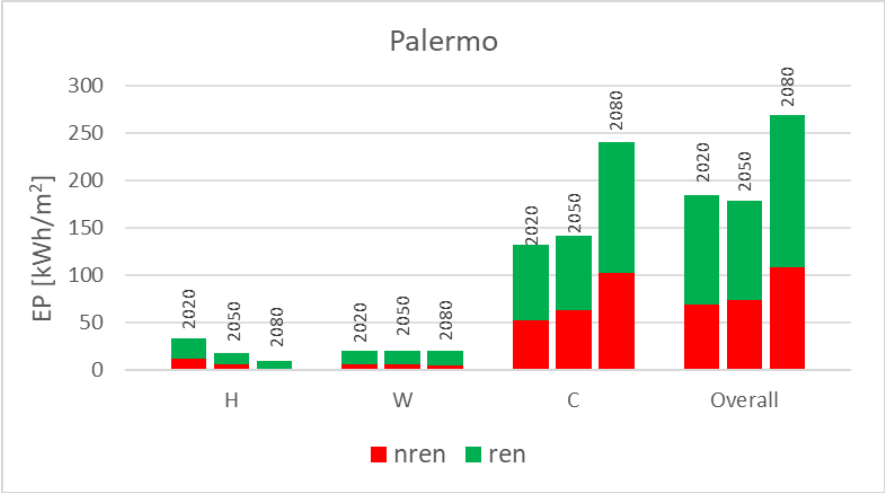


Figure 40: Annual primary energy for heating (H), domestic hot water (W), cooling (C), and overall, of the building in Palermo, in 2010, 2050 and 2080

Table 12: Relative changes of non-renewable, renewable, and total primary energy for Milan, Rome, and Palermo, in 2050 and 2080 compared to 2010

| | Milan | | Rome | | Palermo | |
|---|---|---|---|---|---|---|
| | 2050s | 2090s | 2050s | 2090s | 2050s | 2090s |
| $EP_{gl,nren}$ | −4.9% | −12.5% | 19.2% | 44.1% | 5.8% | 57.1% |
| $EP_{gl,ren}$ | −4.2% | 4.5% | 1.2% | 31.2% | −8.8% | 38.7% |
| $EP_{gl,tot}$ | −4.5% | −1.9% | 8.3% | 36.3% | −3.4% | 45.6% |

The annual delivered energy by each energy carrier (i.e., electricity from the grid, on-site PV electricity, and on-site aerothermal energy), expressed by unit of conditioned net floor area, is shown in Figures 41, 42 and 43, for the building in

Milan, Rome, and Palermo, respectively. In addition, the PV surplus is shown in the last set of columns of the same Figures. The results show that the delivered energy decreases for heating, remains constant for domestic hot water and increases for cooling for all the scenarios. Looking at the overall delivered energy, it is apparent that electricity from the grid will increase in the future for Rome and Palermo and decreases for Milan. The reason lies in the dominance of the heating energy need in Milan. The on-site aerothermal energy increases in all scenarios, while this increase is more significant in 2090s and for Rome and Palermo. This comes from the fact that the higher outside temperature leads to more aerothermal energy extraction by the heat pump. Furthermore, the on-site PV electricity slightly decreases in all future scenarios. This may be associated with the reduction in the voltage that PVs can generate because of higher temperatures. Besides, the amount of direct and diffuse radiation varies in the future due to the changes in cloud cover and atmospheric aerosol loadings. This leads to lower efficiency of PVs. In addition, the PV surplus decreases in every scenario (except in Palermo for 2050s) since not only the on-site PV electricity decrease but also the electricity demand increases.

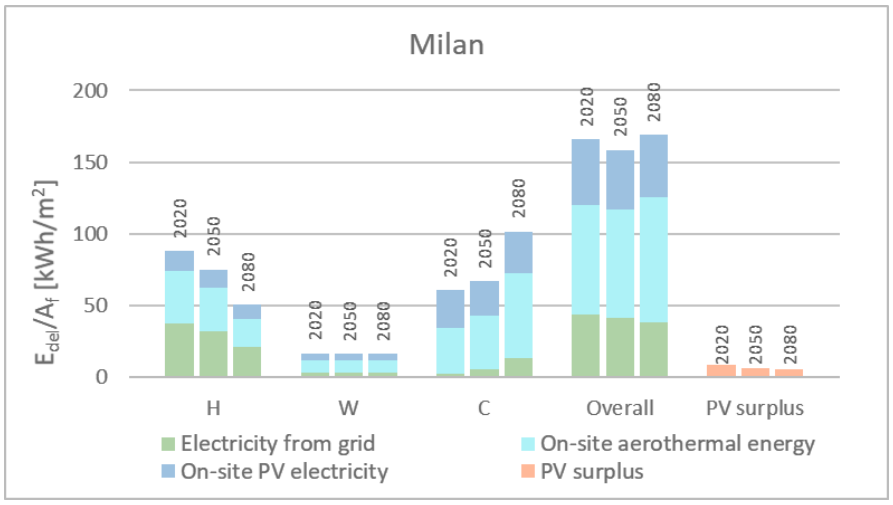


Figure 41: Annual delivered energy for heating (H), domestic hot water (W), cooling (C), overall, and PV surplus in Milan in 2010, 2050 and 2080

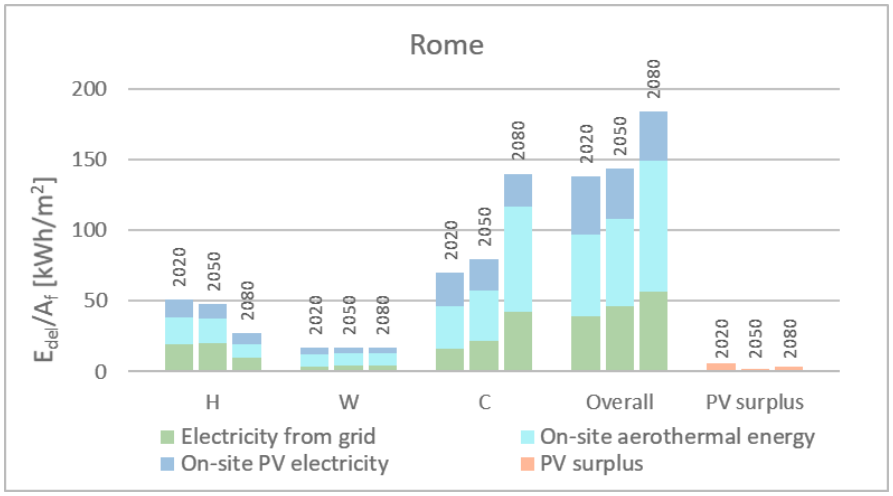


Figure 42: Annual delivered energy for heating (H), domestic hot water (W), cooling (C), overall, and PV surplus in Rome in 2010, 2050 and 2080

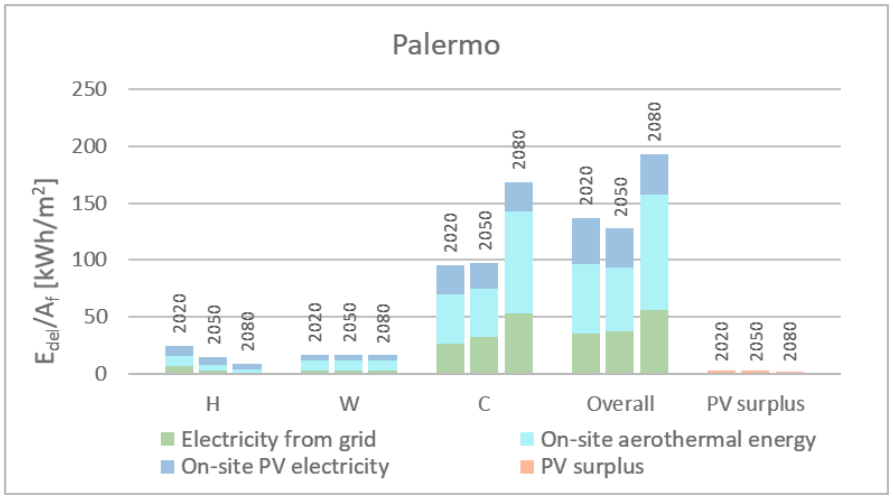


Figure 43: Annual delivered energy for heating (H), domestic hot water (W), cooling (C), overall, and PV surplus in Palermo in 2010, 2050 and 2080

Finally, in Table 13, the renewable energy ratio ($RER_{H+W+C}$), the mean seasonal coefficient of performance ($COP_m$), and the mean seasonal energy efficiency ratio ($EER_m$) are presented for each city in every period. In all scenarios, the compliance with the *RER* requirement for the NZEB is met (i.e., higher than 50%, according to

the current Italian legislation). However, the changes in this value are not significant. In addition, $COP_m$ increases for Rome and Palermo in all scenarios (except in Rome for 2050s), as the increase in temperature due to climate change makes the heat pump more efficient in winter. For Milan, the $COP_m$ decreases in all scenarios because of the higher decrease in the heating load factor compared to the other two cities, despite higher outside temperatures. Besides, $EER_m$ increases in all scenarios, except in 2050s for Palermo. This is due to the fact that by increasing the energy need for cooling in the future, the cooling load factor increases too.

It is important to indicate that the existence of exceptions in results and discussion may be due to the fact that the weather data have not been bias-adjusted to reduce long-term bias associated with climate model data.

Table 13: Renewable energy ratio, mean coefficient of performance, and mean energy efficiency ratio for Milan, Rome, and Palermo in 2010, 2050 and 2080

| | Milan | | | Rome | | | Palermo | | |
|---|---|---|---|---|---|---|---|---|---|
| | 2010s | 2050s | 2090s | 2010s | 2050s | 2090s | 2010s | 2050s | 2090s |
| $RER_{H+W+C}$ | 62% | 62% | 66% | 60% | 56% | 58% | 63% | 59% | 60% |
| $COP_m$ | 1.96 | 1.91 | 1.89 | 1.90 | 1.87 | 1.94 | 2.10 | 2.18 | 2.32 |
| $EER_m$ | 2.72 | 2.85 | 2.98 | 2.07 | 2.13 | 2.48 | 2.19 | 2.12 | 2.52 |

The aim of the present chapter was to investigate the energy performance of NZEBs in future scenarios of climate change. Three locations belonging to different Italian climatic zones were selected to perform the analysis: Milan, Rome, and Palermo. The NZEB energy performance requirements according to Italian regulations were

compared for the mid-term and the long-term future periods with the present time. The main findings are summarized as follows:

1. The impacts of climate change on the NZEBs energy performance highly depend on the climatic zone. As an example, although in all scenarios, the NZEB requirements are not met, it was demonstrated that the NZEBs in Milan are less sensitive to climate change compared to Rome and Palermo.
2. The studied period also affects the evaluation results significantly. For 2090s, compared to 2050s, the incompliance with the NZEB requirements is more severe. For instance, the annual energy needs for cooling in 2050 may increase up to 8.2 % (Milan), while this value may raise up to 94.1% (Rome) in 2090s.
3. The analysis performed on renewable and non-renewable primary energy showed that for renewable energy, the changes depend on the type of energy source. More in detail, while the on-site aerothermal energy increases, the on-site PV electricity decreases for all scenarios. On the other hand, the non-renewable delivered primary energy increases for Rome and Palermo, which once more verifies the importance of the climatic zone for such analyses.

Overall, buildings will miss the target of meeting nearly zero energy in the future, so a new configuration is needed to keep the NZEB goals in the future. These results highlight the significance of considering future weather for the energy performance assessment of NZEBs and establishing building adaptation measures for climate change besides NZEB measures to ensure a holistic approach.

# 5. Resilient cooling technologies

## 5.1 Literature review on resilient cooling solutions

Climate change will have impacts on buildings' energy performance and their cooling systems. As explained earlier in chapter 1, the major and critical impacts of climate change on buildings include overheating, which results in more cooling energy consumption and in energy shortage. Accordingly, providing cooling technologies that are energy efficient now and still functional in the future is crucial. In other words, resilient cooling solutions are those that both help to mitigate the negative impacts of buildings on the environment and adapt to future scenarios so that future risks are prevented. According to Zhang et al. (2021), resilient cooling solutions favour from efficient “absorptive capacity, adaptive capacity, restorative capacity, and recovery speed.” As mentioned earlier, this thesis has been developed in nexus with the research activities of Buildings and Communities Programme (EBC) Annex 80 ‘‘Resilient Cooling of Buildings” which studies the resilience of cooling technologies and solutions and divides cooling strategies into four groups presented in table 14.

Table 14: Classification of the most widespread cooling technologies according to Annex 80 ‘‘Resilient Cooling of Buildings”

| Categories | The most widespread technologies |
|---|---|
| Reducing heat gains to indoor environments and people | • Advanced solar shading/advanced glazing technologies<br>• Cool envelope materials<br>• Green roofs, roof pond, green facades, ventilated roofs, and ventilated facades<br>• Thermal mass utilization, including PCM and off-peak ice storage |
| Removing sensible heat from indoor environments | • Ventilative cooling<br>• Adiabatic/evaporative cooling<br>• Compression refrigeration<br>• Absorption refrigeration, including desiccant cooling<br>• Natural heat sinks, such as groundwater, borehole heat exchangers, ground labyrinths, earth tubes, and sky radiative cooling<br>• High-temperature cooling system: Radiant cooling, chill beam |
| Enhancing personal comfort apart from cooling whole spaces | • Comfort ventilation (elevated air movement)<br>• Micro-cooling and personal comfort control |
| Removing latent heat from indoor environments | • High-performance dehumidification, including desiccant humidification |

The cooling solutions which have been adopted in this study are from the first and second categories. The first two, which aim at reducing heat gains to indoor environments and people, are advanced solar shading/advanced glazing technologies besides the cool envelop materials. The third solution is ventilative cooling, which is among the solutions that help remove sensible heat from indoor environments. More information is given on these three cooling solutions in the following paragraphs.

### 5.1.1 Advanced solar shading/advanced glazing

The first cooling solution is advanced solar shading/advanced glazing technologies, which refers to “reducing heat gains to indoor environments and people.” The characteristics of glazing and shading technologies, the way they are combined, and the relevant functional classification - static and dynamic, besides manual and automatic- could determine the resilience of the cooling solution. Windows can have a significant impact on peak cooling loads, cooling energy use, and occupant comfort (C. Zhang et al., 2021). By absorbing, transmitting, and reflecting solar energy, thanks to the materials used in the glass and glazing system's construction, glazing technologies can control the cooling loads caused by solar gain. To increase the thermal management capability of the glazing, traditional clear glass which has a very high solar transmittance, is equipped with coatings and body tints to increase their reflection/absorption. Low thermal-infrared emittance ("low-E") coatings are the most efficient and extensively used glazing solutions that will limit solar heat gain and lower the window's thermal transmittance (or "U-value") when appropriately positioned within an insulating glass unit. While effectively lowering solar gain, low-E coatings could offer spectrum control and admit the majority of daylight, which also decreases the building cooling loads related to electric lighting (Rubin et al., 1999). Low-E coatings have two main functions in energy management. Since long-wave radiative heat transmission is decreased by the high reflectance of all low-E coatings between 4 μm and 50 μm, the insulated glass unit's overall thermal conductance is decreased. The initial generation of low-E coatings, which were employed in passive solar-heated buildings, had a high solar spectrum transmittance. The reflectance transition wavelength was reduced from around 4 μm to about 0.7 μm by the second generation of coatings available since the 1990s, followed by subsequent improvements in multilayer coatings. As a result, the majority of the near-infrared radiation in sunlight (0.7-2.5 μm) is reflected. The

most popular low-E coatings nowadays are those that are spectrally selective. Some are applied immediately to the hot glass on the float line, while the majority are magnetron sputtered under vacuum after the glass is created. Low-E coating emissivity varies from roughly 0.10-0.15 for pyrolytic coatings to 0.03-0.08 for the majority of post-processed sputtered coatings; the emissivity of glass is 0.84. These highly calibrated multilayer optical filters, which typically have low absorptance and high reflectivity in the NIR, as well as varying degrees of daylight transmittance, are made of sputtered coatings. The "light to solar gain" ratio, which is defined as visual transmittance divided by solar heat gain coefficient, is frequently used to describe spectrally selective coatings that permit daylight but restrict overall solar gain. The best spectrally selective "triple silver" sputtered coatings have an LSG ratio of about 2.4, while bronze-tinted glazing has an LSG ratio of about 0.5 (Kirankumar et al., 2017; Rissim & Hallie, 2013; Schaefer et al., 1997). In addition, several different ‘‘smart glazing” products are manufactured to overcome the limitations of fixed solar optical and thermal properties of glasses. Thermochromic glasses, for example, can change the solar optical features of the window based on changes in temperature (Aburas et al., 2019). Turning now to the solar shading technologies, the options come in a variety of forms, are made of various materials, and can be used in different types of structures. Static or dynamic shading systems can be mounted to the glass from the outside or the inside. Although less cost-efficient, shading equipment is more energy-efficient in controlling solar loads when positioned on the building's exterior. Some well-known shading solutions include blinds, and drapes on the interior and screens, operable shades, and external fins/overhangs. There are also more complicated solutions that control the airflow and manage heat removal or recovery by using the between the shading and glazing. The most recent kind of exterior solar shading has the ability to include PV arrays for power generation (X. Zhang et al., 2018).

### 5.1.2 Cool envelop materials (CEMs)

The second cooling strategy relevant to this study is the application of cool envelop materials (CEMs), including cool roofs, green facades or roofs, roof ponds, etc. As mentioned earlier, four categories are suggested for resilience cooling solutions, among which the “absorptive” capacity is the one that the CEMs provide (C. Zhang et al., 2021). CEMs are solar-opaque surfaces using a reflecting product in order to minimize the net radiative heat gain and have a less radiative heat gain compared

to traditional envelope materials. This helps to lessen heat flow into the occupied space. According to the critical review and assessment by C. Zhang et al. (2021), the CEM strategies include "static high solar reflectance (light-coloured or ultrabright white CEM), static high near-infrared (NIR) reflectance (cool-coloured CEM), temperature-sensitive high solar reflectance (thermochromic CEM), angle-sensitive high solar reflectance (directionally selective reflector CEM), static solar retroreflection (solar-retroreflective CEM), and static near-unity solar reflectance + static selective thermal emittance (daytime sky radiator CEM)." When power is available, CEMs reduce indoor temperatures in an air-conditioned building by conserving cooling energy; when power is unavailable, or the building lacks cooling equipment, they lower indoor temperatures in an unconditioned building; and finally in case of undersized cooling equipment and in the presence of power for an extremely hot day, CEMs combine energy savings and indoor temperature reduction. From the category of CEMs, this study focuses on cool roofs, which are demonstrated to be effective, especially in climate zones with high solar radiation on no heating requirement (Dabaieh et al., 2015; Garg et al., 2016; Kolokotroni et al., 2018; Mavrogianni et al., 2011; Radhi et al., 2017). The resilience of this technology is also claimed to be enhanced in hot-dry climates rather than humid ones. The reason lies in the reduction of solar reflectance due to weathering in humid regions. In addition, because of more cloudiness, the sky radiative cooling effect becomes smaller in tropical regions, which results in the lower performance of the solution (Torres-Quezada et al., 2019). On the other hand, cool roofs are more efficient in low-rise buildings since they occupy the top floor of construction.

### 5.1.3 Ventilative cooling

The other cooling solution is ventilative cooling which gets the advantage of outdoor air-cooling potential through the wind airflow, buoyancy forces, or fans. It is also possible to use the combination of these techniques. According to Annex 80 categories based on their approaches to cooling people or the indoor environment, ventilative cooling is classified as a solution that removes sensible heat from indoor environments. A distinction can be made between ventilation aimed at daytime comfort (or direct cooling) and night cooling (or indirect). Daytime comfort ventilation introduces the flow of outside air through the building during the day to directly remove heat gains. It aims to improve the thermal comfort of the occupants through the transport of convective heat, increasing the evaporative cooling effect

on the occupants' skin and decreasing the internal air temperature. Night cooling has a double effect: on the one hand, it uses the thermal mass of the building during the night, which acts as a heat sink during the busy period, and on the other hand, it reduces the indoor air temperature during the hours (C. Zhang et al., 2021). The availability of heat sinks (external heat mass) with appropriate temperature gradients and coupling between the thermal mass and sink are major determinants of ventilative cooling systems' efficiency (Heiselberg & Kolokotroni, 2017a; Santamouris et al., 2010). One of the key advantages of VC is the use of natural ventilation, which is one of the most energy-efficient cooling sources and can improve air quality -assuming the outdoor air is less polluted and cooler than the inside air- while boosting users' thermal comfort. However, the main limitation refers to the dependence of this solution on the occupant's behaviour which is influenced by psychological, cultural, educational, social, and lifestyle factors (Heiselberg & Kolokotroni, 2017b). It has been demonstrated by some studies, including the one by Artman et al. (2008), that climate change will affect ventilation cooling performance, such as the night-time ventilative cooling potential, and it is needed to reassess the resilience of this strategy. Accordingly, some other studies analysed the adaptability of various natural ventilation strategies to future climatic conditions discovering that buildings using advanced natural ventilation systems are more resilient to future climate change than structures using single-side natural ventilation (Lomas & Ji, 2009). Similar to the previous solutions, since local climatic variables have an impact on ventilative cooling systems, they must be re-evaluated in light of changing climes. In this thesis, mechanical ventilative cooling is applied, which is claimed by some researchers, including Burman & Mumovic (2018), to be more resilient despite increasing energy consumption.

## 5.2 Case study, Technologies, and KPIs

For evaluating the resilience of the reviewed cooling technologies, a set of analysis is performed for a representative case study in Rome. In synergy with the selection criteria of IEA EBC ANNEX 80 Weather Data Task Group, Rome has been selected since it is a city with relatively high population and population growth and belongs to the climate zone 3A (Warm Humid) of ASHRAE classification (ASHRAE, 2020). With the aim of extending the research outcomes at a broader territorial scale, the case study was selected in a way to be representative of a specific category, that is, the Italian single-family house built in the period 1946-1960

(Ballarini et al., 2014) described in details in section 2.2. In a recent study (Tootkaboni et al., 2021), this type of building was found to be more sensitive to climate change due to its high shape factor.

The thermo-physical features of the building envelope components are provided in Table 15, assuming the building type both in the original pre-retrofit situation and in the retrofitted state. This double condition allows for assessing the effect of the passive cooling strategies both on low energy-efficiency buildings and on already insulated buildings. The *U*-values of the envelope components in the pre-retrofit state refer to typical technologies of the construction period (solid brick masonry and single-glazing windows). The retrofitted state presents components insulated in accordance with the notional reference building for the climatic zone of Rome, as expressed by the Italian energy regulations (Italian Republic, Interministerial Decree of June 26th, 2015), which also represents the nearly zero-energy building target. The post-retrofit windows present a low-E double-glazing. In addition, while the original building is not equipped with solar shading devices, these are provided for in the retrofitted building (external wooden Venetian blinds).

As far as the technical building systems are concerned, the building in the pre-retrofit state is equipped with a gas standard boiler and radiators for space heating and a split system for space cooling. In the post-retrofit phase, both heating and cooling are provided by a reversible air-to-water heat pump with fan coils as heat emitters. The air conditioning is auto sized to design days according to each weather condition. Since passive cooling technologies are simulated, the auto-sizing of the HVAC system will produce energy savings or improvements in thermal comfort that are not solely attributable to passive cooling technologies but rather to the compound effect of cooling technologies, plus changes in HVAC system sizing. As a result, the baseline model should be used to estimate the HVAC capacities for heating and cooling coils, and these fixed capacities should be applied throughout the performance assessment of passive cooling technology. The simulation engine, user behaviour, profiles of internal gains, operation mode of the technical building system, heating, and cooling setpoints, and the operation of blinds are the same as explained in section 2.3.2.

Table 15: Thermo-physical parameters of the envelope components

| Component | Parameter | Pre-retrofit | Post-retrofit |
|---|---|---|---|
| External wall | $U$ [W·m$^{-2}$K$^{-1}$] | 1.48 | 0.29 |
| Roof | $U$ [W·m$^{-2}$K$^{-1}$] | 1.65 | 0.26 |
| | $\alpha_s$ [-] | 0.75 | 0.75 |
| | $\rho_s$ [-] | 0.25 | 0.25 |
| Bottom floor | $U$ [W·m$^{-2}$K$^{-1}$] | 2.00 | 0.29 |
| Windows | $U$ [W·m$^{-2}$K$^{-1}$] | 4.9 | 1.30 |
| Glazing | $U$ [W·m$^{-2}$K$^{-1}$] | 5.7 | 1.20 |
| | $g$ [-] | 0.85 | 0.59 |
| | $\tau_v$ [-] | 0.90 | 0.80 |
| Shading | $\tau_s$ [-] | N/A | 0.40 |
| | $\rho_s$ [-] | N/A | 0.12 |

Among the reviewed technologies in the previous chapter, the resilience of four solutions is evaluated for the case study explained above. The cooling solutions were selected from the first and second cooling categories provided by IEA EBC Annex 80, which are "reducing heat gains to indoor environments and people, removing sensible heat from indoor environments." From the first category, ultra-selective double-glazed windows, external roller blinds, and cool roof tiles are

analysed, and from the second category, mechanical ventilative cooling is chosen. The ultra-selective double-glazed window is a static technology that incorporates low thermal-infrared emittance (low-E) coatings with spectral control to reduce the window heat loss and solar heat gain while admitting most daylight. The external roller blind is a dynamic technology with a low solar transmittance that strongly reduces the solar heat gain due to its external position and can be controlled to optimise both thermal and visual comfort and energy demands for heating, cooling, and lighting. Cool roof tiles are a static technology that reduces net radiative heat gain at the envelope (solar + thermal infrared radiation) thanks to the high solar reflectance.

For applying mechanical ventilative cooling, the air exchange rate was calculated using the ventilative cooling potential tool (VC Tool), which was developed within the Annex 62 project (Heiselberg, 2018). By taking into account building envelope thermal attributes, internal gains, ventilation requirements, and occupancy patterns, the *VC Tool* (Venticool, 2018) intends to evaluate the potential efficacy of ventilative cooling systems. The tool uses a method that considers well-mixed, single-zone energy balance with heat transfer surfaces defining its boundaries. In order to keep indoor air temperatures at a certain internal heating setpoint temperature, it is presumable that a heating balance point for the external air temperature could be established below which heating must be applied. Hence, direct ventilation helps keep indoor comfort when the temperature of the external dry bulb is more than the temperature of the heating balance point. Ventilative cooling is no longer effective at or below the heating balance point temperature. However, heat recovery ventilation should be employed to maintain the required minimum air change rates for keeping indoor air quality and minimizing heat losses.

In the *VC Tool*, five ventilative cooling modes (0–4) have been identified (Belleri & Chiesa, 2018). Mode [0]: “when the outdoor temperature is below the heating balance point temperature, no ventilative cooling is required since heating is needed”; Mode [1]: “direct ventilation with airflow rate maintained at the minimum required for indoor air quality can potentially ensure comfort when the outdoor temperature exceeds the balance point temperature, yet it falls below the lower temperature limit of the comfort zone”; Mode [2]: “Direct ventilative cooling with increased airflow rate can potentially ensure comfort when the outdoor temperature

is within the range of comfort"; Mode [3]: "direct evaporative cooling (DEC) can potentially ensure comfort even if direct ventilation alone is not useful because the outdoor temperature exceeds the upper-temperature limit"; Mode [4]: "Direct ventilative cooling is not useful when the outdoor temperature exceeds the upper-temperature limit of the comfort zone, and furthermore this limit is also overtaken from the expected DEC outlet temperature." The Ventilative Cooling mode [2] was employed in this study. The tool determines the necessary airflow rate for ventilative cooling mode 2 in addition to dividing the total number of hours the building is occupied into the specified groups. When the external temperature falls within the range of comfort zone temperatures, direct ventilative cooling with enhanced airflow rate could be able to guarantee comfort. In this instance, the tool determines the airflow rate necessary to keep the indoor air temperature within acceptable ranges.

The following three key performance indicators (KPIs) were used for the performance assessment of the selected cooling solutions:

- *HE* [%], i.e., hours of exceedance, which are the number of hours in which the operative temperature of the zone is greater than the upper limit temperature

- $EP_{C,\mathrm{nd}}$ [kWh/m$^2$], annual thermal energy need for space cooling

- $E_{el,C}$ [kWh/m$^2$], annual electrical energy consumption (from the grid) for cooling and ventilation

The above indicators were chosen from the list of KPIs officially adopted in IEA EBC Annex 80 to represent the summer performance of the building according to the following criteria: a) thermal discomfort in free-floating conditions (absence of cooling or power outage) or in case of power shortage, b) thermal performance of the fabric in cooling operation, and c) energy performance of the building (including HVAC system) in cooling operation.

All the adopted indicators are based on international standards. *HE* accounts for the number of hours exceeding the acceptable range of the indoor operative temperature. For free-floating condition, the adaptive comfort method is assumed according to the Annex-H of EN ISO 7730, 2005. $EP_{C,\mathrm{nd}}$ reflects the basic energy

needs of the building in ideal thermal conditions (uniform and ideally controlled indoor temperature) without interaction with specific technical building systems (EN ISO 52016-1, 2017). $E_{el,C}$ represents the energy delivered to the building for cooling by adding the effect of the energy losses of the cooling system (EN ISO 52000-1, 2017). The analysis of the case study is performed twice: once in section 4.3 for assessing the resilience of cooling technologies using thermal comfort and energy performance metrics (explained KPIs) and then in section 4.4 to deepen this assessment by applying a sensitivity analysis to compare the impact of each technology and the relevant parameters on the KPIs.

## 5.3 Analysing the resilience of cooling technologies

### 5.3.1 Modelling assumption and Simulation

For performing the resilience analysis of the selected technologies explained above, for each, a set of parameters are selected to represent their technical characteristics to be used in simulations. Initially, a range for the relevant parameters -according to the criteria explained in section 5.2- is defined, which will later be used to perform the sensitivity analysis. Besides, for all these parameters, a configuration is selected to run the simulations in this section.

For ultra-selective double-glazed windows, the considered parameters are thermal transmittance ($U_w$) W/(m².K), total Solar factor ($g$) %, and light transmittance ($\tau_v$) %. For $U_w$ value, the upper range is equal to 1.8 W/(m².K) according to the Italian energy regulations (M.D 26 June 2015) for the notional reference building in the climatic zone of Rome. For $g$ and $\tau_v$ ranges are $g \leq 30\%$ and $\tau_v \geq 60\%$, as suggested by the critical review and qualitative assessment of Annex 80 on advanced glazing technology (C. Zhang et al., 2021). Using the European AGC glass configurator dataset, glass products manufactured or processed by AGC company in the market within these ranges were found. These products were used to fix the lower range of the $U_w$ value (0.9 W/(m².K)) in a realistic way. For the external roller blind, the considered parameters are solar transmittance ($\tau_{s,blind}$) and solar reflectance ($\rho_{s,blind}$). Based on the Italian energy regulations (M.D 26 June 2015), the total solar energy transmittance of the glazing, including the solar protection device ($g_{gl+sh}$), must be equal to 0.35. Accordingly, considering the window properties of the pre-retrofitted building, the range of $\tau_{s,blind}$ is calculated according to ISO 52022-1 (CEN, 2017),

which must be less than 0.25. Afterward, using blinds from the European solar shading database, the lower range (equal to 0.01) is found. After defining the $\tau_{s,blind}$, it has been tried to fix the $\alpha_{s,blind}$ (0.65) in a way to arrive at an acceptable range of $\rho_{s,blind}$. Turning now to the cool roof tiles, the considered parameters are solar absorbance ($\alpha_{s,roof}$) and solar reflectance ($\rho_{s,roof}$). According to EN ISO 22969, the $\rho_{s,roof}$ for a pitched roof should be greater than 30%. Similarly, the available products in Cool Roof Rating Council database were referred to finding the upper limit, which equals 70%. Afterward, the range for $\alpha_{s,roof}$ is defined considering the range of $\rho_{s,roof}$ for a pitched roof. For mechanical ventilative cooling, using the VC tool for the described case study, the airflow rate equal to 2.8 ACH was calculated. The tool also defines the standard deviation, which in this case is 1.75, according to which the range of the airflow rate was determined. All the values and ranges of the parameters and the selected configuration for running the simulations in this section are presented in table 16. The simulations are performed as presented in figure 44. In total, 90 simulations were run.

Table 16: Parameters of studied cooling technologies

| Technologies | Parameter | Resilient technologies | |
|---|---|---|---|
| | | Selected configuration | The range for sensitivity analysis |
| Glazing | *Window thermal transmittance ($U_w$)* W/(m².K) | $U_w$=1.2 | (g) ≤ 30% |
| | *Total Solar factor (g)* % | *g* =30% | ($\tau_v$) ≥ 60%. |
| | *Light transmittance($\tau_v$)* % | $\tau_v$ =64% | 0.9≤ $U_w$ ≤1.8 |
| | *Solar transmittance ($\tau_s$)* % | $\tau_s$ =21% | |
| Shading | *Solar transmittance ($\tau_{s,blind}$)%* | $\tau_{s,blind}$= *13%* | *1% ≤ $\tau_{s,blind}$ ≤ 25%* |
| | *Solar reflectance ($\rho_{s,blind}$) %* | $\rho_{s,blind}$ = *42%* | $\alpha_{s,blind}$ =*65%* |
| Cool roofs | *Solar absorbance ($\alpha_{s,roof}$) %* | $\alpha_{s,roof}$ = 50% | 0.3≤ $\alpha_{s,roof}$ ≤0.7 |
| | *Solar reflectance ($\rho_{s,roof}$) %* | $\rho_{s,roof}$= 50% | 0.3≤ $\rho_{s,roof}$ ≤0.7 |
| Ventilative cooling | Air change rate by mechanical ventilative cooling ($h^{-1}$) | 2.8 | 1 ≤ *ACH*≤ 5 |

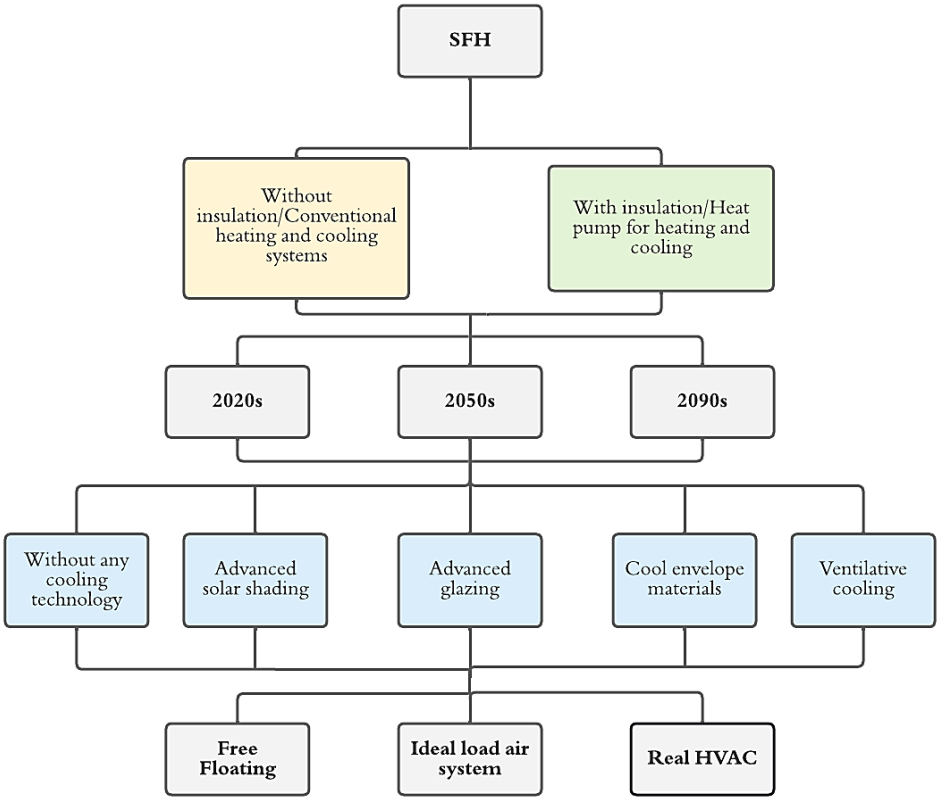


Figure 44: Simulation flow chart of analysing the resilience of cooling technologies

## 5.3.2 Results and discussion

The results obtained from the simulations are shown in Figures 45 to 50. The first two refer to the annual thermal energy need for space cooling ($EP_{C,\mathrm{nd}}$) in 2010, 2050, and 2090. Besides, Figures 47 and 48 represent the annual electrical energy consumption (from the grid) for cooling and ventilation ($E_{el,C}$). In each graph, the base case and the case with the activation of the different cooling strategies are compared. An increase of up to 55 % for the pre-retrofitted and 40 % for the post-retrofitted case is shown in $EP_{C,\mathrm{nd}}$ over time due to climate change. Furthermore, the increase of $E_{el,C}$ is up to 70 % for the pre-retrofitted and 60 % for the post-retrofitted building. For post-retrofitted buildings, the variations of $EP_{C,\mathrm{nd}}$, and $E_{el,C}$ are less than the pre-retrofitted ones. It can be argued that the post-retrofitted building is less sensitive to the effects of climate change.

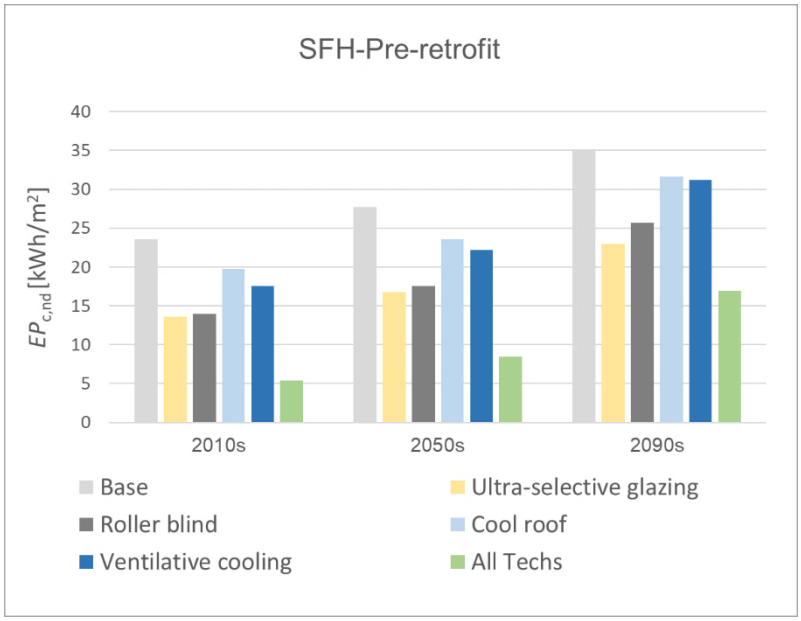


Figure 45: Annual thermal energy need for space cooling in 2010s, 2050s, and 2090s for pre-retrofit building

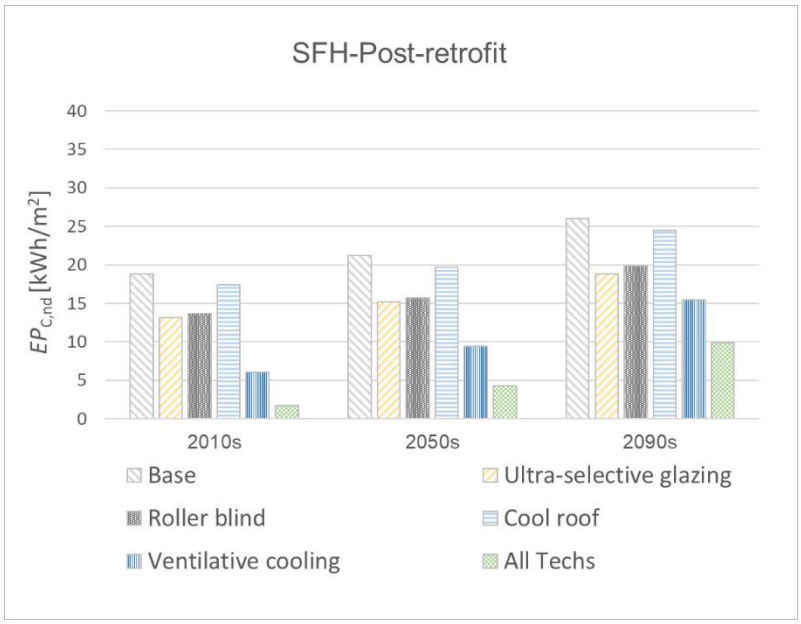


Figure 46: Annual thermal energy need for space cooling in 2010s, 2050s, and 2090s for post-retrofit building

The reduction in the $EP_{C,nd,}$ and $E_{el,C}$ caused by either of the cooling solutions are more significant in the pre-retrofitted building. In addition, it is shown that the most effective solution on $EP_{C,nd,}$ and $E_{el,C}$ for the pre-retrofit condition is ultra-selective glazing. In post-retrofit condition, ventilative cooling becomes more effective in reducing $EP_{C,nd}$ while the effect of ventilative cooling, considering the electricity consumption of the fans, is almost the same as ultra-selective glazing on reducing $E_{el,C}$. In general, the positive effect of mechanical ventilative cooling solution will diminish over time as this solution works in relation to the outside air temperature, which will increase due to climate change in the future.

The cool roof has a minor effect, as the building has a pitched roof with an unconditioned attic. This effect is negligible for the electrical energy consumption in the post-retrofitted building in all three periods. If all cooling solutions are applied, the $EP_{C,nd,}$ and $E_{el,C}$ can be reduced to the degree that in 2090 they are even less than the present base case. This result is valid for both buildings' conditions.

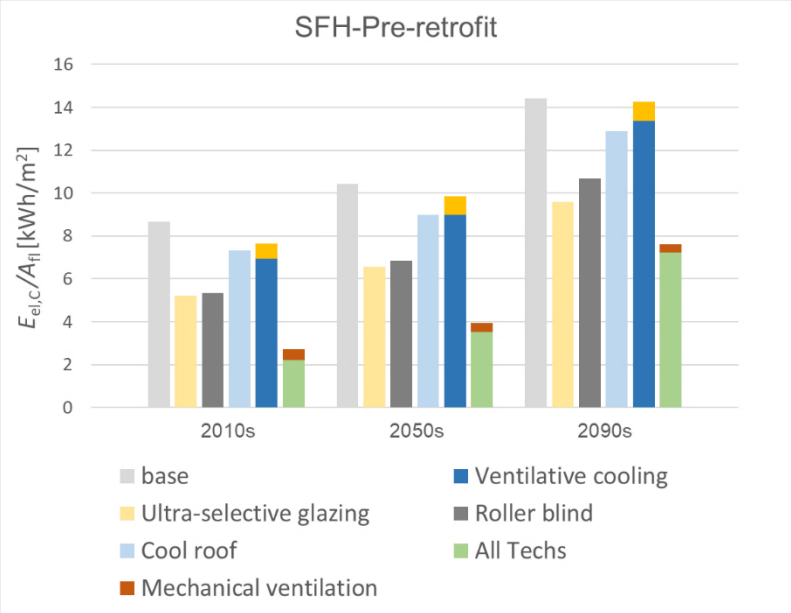


Figure 47: Annual electrical energy consumption (from the grid) for cooling and ventilation in 2010s, 2050s, and 2090s for pre-retrofit building

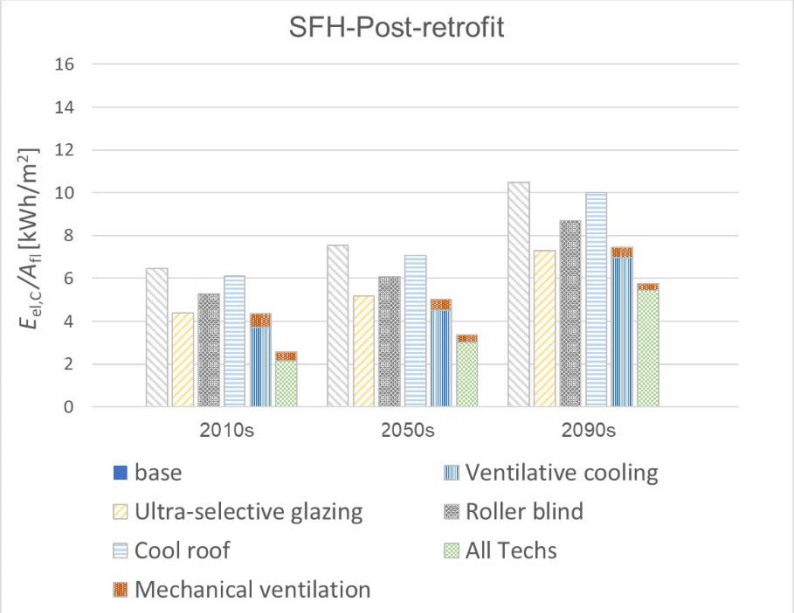


Figure 48: Annual electrical energy consumption (from the grid) for cooling and ventilation in 2010s, 2050s, and 2090s for post-retrofit building

As mentioned earlier, when it comes to the impacts of climate change on buildings, it is necessary to take the overheating risk into account. For this purpose, by running free-floating simulations, hours of exceedance in 2010s, 2050s, and 2090s are calculated and presented in Figures 49 and 50. Results report that the hours of exceedance increase due to climate change in both conditions. However, in post-retrofitted buildings, occupants will experience overheating equal to 4925 hours in future scenarios, while this amount reaches a maximum of 1603 hours for pre-retrofitted buildings in 2090s. This result is due to the unwanted effect of insulation that causes heat trap in the building in a free-floating regime.

It is shown that the cooling solutions can reduce exceedance hours. For both conditions, the effect of ventilative cooling is more than other solutions. For the pre-retrofit case, by applying ventilative cooling, the hours of exceedance in 2090 are reduced to 856 hours. For post-retrofitted case, this reduction is even more and reaches to 660 hours in 2090. The difference between the effectiveness of ventilative cooling in comparison to the impact of other solutions is significantly more in post-retrofit condition. This result is valid even considering the overmentioned fact that the positive effect of mechanical ventilative cooling solution will diminish due to climate change. The results show the capacity of this

cooling solution to adapt to the unwanted effects of insulation in the post-retrofitted building, which also demonstrates its resilience. The impact of ultra-selective glazing and roller blind is almost the same and significantly higher than the cool roof. By applying all the cooling solutions, hours of exceedance reduce significantly for both cases. However, the hours of exceedance in the post-retrofitted building for the worst case (2090) equals 73 hours which is much less than the pre-retrofitted case (237 h).

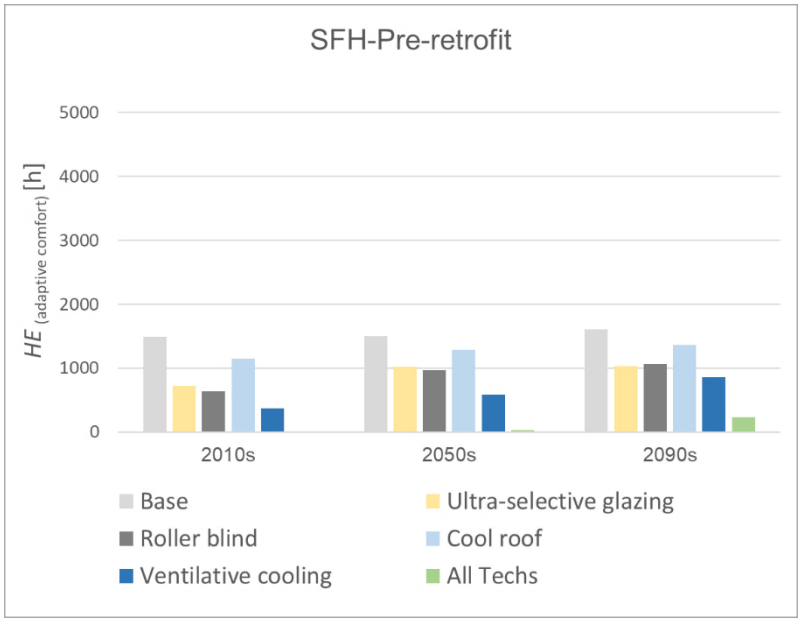


Figure 49: Hours of exceedance in 2010s, 2050s, and 2090s for pre-retrofit building, in free-floating condition

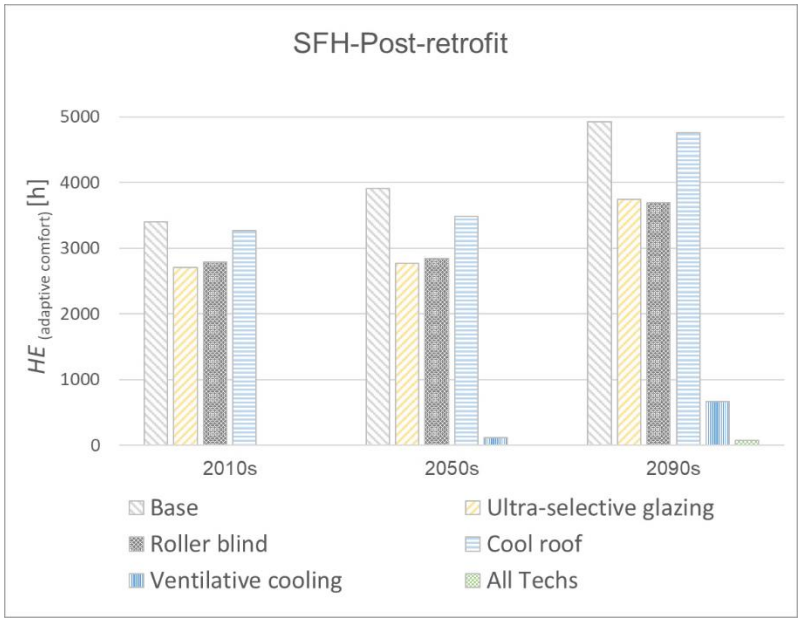


Figure 50: Hours of exceedance in 2010s, 2050s, and 2090s for post-retrofit building, in free-floating condition

This section aims to examine the climate resilience of four passive cooling solutions regarding the future performance of Italian residential buildings. The current results indicate that among selected solutions -depending on the building's condition- the mechanical ventilative cooling and the ultra-selective double-glazed window have the most significant impact on reducing the effect of climate change on thermal energy need for space cooling, electrical energy consumption from the grid for cooling and ventilation, and hours of exceedance in free-floating condition. The findings also revealed that applying all four mentioned cooling solutions could significantly develop the energy performance of the buildings so that in the worst future case scenario (2090), the energy performance will be enhanced. This improvement is more considerable for the post-retrofitted building. These findings shed new light on the trade-off between energy efficiency and climate resiliency. In this case, it is necessary to identify cooling solutions that help to mitigate climate change and foster adaptation to it to ensure both sustainability and climate resilience for the built environment.

## 5.4 Sensitivity analysis

In many areas of research, it is crucial to know how variation in input affects the outcome. When the outcome is a function of multiple factors, measurement of the magnitude of change in output caused by a change in each factor, or interaction between factors, allows for more efficient policy making and intervention, particularly when the limitation in data creates uncertainty in understating the function. Sensitivity analysis aims to find and quantify the source of uncertainty in the outcome. It is defined as "The study of how the uncertainty in the output of a model (numerical or otherwise) can be apportioned to different sources of uncertainty in the model input" (Saltelli et al., 2004).

The sensitivity analysis methods are diverse and chosen according to the research question or design. In general, they can be classified into two main sub-categories: local and global. The local methods measure "the effect of a given input on a given output." This measurement is usually done by computing derivative $\partial Y/\partial X_i$, where$X_i$ is the input of interest. The method of local sensitivity analysis is derivative based. It has the advantage of being efficient in computing time but inefficient in terms of the analyst's time since it requires the repeated intervention of the analyst when ad hoc coding is needed (Saltelli et al., 2008). But perhaps the more critical shortcoming of this method is "that it is unwarranted when the model input is uncertain and when the model is of unknown linearity." Derivatives are defined at one point and provide no information on the whole range of the input. This shortcoming becomes salient when the system is non-linear. Moreover, local approaches cannot measure the effect of interaction between inputs (Puy et al., 2022).

Unlike the local approach, global sensitivity analysis suits questions with uncertain inputs. Global sensitivity is based "on the consideration that a handful of data points judiciously thrown into that space is far more effective, in the sense of being informative and robust, than estimating derivatives at a single data point in the centre of the space." A commonly used global sensitivity analysis method is Sobol's variance-based method, which is applied in this study and will be explained in the following section.

### 5.4.1 Methodology and theory

Variance-based sensitivity analysis can measure sensitivity across the entire input space and compute the sensitivity of interaction between inputs. The basic idea is to use variance to describe uncertainty in the model output (Puy et al., 2022). The variance of output is decomposed to variances of inputs and their interactions. This method was introduced by Sobol (Sobol, 2001).

The model is in the format Y=f (X), where X is a vector of "k" inputs and Y is a scalar output. $X_{1...}X_k$ are independent inputs, each defined by a probability distribution. It is assumed that F(X) is square-integrable. Y can be defined in the following format:

$$Y = F(X) = f_0 + \sum_i f_i(x_i) + \sum_i \sum_{i<j} f_{ij}\left(x_i, x_j\right) + \cdots + f_{1,2,\ldots,k}(x_1, x_2, \ldots, x_k) \quad (12)$$

Where:

$$f_0 = E(Y), \qquad f_i(X_i) = E(Y|X_i) - f_o \qquad f_{ij}\left(X_i, X_j\right) = E\left(Y|X_i, X_j\right) - f_o - f_i - f_j \quad , \ldots . \quad (13)$$

The variance of Y can be decomposed in the following way:

$$V(Y) = \sum_i V_i + \sum_i \sum_{i<j} V_{ij} + \cdots + V_{1,2,\ldots,k} \quad (14)$$

Where:

$$V_i = V_{x_i}(E_{x_i}(Y|X_i))$$
$$V_{ij} = V_{x_i,x_j}(E_{x_{i,j}}(Y|X_i)) - V_{x_i}(E_{x_i}(Y|X_i)) - V_{x_j}(E_{x_j}\left(Y|X_j\right)) \quad (15)$$

Based on these variances, Sobol's indices are defined as follows:

$$S_i = \frac{V_i}{V(Y)} \qquad S_{ij} = \frac{V_{ij}}{V(Y)} \quad \ldots\ldots \quad (16)$$

Where $S_i$s are first-order indices, $S_{ij}$s are second-order indices, and similarly for higher-order indices. $S_i$ is the fraction of $V(Y)$, which could be reduced if $X_i$ were fixed. Similar interpretations hold for higher-order indices. By dividing two sides of equation (14) by $V(Y)$, we have:

$$\sum_{i=1}^{k} S_i + \sum_i \sum_{i<j} S_{ij} + \cdots + S_{1,2,\ldots,k} = 1 \quad (17)$$

In the case of no interaction between inputs $\sum_{i=1}^{k} S_i = 1$. In reality, this is rarely the case, and first-order indices are not enough to explain the output variance (Puy et al., 2022).

It can be seen that with an increase in the number of inputs, the number of interaction terms will increase exponentially (there are $2^{k-1}$ terms in equation (17)). This makes the computation of second and higher-order indices difficult. To tackle this issue, Homma and Saltelli (1996) introduced the total-order index $T_i$:

$$T_i = 1 - \frac{V_{x_i}(E_{x_i}(Y|X_i))}{V(Y)} = \frac{E_{x_i}(EV_{x_i}(Y|X_i))}{V(Y)} \quad (18)$$

A (quasi) Monte Carlo method is used to compute these indices. First, two $N \times k$ matrices (A & B) of random sample points are generated, where "k" is the number of parameters and N is the sample size. Each column in these two matrices is a model input, i.e., the probability distribution of a parameter, and each row is a sample point. The next step is the creation of $A_B^{(i)}$ or $B_A^{(i)}$ matrices. $A_B^{(i)}$ is the matrix that is constructed by replacing the column (i) of matrix A with the same column of matrix B. $B_A^{(i)}$ matrices are built similarly. Then, estimators of Sobol's indices can be computed from these matrices.

A range of estimators has been defined by scholars for the estimation of Sobol's indices. In this study, the Sensobol package in R is utilized, which provides a set of combinations of first, second, and total order indices (Puy et al., 2022). The analysis is limited to first and total-order indices. "Saltelli" first order and "Sobol" total-order estimators are used, which are defined below:

"Saltelli" first order estimator: (Saltelli et al., 2010)

$$\frac{\frac{1}{N}\sum_{v=1}^{N} f(B)_v[f\left(A_B^{(i)}\right)_v - f(A)_v]}{V(Y)} \quad (19)$$

"Sobol" total order estimator: (Sobol′, 2001)

$$\frac{\frac{1}{N}\sum_{v=1}^{N} f(A)_v[f(A)_v - f\left(A_B^{(i)}\right)_v]}{V(Y)} \quad (20)$$

### 5.4.2 Application and simulations

The sensitivity analysis in this study aims to determine the contribution of variances of building conditions (insulation level of envelopes) and cooling technologies to the variances of building energy performance and thermal comfort. Accordingly, the outputs (Ys) are:

- *HE* [%], i.e., hours of exceedance in the second floor of the case study, which are the number of hours in which the operative temperature of the zone is greater than the upper limit temperature
- $EP_{C,nd}$ [kWh/m$^2$], annual thermal energy need for space cooling
- $E_{el,C}$ [kWh/m$^2$], annual electrical energy consumption (from the grid) for cooling

These KPIs are dependent on the parameters representing the building's conditions and cooling technologies. These input parameters are selected and listed in table 17. All of them have uniform distribution within the specified range. For the resilient cooling solutions, the procedure for defining the ranges is explained in chapter 4.3.1. In addition, for considering the condition of the building, the ranges of insulation materials thicknesses for different envelopes are specified. In this case, the lower limit refers to the absence of insulation material, and the upper range is calculated according to the value of the thermal transmittance in accordance with the notional reference building for the climatic zone of Rome, as expressed by the Italian energy regulations (Italian Republic, Interministerial Decree of June 26th, 2015).

Table 17: sensitivity analysis input parameters and their distribution ranges

| | Parameter | Distribution |
|---|---|---|
| Glazing | *Window Thermal transmittance ($U_w$)* W/(m².K) | *U* ( 0.9, 1.8 ) |
| Shading | *Solar transmittance ($\tau_{s,blind}$ )%* | *U* ( 1, 25 ) |
| Cool roofs | *Solar absorbance ($\alpha_{s,roof}$) %* | *U* ( 30, 70 ) |
| Ventilative cooling | Air change rate by mechanical ventilative cooling (ACH) $h^{-1}$ | *U* ( 1, 5 ) |
| Wall thermal transmittance | The thickness of insulation material *($d_{ins,wall}$) m* | *U* ( 0, 0.40 ) |
| Roof thermal transmittance | The thickness of insulation material *($d_{ins,roof}$) m* | *U* ( 0, 0.35 ) |
| Bottom floor thermal transmittance | The thickness of insulation material *($d_{ins,floor}$) m* | *U* ( 0, 0.40 ) |

To start the analysis, the command Sobol_matrices() in the package is used to generate the required matrices of inputs. The command requires the following parameters: character vectors (c ("A," "B," "AB")), N (size of sample), names of the model parameters, order of indices, and "type," which indicates the approach to construct the sample matrices. The default approach is QRN (quasi-random numbers).

After A, B, and $A_B^{(i)}$ matrices are generated, they will be exported to JEPlus(*JEPlus,v2.1.0*, 2020) for simulation and the generation of the output vector (Y). The JEPlus tool has been developed to use EnergyPlus for complicated parametric analysis. It offers a graphical user interface (GUI) for setting design parameters, editing models, controlling simulation runs, and gathering data. The GUI allows for the rapid creation of hundreds of thousands of simulation cases. The tool is an open-source project built in Java. For using the software, it is needed to choose a construction model (an IDF or group of IMF files) and enter search words in the positions of the parameters; then, it is required to provide all possible values for the parameters in JEPlus; JEPlus then chooses a set of values and calls EnergyPlus. This enables us to easily set up numerous simulations runs to investigate the design possibilities.

Since the number of parameters in the sensitivity analysis is seven, there will be 7 $A_B^{(i)}$ matrices and, therefore, nine quasi-randomly generated matrices. The exported matrix from R has the dimension 9N×7, where N is the sample size. The smallest sample size for the Sobol indices (including first and total-order indices) is n(2k+2), where n is the least number of model evaluations needed to estimate a single effect; n can range from 16, 32, 64…1024; and k is the total number of variables (Homma et al., 2012). In my case, considering the computational cost, a sample size of 3000 is chosen, which is between 2048 (=128(2k+2)) and 4096 (=256(2k+2)). Therefore, the number of simulations equals 27000 for three time periods and three outputs. A smaller sample size might fail to achieve convergence in the computation of indices, and a larger one would be unfeasible. In any case, the convergence of the indices must be controlled in the study.

After the simulation is completed, the output matrices will be imported to R again to compute the Sobol indices with the command sobol_indices(). For this command, character vectors (c ("A," "B," "AB")), N (size of sample), names of the model parameters, order of indices, and the type of estimators (first=" Saltelli," total="

Sobol," order=" first") and "type" which is QRN by default. The function bootstraps the Sobol indices, and the number of replications is considered equal to 1000. In addition, the confidence interval equals 0.95.

Finally, the convergence of Sobol's indices is checked by the command sobol_convergence(). The package allows checking convergence "backward." If the initial sample is N, it is possible to check how the convergence evolves up to N. The command divides the original sample into sub-sample and plots the convergence of Sobol's indices as the size of the sub-sample increases.

### 5.4.3 Results and discussion

In this section, the results coming from the Sobol sensitivity analysis are reported for all three KPIs considering three time periods (2010s, 2050s, and 2090s). Each Figure represents the Sobol indices of input variables.

The first three figures in this section represent the Sobol first (red) and total (green) indices of window thermal transmittance ($U_w$) W/(m².K), shading solar transmittance ($\tau_{s,blind}$ )%, roof solar absorbance ($\alpha_{s,roof}$) %, air change rate by mechanical ventilative cooling (ACH) $h^{-1}$, the thickness of insulation material ($d_{ins,wall}$) m, the thickness of insulation material ($d_{ins,roof}$) m, and thickness of insulation material ($d_{ins,floor}$). These indices reflect each parameter's contribution to the variance of annual thermal energy need for space cooling ($EP_{C,nd}$ [kWh/m$^2$]).

Figures 51,52, and 53 consecutively represent the results for 2010s, 2050, and 2090s. It is evident from the figures that in all three periods, the difference between the first and the total order is not significant, which means interactions between the parameters are not a considerable source of variance in the $EP_{C,nd.}$ For all three periods, the variance of wall insulation thickness has the most contribution to the variance of the output. This demonstrates the high importance of the building's condition. For 2010s, after the wall insulation thickness, the variance of air change rate by mechanical ventilative cooling has more significance. However, this pattern changes in 2050s and 2090s towards the more contribution of roof insulation thickness. This might be due to the fact that the effect of ventilative cooling diminishes over time as this solution works in relation to the outside air

temperature, which will increase due to climate change in the future. This confirms that the importance of the building's condition will increase over time. Turning now to the parameters representing the cooling solutions, in all three periods, the most contribution refers to air change rate by mechanical ventilative cooling ($h^{-1}$). Finally, figure 54 presents that the convergence of all mentioned Sobol indices for annual thermal energy need for space cooling is verified, which confirms the adequacy of the sample size.

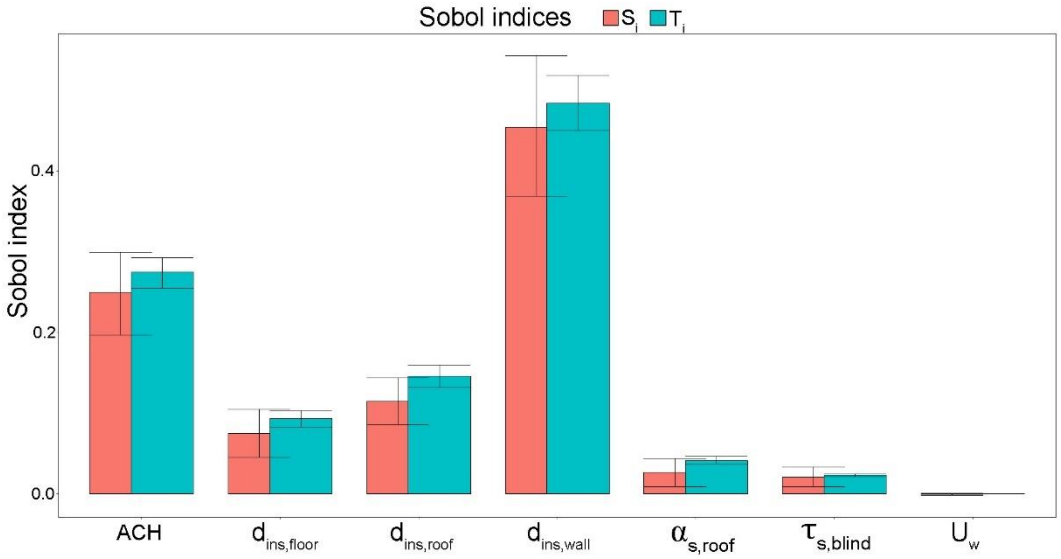


Figure 51: First and total order of the Sobol indices of the input parameters for annual thermal energy need for space cooling in 2010s

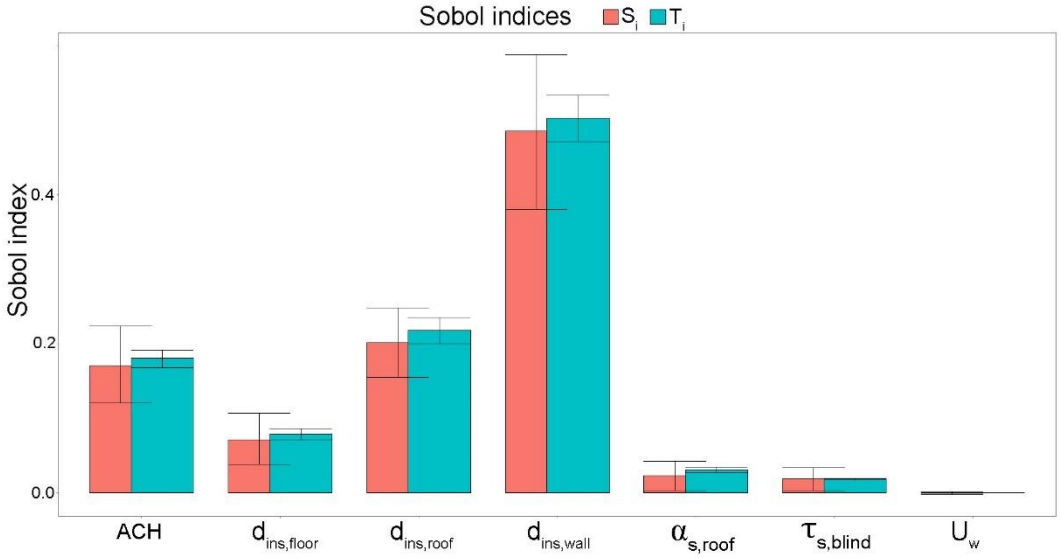


Figure 52: First and total order of the Sobol indices of the input parameters for annual thermal energy need for space cooling in 2050s

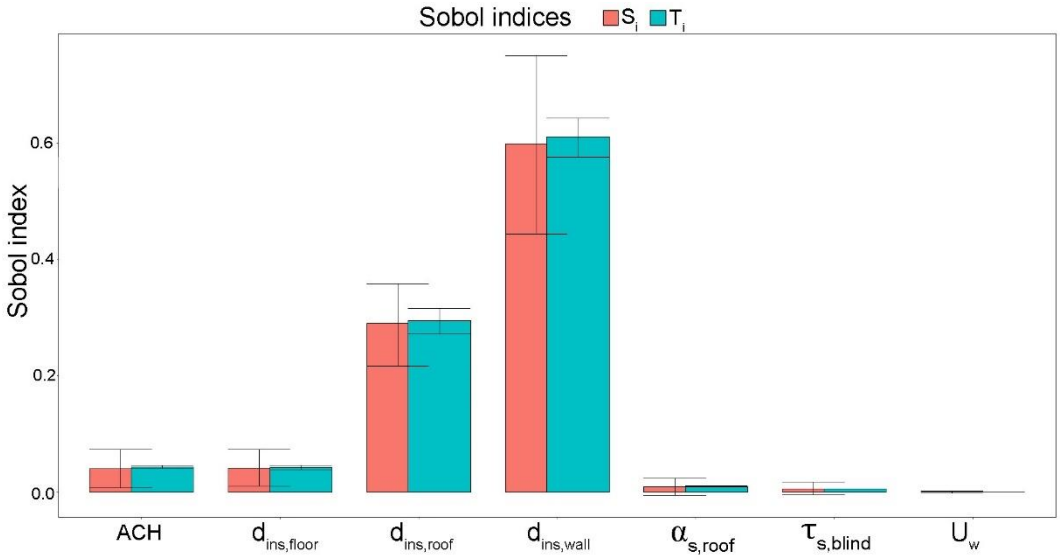


Figure 53: First and total order of the Sobol indices of the input parameters for annual thermal energy need for space cooling in 2090s

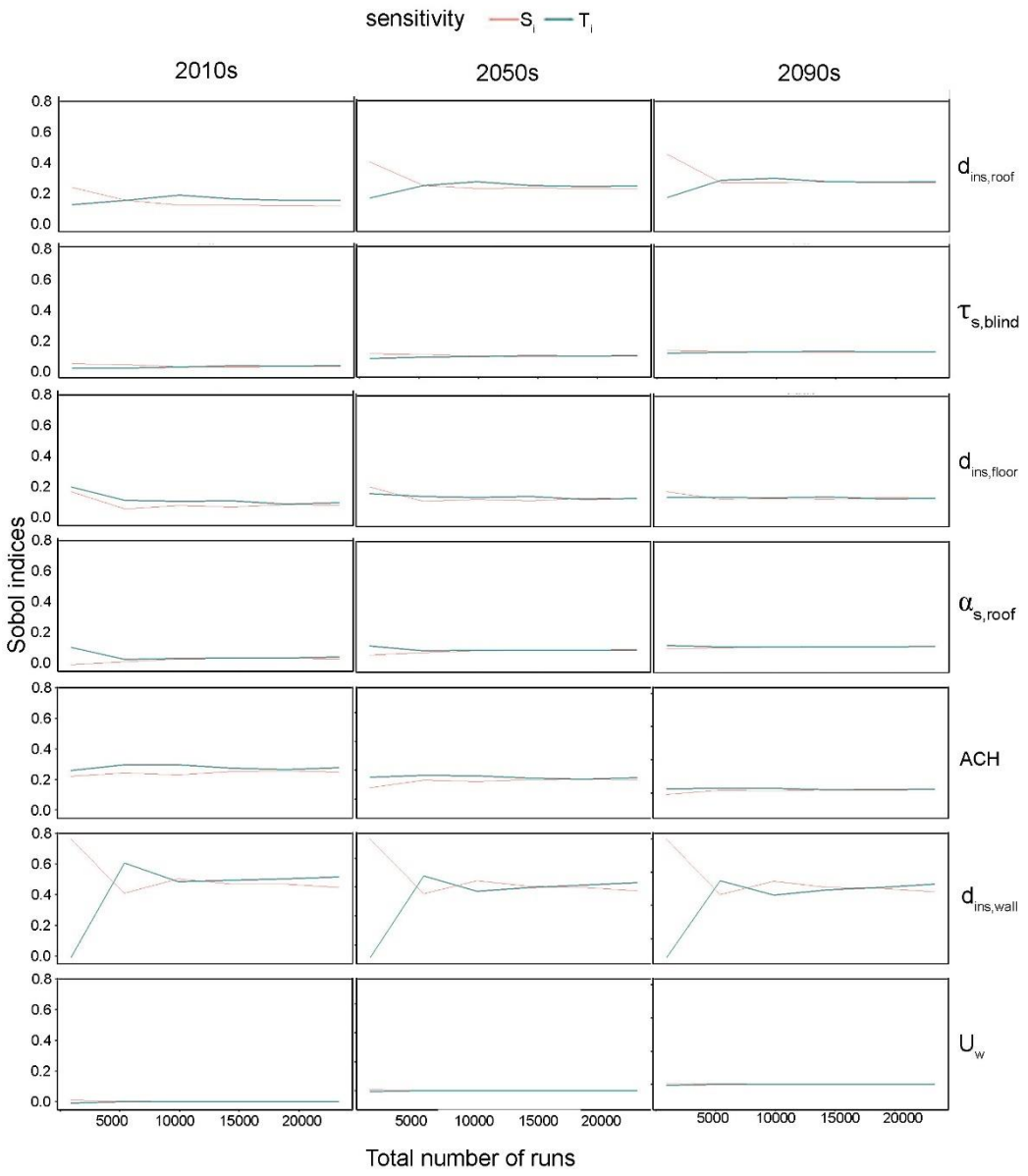


Figure 54: The plot of convergence of the input parameters for annual thermal energy need for space cooling in 2010s, 2050, and 2090s

Turning now to the annual electrical energy consumption (from the grid) for cooling ($E_{el,C}$ [kWh/m$^2$]), the variance of ACH is the most effective on the output variance in 2010s, as shown in figure 55. This result is due to the fact that more electrical energy is consumed when ACH is higher. However, the contribution of ACH reduces in 2050s (figure 56) and more significantly in 2090s (figure 57). The reason is the same as mentioned before and refers to the rise of outside temperature due to climate change previously shown in table 5 in section 3.4.1. In 2050s, and 2090s, the variance of wall insulation thickness is more effective, and in 2090s, the roof insulation thickness becomes the second important contributor in the variation of $E_{el,C}$. This confirms once more that the building's condition plays a crucial role in the future climate. Finally, figure 58 presents that the convergence of all mentioned Sobol indices for annual electrical energy consumption (from the grid) for cooling is verified, which confirms the adequacy of the sample size also in this case.

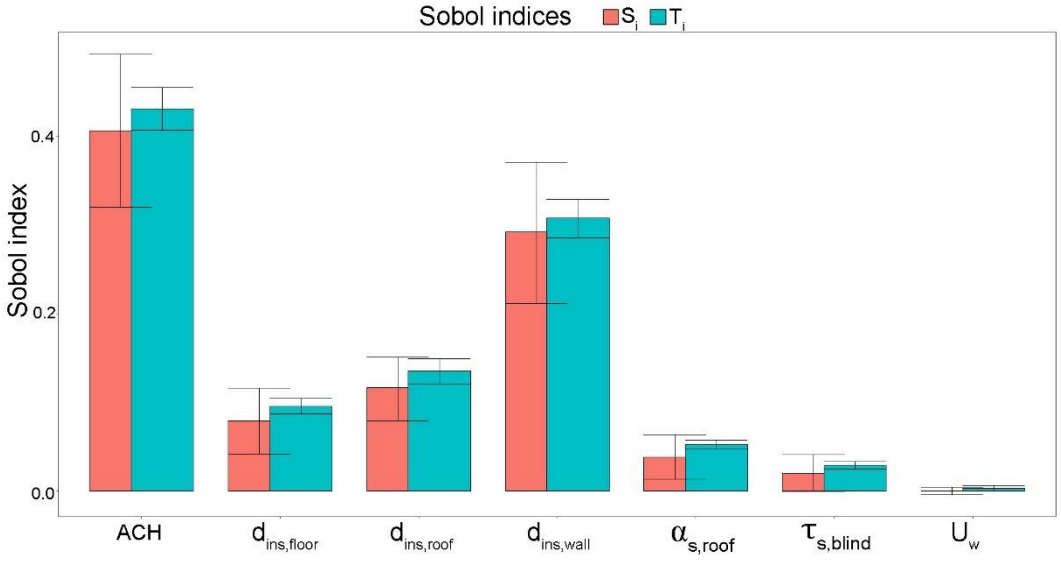


Figure 55: First and total order of the Sobol indices of the input parameters for annual electrical energy consumption (from the grid) for cooling in 2010s

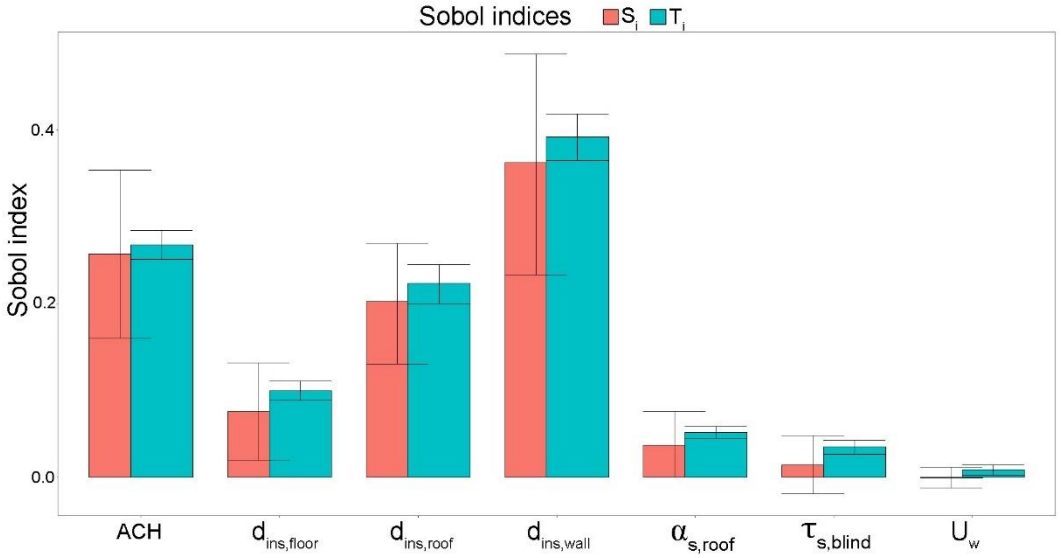


Figure 56: First and total order of the Sobol indices of the input parameters for annual electrical energy consumption (from the grid) for cooling in 2050s

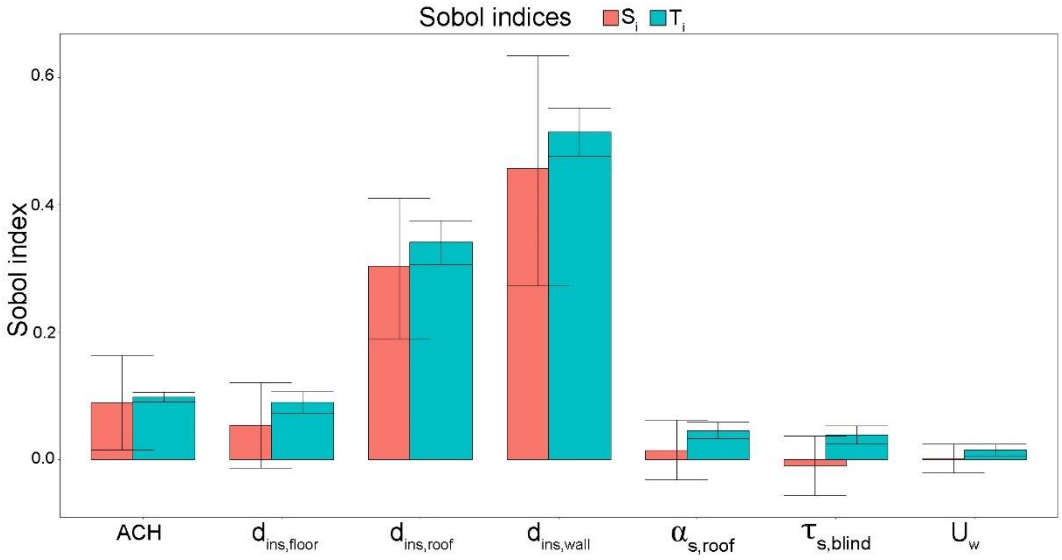


Figure 57: First and total order of the Sobol indices of the input parameters for annual electrical energy consumption (from the grid) for cooling in 2090s

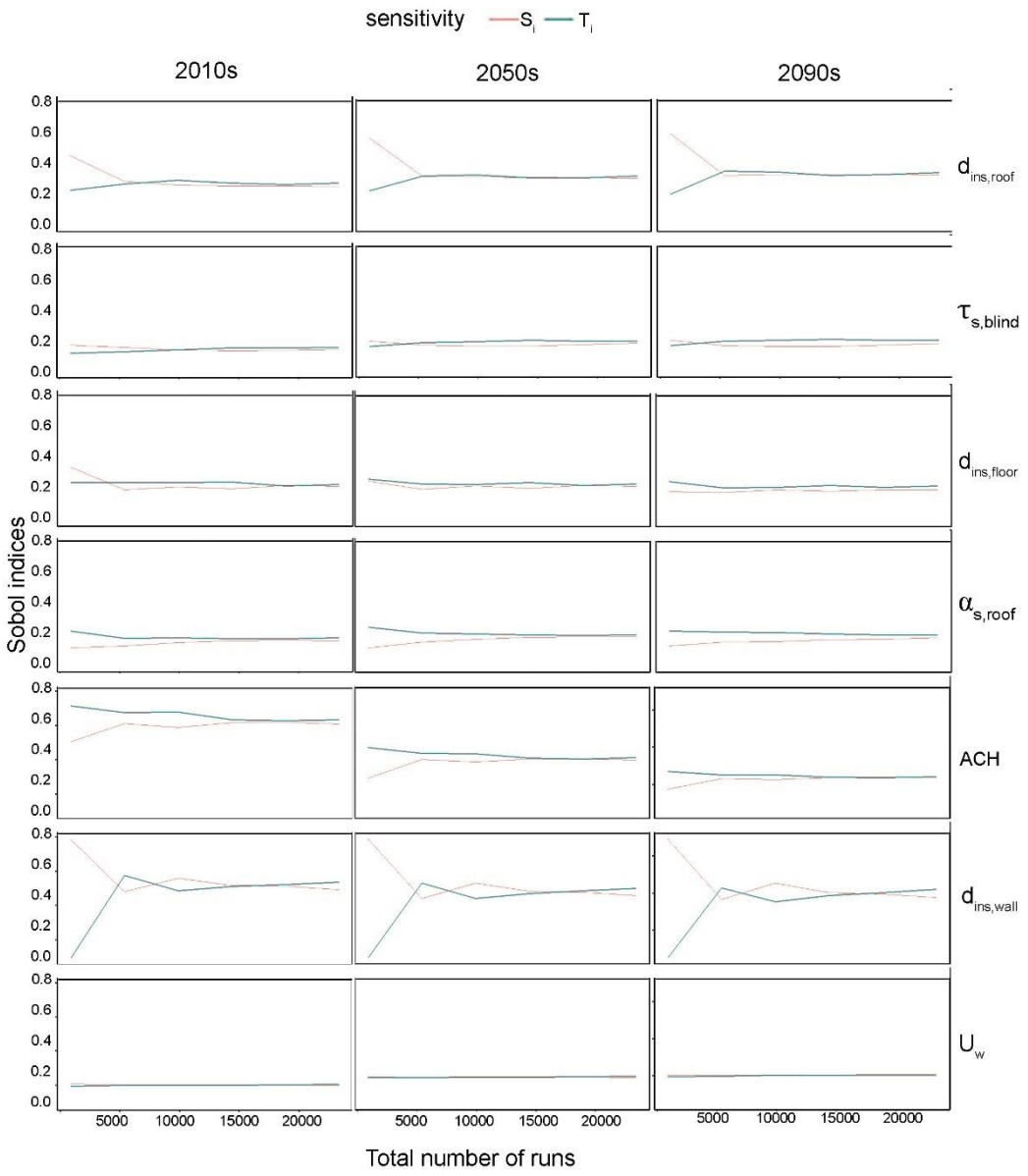


Figure 58: The plot of convergence of the input parameters for annual electrical energy consumption (from the grid) for cooling in 2010s, 2050, and 2090s

The last set of results refers to hours of exceedance -on the second floor- which is the number of hours in which the operative temperature of the zone is greater than the upper limit temperature (HE [%]). First, it is seen that the difference between the first and the total order of Sobol indices of parameters is considerable. This means that when analysing the building in free floating condition, the interactions between parameters are a significant source of variance in the output. In all three periods, the variation of ACH has the most contribution to the variation of hours of warm discomfort, and even its effect reduces over time. The second important contributor in 2010s and 2050s is the thickness of floor insulation, while in 2090s the importance of roof insulation thickness becomes more. It has also been discovered between the parameters representing the cooling solutions, solar absorbance of roof tiles, and solar transmittance of the blinds contribute more to the variation of *HE* if we compare them to their contribution to the variations of $EP_{C,nd,}$ and $E_{el,C}$. Besides, figure 62 presents that the convergence of all mentioned Sobol indices for hours of exceedance is verified, which confirms the adequacy of the sample size also in this case.

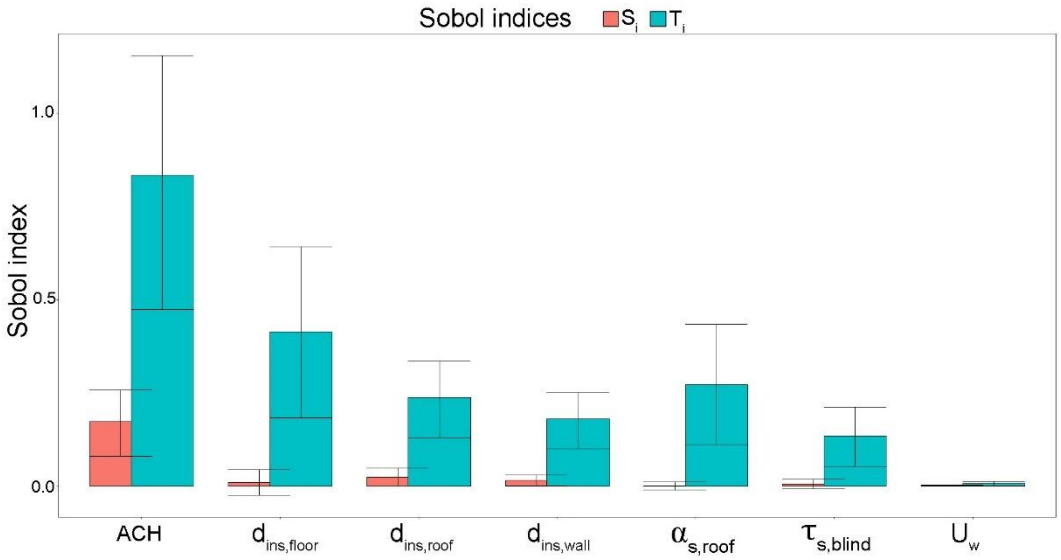


Figure 59: First and total order of the Sobol indices of the input parameters for hours of exceedance in second floor in 2010s

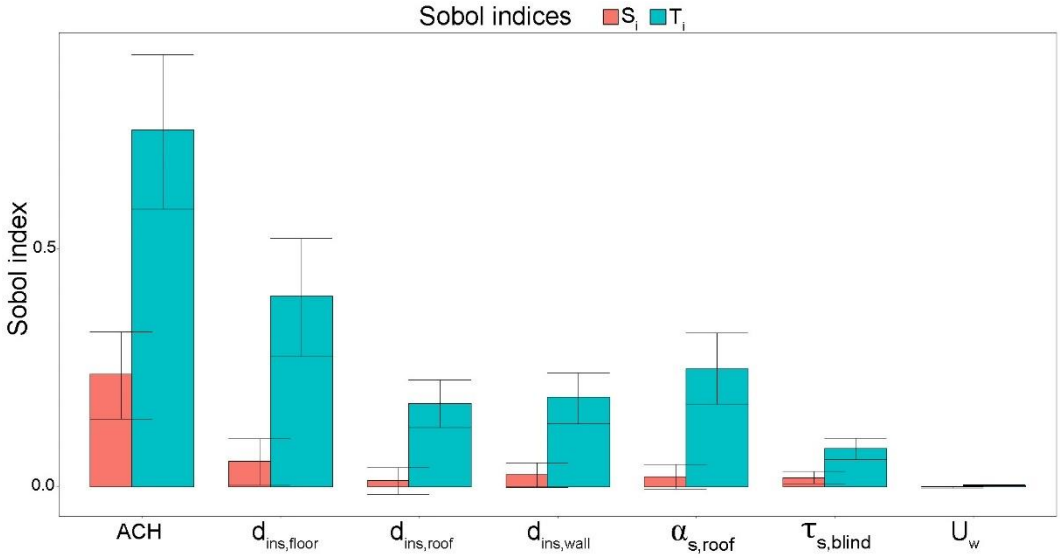


Figure 60: First and total order of the Sobol indices of the input parameters for hours of exceedance in second floor in 2050s

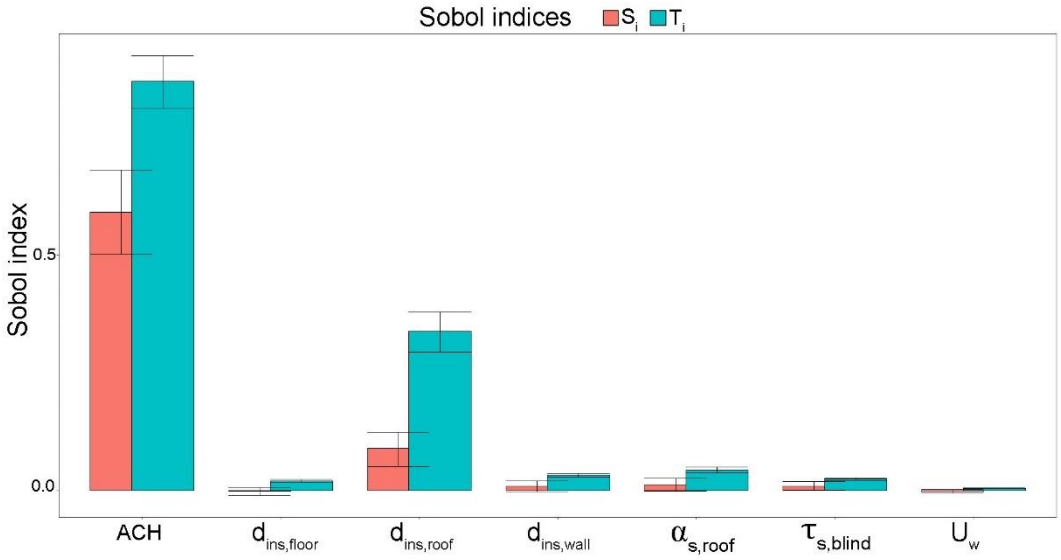


Figure 61: First and total order of the Sobol indices of the input parameters for hours of exceedance in second floor in 2090s

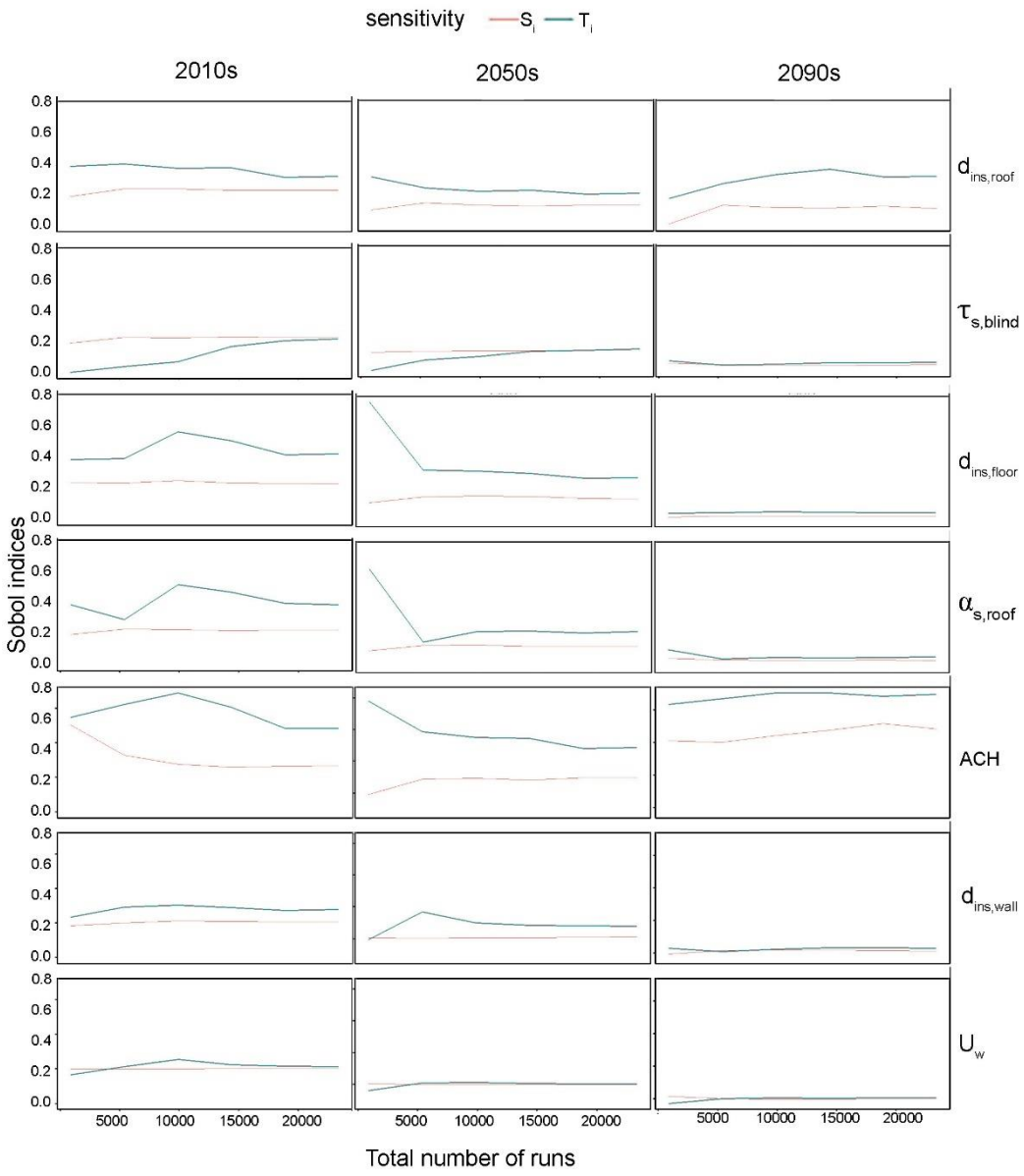


Figure 62: The plot of convergence of the input parameters for hours of exceedance in second floor in 2010s, 2050, and 2090s

# 6. Conclusions

This study set out to inform the growing concern on how climate change may affect buildings' future energy performance, particularly with regard to the rise in cooling demand and overheating risk. In order to investigate buildings' energy efficiency, optimization, and thermal comfort in a changing climate (long-term assessment), this research analyses the building stock in Italy on a regional level. For performing such an analysis, it was first necessary to create a reliable future weather data set. Accordingly, the reliability of future weather data generation methods was studied. Among the major downscaling methods of the regional climate models, it is seen that the morphing approach (statistical downscaling) can provide appropriate information to do a comparative study on long-term changes in building energy performance. However, the method's current inconsistency could result in significant prediction errors. Therefore, it is concluded that when the goal is to design, evaluate, and communicate resilient solutions to withstand as well as prevent the future impacts of climate change on building energy performance, the dynamical downscaling method is more dependable.

Since the Morphing method is adequate for comparative study on long-term changes in building energy performance, in the first step, this method was applied to perform a preliminary analysis. The aim was to shed light and provide an overview of the climate change impacts on Italian residential buildings' performance and fill the research gap referring to the lack of regional scale studies on Italian building stock. Additionally, the impact envelope insulation under each of these circumstances was examined in order to take into account how the refurbishment will affect the performance of buildings in the future, particularly in light of the national policies that are frequently used. The results for various residential building types clearly demonstrate that there is a significant increase in cooling electricity consumption and a slight decrease in heating energy use. Moreover, there is a substantial rise in the risk of overheating in existing structures. More importantly, buildings with a higher shape factor are discovered to be more sensitive to the impacts of climate change. Applying refurbishment could help to reduce this sensitivity. However, despite being always beneficial, the impact of

building refurbishment will diminish over time, which shows the necessity of re-evaluating the efficiency of refurbishment solutions. Different future weather scenarios and case studies do not all face the same climate change impacts. These impacts are more intense in the long term and more severe in some specific climate zones, making it more urgent to perform a regional and localized analysis to develop adaptation measures. A similar analysis was also performed for Nearly Zero Energy Buildings (NZEBs). It was once more seen that the climate zone and the period of analysis play a vital role in the intensity of climate change impacts on NZEBs. In addition, climate change will also affect the performance of renewable energy resources, and the magnitude of change depends on the type of energy source. In general, buildings won't achieve the vision of NZEBs in the future, suggesting a new configuration is needed in order to maintain the NZEB targets. To this aim, it was helpful to examine the capability of different cooling technologies to provide more climate-resilient buildings.

Therefore, a set of cooling solutions were assessed regarding the future performance of Italian residential buildings for a representative case study in Rome. The findings show that the mechanical ventilative cooling and ultra-selective double-glazed windows -depending on the building's condition- have the greatest impact on reducing the impact of climate change on the thermal energy required for space cooling, the electrical energy consumed from the grid for cooling and ventilation, and hours of exceedance in the free-floating condition. This analysis also showed that using all the considered cooling strategies might greatly improve a building's energy efficiency, resulting in a significant improvement even in the worst-case scenario (2090s).

Subsequently, a global sensitivity analysis (Sobol method) was conducted to more precisely assess the effect of variations in building conditions (insulation level of envelopes) and cooling technologies on variations in building energy performance and thermal comfort. This analysis was performed for three time periods (2010s, 2050s, and 2090s) and the same case study. It is noticeable that, for all three time periods, the variation in wall insulation thickness has the greatest contribution to the variation in the annual thermal energy need for space cooling, which demonstrates the key role of the building's condition. Turning now to the annual electrical energy consumption (from the grid) for cooling, it was confirmed once more that in the future climate, the building's condition plays a crucial role. In

addition, for both of these key performance indicators, the first and total orders do not differ much, indicating that interactions between the parameters do not contribute a large amount of variance. Unlikely, the difference between the first and the total order of Sobol indices is more considerable when analysing the hours of exceedance, and this indicates that the interactions between factors are a substantial source of output variance when analysing the building in a free-floating condition. Even though its impact decreases with time, the variance of the mechanical ventilative cooling air flow rate in all three periods contributes the most to the variation of warm discomfort hours.

Finally, the scope of this study was limited in terms of computational cost for processing RCM data for more climate zones and difficulties in finding appropriate observational data for performing bias adjustment. Further studies could be performed for more climate zones since the importance of regional and local analysis was demonstrated. Another source of limitation in this study was the high computational cost of performing building simulations with adequate size for applying the sensitivity analysis. Although a relatively large sample size was created in this research, more simulations could help to study further scenarios. For example, fixing the parameters regarding the building condition and analysing more cooling solutions or comparing the active and passive resilient cooling solutions to widen the analysis of the resilient cooling solutions could be helpful.

The findings of this study add to the rapidly expanding field of built environment climate resilience and establish the urgency of providing building adaptation measures for climate change. Taken together, these findings offer recommendations for future policies. Resilient cooling strategies should be assessed in future whole-building performance assessment tools and calculation methods. All thresholds/recommendations/input data should be revised based on climate change impacts. Climate resilience policies should not be developed as standalone policies, but fully integrated with policies concerning indoor environmental quality, energy efficiency, fuel poverty, decarbonisation, environmental sustainability, etc. Finally, it is recommended that climate resilience key performance indicators should also be standardised and inserted into official reports, such as energy performance certificates and energy audit reports.

# 7. References


Aburas, M., Soebarto, V., Williamson, T., Liang, R., Ebendorff-Heidepriem, H., & Wu, Y. (2019). Thermochromic smart window technologies for building application: A review. *Applied Energy*, *255*, 113522. https://doi.org/10.1016/J.APENERGY.2019.113522

American Meteorological Society. (2013). *Regional climate model. In Glossary of Meteorology; American Meteorological Society*.

Artmann, N., Gyalistras, D., … H. M.-B. R. &, & 2008, undefined. (2008). Impact of climate warming on passive night cooling potential. *Taylor & Francis*, *36*(2), 111–128. https://doi.org/10.1080/09613210701621919

ASHRAE. (2020). Climatic data for building design standards. *ASHRAE Standard 169*, *8400*, 384.

ASHRAE–American Society of Heating. (2017). *Handbook, Ventilating and Air-Conditioning Engineers*.

Attia, S., Energies, C. G.-, & Gobin, C. (2020). Climate change effects on belgian households: A case study of a nearly zero energy building. *Energies*. https://doi.org/10.3390/en13205357

Baglivo, C., Congedo, P. M., Murrone, G., & Lezzi, D. (2022). Long-term predictive energy analysis of a high-performance building in a mediterranean climate under climate change. *Energy*, *238*, 121641. https://doi.org/10.1016/J.ENERGY.2021.121641

Ballarini, I., Corgnati, S. P., & Corrado, V. (2014). Use of reference buildings to assess the energy saving potentials of the residential building stock: The experience of TABULA project. *Energy Policy*, *68*, 273–284. https://doi.org/10.1016/J.ENPOL.2014.01.027

Ballarini, I., & Corrado, V. (2017). A new methodology for assessing the energy consumption of building stocks. *Energies*. https://doi.org/10.3390/en10081102

Ballarini, I., Pichierri, S., & Corrado, V. (2015). Tracking the Energy Refurbishment Processes in Residential Building Stocks. The Pilot Case of Piedmont Region. *Energy Procedia*, *78*, 1051–1056. https://doi.org/10.1016/J.EGYPRO.2015.11.069

Barnaby, C., Simulation, U. C.-B. performance, & 2012, U. (2011). Weather data for building performance simulation. *Taylorfrancis.Com*.

Belcher, S. E., Hacker, J. N., & Powell, D. S. (2005). Constructing design weather data for future climates. *Building Services Engineering Research and Technology*. https://doi.org/10.1191/0143624405bt112oa

Belleri, A., & Chiesa, G. (2018). *Ventilative Cooling potential tool. User guide. IEA – EBC Programme – Annex 62 Ventilative Cooling*.

Berardi, U., & Jafarpur, P. (2020). Assessing the impact of climate change on building heating and cooling energy demand in Canada. *Renewable and Sustainable Energy Reviews*, *121*. https://doi.org/10.1016/j.rser.2019.109681

Boland, J., Ridley, B., & Brown, B. (2008). Models of diffuse solar radiation. *Renewable Energy*, *33*(4), 575–584. https://doi.org/10.1016/J.RENENE.2007.04.012

Bravo Dias, J., Carrilho da Graça, G., & Soares, P. M. M. (2020). Comparison of methodologies for generation of future weather data for building thermal energy simulation. *Energy and Buildings*, *206*. https://doi.org/10.1016/J.ENBUILD.2019.109556

Bürger, G., Schulla, J., Research, A. W.-W. R., & 2011, undefined. (2011). Estimates of future flow, including extremes, of the Columbia River headwaters. *Wiley Online Library*, *47*(10), 10520. https://doi.org/10.1029/2010WR009716

Burman, E., & Mumovic, D. (2018). *The impact of ventilation strategy on overheating resilience and energy performance of schools against climate change: the evidence from two UK secondary schools*. 2018. https://discovery.ucl.ac.uk/id/eprint/10055059/

Cannon, A. (2016). Multivariate bias correction of climate model output: Matching marginal distributions and intervariable dependence structure. *Climate*. https://journals.ametsoc.org/view/journals/clim/29/19/jcli-d-15-0679.1.xml

Cannon, A. J. (2018). Multivariate quantile mapping bias correction: an N-dimensional probability density function transform for climate model simulations of multiple variables. *Climate Dynamics*, *50*(1–2), 31–49. https://doi.org/10.1007/S00382-017-3580-6

Cannon, A., Sobie, S., Climate, T. M.-J. of, & 2015. (2015). Bias correction of GCM precipitation by quantile mapping: how well do methods preserve changes in quantiles and extremes? *Journals.Ametsoc.Org*. https://journals.ametsoc.org/view/journals/clim/28/17/jcli-d-14-00754.1.xml

Cartalis, C., Synodinou, A., Proedrou, M., Tsangrassoulis, A., & Santamouris, M. (2001). Modifications in energy demand in urban areas as a result of climate changes: An assessment for the southeast Mediterranean region. *Energy Conversion and Management*. https://doi.org/10.1016/S0196-8904(00)00156-4

*CCWorldWeatherGen* /climate-change-world-weather-file-generator-for-world-wide-weather-data-ccworldweathergen/*University of Southampton Blogs*. (2012). https://energy.soton.ac.uk/

CEN. (2005). *EN ISO 15927-4 Hygrothermal Performance of Buildings Calculation and Presentation of Climatic Data, Part 4: Hourly Data for Assessing the Annual Energy Use for Heating and Cooling; European Committee for Standardization*.

Energy performance of buildings - Overarching EPB assessment - Part 1: General framework and procedures (EN ISO 52000-1)., (2017).

CEN. (2017). *ISO - ISO 52022-1:2017 - Energy performance of buildings — Thermal, solar and daylight properties of building components and elements — Part 1: Simplified calculation method of the solar and daylight characteristics for solar protection devices combined w*. https://www.iso.org/standard/65785.html

Chai, J., Huang, P., & Sun, Y. (2019). Investigations of climate change impacts on net-zero energy building lifecycle performance in typical Chinese climate regions. *Energy*. https://doi.org/10.1016/j.energy.2019.07.055

Chaudry, M., Ekins, P., Ramachandran, K., & Shakoor, A. (2011). *Building a resilient UK energy system*.

Comitato Termotecnico Italiano. (2020). *Technical Commission 241, doc. no. 181, Italian National Annex of the EN 16798-1 technical standard (working draft for internal use)*.

*CORDEX Data Extractor*. Retrieved December 2, 2020, from https://agrimetsoft.com/CordexDataExtractor

Corrado, V., & Ballarini, I. (2016a). Refurbishment trends of the residential building stock: Analysis of a regional pilot case in Italy. *Energy and Buildings*. https://doi.org/10.1016/j.enbuild.2016.06.022

Corrado, V., & Ballarini, I. (2016b). Refurbishment trends of the residential building stock: Analysis of a regional pilot case in Italy. *Energy and Buildings*, *132*, 91–106. https://doi.org/10.1016/J.ENBUILD.2016.06.022

Dabaieh, M., Wanas, O., Hegazy, M. A., & Johansson, E. (2015). Reducing cooling demands in a hot dry climate: A simulation study for non-insulated passive cool roof thermal performance in residential buildings. *Energy and Buildings*, *89*, 142–152. https://doi.org/10.1016/J.ENBUILD.2014.12.034

D'Agostino, D., Parker, D., Epifani, I., Crawley, D., & Lawrie, L. (2022). How will future climate impact the design and performance of nearly zero energy buildings (NZEBs)? *Energy*, *240*, 122479. https://doi.org/10.1016/j.energy.2021.122479

Davoudi, S., Shaw, K., Haider, L. J., Quinlan, A. E., Peterson, G. D., Wilkinson, C., Fünfgeld, H., McEvoy, D., & Porter, L. (2012). Resilience: A Bridging Concept or a Dead End? "Reframing" Resilience: Challenges for Planning Theory and Practice Interacting Traps: Resilience Assessment of a Pasture Management System in Northern Afghanistan Urban Resilience: What Does it Mean in Planni. *Planning Theory and Practice*, *13*(2), 299–333. https://doi.org/10.1080/14649357.2012.677124

de Masi, R. F., Gigante, A., Ruggiero, S., & Vanoli, G. P. (2021). Impact of weather data and climate change projections in the refurbishment design of residential buildings in cooling dominated climate. *Applied Energy*, *303*, 117584. https://doi.org/10.1016/J.APENERGY.2021.117584

Dino, I. G. I., Meral Akgül, C., & Energy, C. A.-R. (2019). Impact of climate change on the existing residential building stock in Turkey: An analysis on energy use, greenhouse gas emissions and occupant comfort. *Renewable Energy*. https://doi.org/10.1016/j.renene.2019.03.150

Duffie, J., & Beckman, W. (1991). Solar Engineering of Thermal Processes. 2nd ed. John Wiley and Sons. New York: USA. In *John Wiley and Sons. New York: USA.*

Eckstein, J. H. (1990). *Detailed modeling of photovoltaic components. Solar Energy Laboratory, University of Wisconsin, Madison.*

*EUROCORDEX: Cordex Archive Specifications*. Retrieved December 2, 2020, from https://is-enes-data.github.io/cordex_archive_specifications.pdf

European Commission, C. final. (2014). *Communication from the Commission to the European Parliament, the Council, the European Economic and Social Committee and the Committee of the Regions, A policy framework for climate and energy in the period from 2020 to 2030*. https://eur-lex.europa.eu/legal-content/EN/TXT/PDF/?uri=CELEX:52014DC0015&from=EN,

Heating systems in buildings - Method for calculation of the design heat load (EN 12831)., (2003).

European Committee for Standardization. (2005). *EN ISO 15927-4 Hygrothermal Performance of Buildings Calculation and Presentation of Climatic Data, Part 4: Hourly Data for Assessing the Annual Energy Use for Heating and Cooling; European Committee for Standardization*.

*European Committee for Standardization (CEN). EN ISO 13789, Thermal Performance of Buildings—Transmission and Ventilation Heat Transfer Coefficients—Calculation Method; CEN: Brussels, Belgium, 2017.*

Finkelstein, J., & Biometrika, R. S. (1971). Improved goodness-of-fit tests. *Academic.Oup.Com*. https://academic.oup.com/biomet/article-abstract/58/3/641/233677

Flato, G., Marotzke, J., Abiodun, B., Braconnot, P., Chou, S. C., Collins, W., Cox, P., Driouech, F., Emori, S., Eyring, V., Forest, C., Gleckler, P., Guilyardi, E., Jakob, C., Kattsov, V., Reason, C., & Rummukainen, M. (2013). Evaluation of Climate Models. In T. F. Stocker, D. Qin, G.-K. Plattner, M. Tignor, S. K. Allen, J. Boschung, A. Nauels, Y. Xia, V. Bex, & P. M. Midgley (Eds.), *Climate Change 2013: The Physical Science Basis. Contribution of Working Group I to the Fifth Assessment Report of the Intergovernmental Panel on Climate Change* (pp. 741–866). Cambridge University Press. https://doi.org/10.1017/CBO9781107415324.020

Flores-Larsen, S., Filippín, C., & Barea, G. (2019). Impact of climate change on energy use and bioclimatic design of residential buildings in the 21st century in Argentina. *Energy and Buildings*. https://doi.org/10.1016/j.enbuild.2018.12.015

Garg, V., Kotharkar, R., Sathaye, J., Rallapalli, H., Kulkarni, N., Reddy, N., Rao, P., & Sarkar, A. (2016). Assessment of the impact of cool roofs in rural buildings in India. *Energy and Buildings*, *114*, 156–163. https://doi.org/10.1016/J.ENBUILD.2015.06.043

Giorgi, F. (2019). Thirty years of regional climate modeling: where are we and where are we going next? *Wiley Online Library*, *124*(11), 5696–5723. https://doi.org/10.1029/2018JD030094

HadCM3, M. O. *Met Office Climate Prediction Model*. Retrieved December 2, 2020, from https://www.metoffice.gov.uk/research/approach/modelling-systems/unified-model/climate-models/hadcm3

Hall, I., Prairie, R., Anderson, H., & Boes, E. (1978). *Generation of a typical meteorological year*. https://www.osti.gov/biblio/7013202

Hawkins, E., & Sutton, R. (2009). The potential to narrow uncertainty in regional climate predictions. *Bulletin of the American Meteorological Society*, *90*(8), 1095–1107. https://doi.org/10.1175/2009BAMS2607.1

Hawkins, E., & Sutton, R. (2011). The potential to narrow uncertainty in projections of regional precipitation change. *Climate Dynamics*, *37*(1), 407–418. https://doi.org/10.1007/S00382-010-0810-6

Heiselberg, P. (2018). *Ventilative Cooling Design Guide Energy in Buildings and Communities Programme* (Issue March). http://www.iea-ebc.org/Data/publications/EBC_Annex_62_Design_Guide.pdf

Heiselberg, P., & Kolokotroni, M. (2017a). *Ventilative Cooling: State-of-the-art review executive summary*. https://vbn.aau.dk/en/publications/ventilative-cooling-state-of-the-art-review-executive-summary

Heiselberg, P., & Kolokotroni, M. (2017b). *Ventilative Cooling: State-of-the-art review executive summary*. https://vbn.aau.dk/en/publications/ventilative-cooling-state-of-the-art-review-executive-summary

Herrera, M., Natarajan, S., Coley, D. A., Kershaw, T., Ramallo-González, A. P., Eames, M., Fosas, D., & Wood, M. (2005). *A review of current and future weather data for building simulation*. https://doi.org/10.1177/01436244

Homma, T., & Saltelli, A. (1996). Importance measures in global sensitivity analysis of nonlinear models. *Reliability Engineering \& System Safety*, *52*(1), 1–17. https://doi.org/10.1016/0951-8320(96)00002-6

Homma, T., Technology, A. S.-J. of N. S. and, & 1995, undefined. (2012). Use of Sobol's quasirandom sequence generator for integration of modified uncertainty importance measure. *Taylor & Francis*, *32*(11), 1164–1173. https://doi.org/10.1080/18811248.1995.9731832

Huang, Y. J., Su, F., Seo, D., & Krarti, M. (2014). Development of 3012 IWEC2 weather files for international locations (RP-1477). *ASHRAE Transactions*.

*IEA EBC Annex 80 - Resilient Cooling of Buildings*. (2013-2023). Retrieved November 7, 2022, from https://annex80.iea-ebc.org/

IPCC. (2013). Annex III: Glossary. In T. F. Stocker, D. Qin, G.-K. Plattner, M. Tignor, S. K. Allen, J. Boschung, A. Nauels, Y. Xia, V. Bex, & P. M. Midgley (Eds.), *Climate Change 2013: The Physical Science Basis. Contribution of Working Group I to the Fifth Assessment Report of the Intergovernmental Panel on Climate Change* (pp. 1447–1466). Cambridge University Press. https://doi.org/10.1017/CBO9781107415324.031

IPCC. (2021). IPCC, 2021: Summary for Policymakers. In: Climate Change 2021: The Physical Science Basis. Contribution of Working Group I to the Sixth Assessment Report of the Intergovernmental Panel on Climate Change. In *Cambridge University Press*. https://doi.org/10.1017/9781009157896

IPCC. (2022). *Climate Change 2022: Mitigation of Climate Change. Contribution of Working Group III to the Sixth Assessment Report of the Intergovernmental Panel on Climate Change* (P. R. Shukla, J. Skea, R. Slade, A. Al Khourdajie, R. van Diemen, D. McCollum, M. Pathak, S. Some, P. Vyas, R. Fradera, M. Belkacemi, A. Hasija, G. Lisboa, S. Luz, & J. Malley, Eds.). Cambridge University Press. https://doi.org/10.1017/9781009157926

IPCC: Global and Sectoral Aspects. (2014). Climate Change 2014 Part A: Global and Sectoral Aspects. In *Climate Change 2014: Impacts, Adaptation, and Vulnerability. Part A: Global and Sectoral Aspects. Contribution of Working*

*Group II to the Fifth Assessment Report of the Intergovernmental Panel on Climate Change*.

IPCC: Mitigation of climate change. (2014). Climate Change 2014 Mitigation of Climate Change. In *Climate Change 2014 Mitigation of Climate Change*. https://doi.org/10.1017/cbo9781107415416

Italian National Agency for New Technologies, (ENEA), & Italian Thermo Technical Committee (CTI). (2021). *The Energy Certification of Buildings, Annual Report 2021*. https://www.pubblicazioni.enea.it/component/jdownloads/?task=download.send&id=552&catid=3&m=0&Itemid=101

Italian Republic, I. D. of J. 26th. (2015). *Interministerial Decree of June 26th, 2015—Calculation Methodologies of the Building Energy Performance and Minimum Energy Performance Requirements (in Italian);*

Jacob, D., Petersen, J., Eggert, B., Alias, A., Christensen, O. B., Bouwer, L. M., Braun, A., Colette, A., Déqué, M., Georgievski, G., Georgopoulou, E., Gobiet, A., Menut, L., Nikulin, G., Haensler, A., Hempelmann, N., Jones, C., Keuler, K., Kovats, S., … Yiou, P. (2014). EURO-CORDEX: New high-resolution climate change projections for European impact research. *Regional Environmental Change*, *14*(2), 563–578. https://doi.org/10.1007/S10113-013-0499-2

Jentsch, M. F. (2012). *Technical Reference Manual for the CCWeatherGen and CCWorldWeatherGen Tools Version 1.2., 2012*. Retrieved December 2, 2020, from http://blog.soton.ac.uk/serg/files/2013/06/manual_weather_tool1.pdf

Jentsch, M. F., Bahaj, A. B. S., & James, P. A. B. (2008). Climate change future proofing of buildings-Generation and assessment of building simulation weather files. *Energy and Buildings*, *40*(12), 2148–2168. https://doi.org/10.1016/J.ENBUILD.2008.06.005

Jentsch, M., James, P., Bourikas, L., Energy, A. B.-R., & 2013, U. (2013). Transforming existing weather data for worldwide locations to enable energy and building performance simulation under future climates. *Elsevier*. https://www.sciencedirect.com/science/article/pii/S0960148113000232?casa_token=lG82W9VdPqEAAAAA:W0RzmCwSsxkCATT_r2cR5KxarfiZ0WLPV33aHcxb11obyyc8OclWfFYRLwXPQ1MgEOpa67aZ4ys

*jEPlus,v2.1.0*. (2020, September). http://www.jeplus.org

Karimpour, M., Belusko, M., Xing, K., Boland, J., & Bruno, F. (2015). Impact of climate change on the design of energy efficient residential building envelopes. *Energy and Buildings*, *87*, 142–154. https://doi.org/10.1016/j.enbuild.2014.10.064

Kasten, F. (1996). The linke turbidity factor based on improved values of the integral Rayleigh optical thickness. *Solar Energy*, *56*(3), 239–244. https://doi.org/10.1016/0038-092X(95)00114-7

Keogh, M., & Cody, C. (2012). The implications of a changing climate for buildings. *Elsevier*.

Kirankumar, G., Saboor, S., & Ashok Babu, T. P. (2017). Investigation of Various Low Emissivity Glass Materials for Green Energy Building Construction in Indian Climatic Zones. *Materials Today: Proceedings*, *4*(8), 8052–8058. https://doi.org/10.1016/J.MATPR.2017.07.144

Kolokotroni, M., Shittu, E., Santos, T., Ramowski, L., Mollard, A., Rowe, K., Wilson, E., Filho, J. P. de B., & Novieto, D. (2018). Cool roofs: High tech low cost solution for energy efficiency and thermal comfort in low rise low income houses in high solar radiation countries. *Energy and Buildings*, *176*, 58–70. https://doi.org/10.1016/J.ENBUILD.2018.07.005

Köppen, W. D. W. der E. (1884). Die Wärmezonen der Erde, nach der Dauer der heissen, gemässigten und kalten Zeit und nach der Wirkung der Wärme auf die organische Welt betrachtet. *Koeppen-Geiger.vu-Wien.Ac.At*. http://koeppen-geiger.vu-wien.ac.at/pdf/Koppen_1884.pdf

Laflamme, E., Linder, E., Extremes, Y. P.-W. and climate, & 2016, U. (2016). Statistical downscaling of regional climate model output to achieve projections of precipitation extremes. *Elsevier*. https://www.sciencedirect.com/science/article/pii/S221209471530058X

Li, D. H. W., Yang, L., & Lam, J. C. (2012). Impact of climate change on energy use in the built environment in different climate zones - A review. In *Energy*. https://doi.org/10.1016/j.energy.2012.03.044

Lomas, K. J., & Ji, Y. (2009). Resilience of naturally ventilated buildings to climate change: Advanced natural ventilation and hospital wards. *Energy and Buildings*, *41*(6), 629–653. https://doi.org/10.1016/J.ENBUILD.2009.01.001

Lucon, O., Ürge-Vorsatz, D., Zain Ahmed, A., Akbari, H., Bertoldi, P., Cabeza, L. F., Eyre, N., Gadgil, A., D Harvey, L. D., Jiang, Y., Liphoto, E., Mirasgedis, S., Murakami, S., Parikh, J., Pyke, C., & Vilariño, M. V. (2014). Chapter 9: Buildings. In *Climate Change 2014: Mitigation of Climate Change. Contribution of Working Group III to the Fifth Assessment Report of the Intergovernmental Panel on Climate Change*.

Mavrogianni, A., Davies, M., Batty, M., Belcher, S. E., Bohnenstengel, S. I., Carruthers, D., Chalabi, Z., Croxford, B., Demanuele, C., Evans, S., Giridharan, R., Hacker, J. N., Hamilton, I., Hogg, C., Hunt, J., Kolokotroni, M., Martin, C., Milner, J., Rajapaksha, I., … Ye, Z. (2011). The comfort, energy and health implications of London's urban heat island: *Http://Dx.Doi.Org/10.1177/0143624410394530*, *32*(1), 35–52. https://doi.org/10.1177/0143624410394530

Mehrotra, R., & Sharma, A. (2016). A multivariate quantile-matching bias correction approach with auto- and cross-dependence across multiple time scales: implications for downscaling. *Journal of Climate*, *29*(10), 3519–3539. https://doi.org/10.1175/JCLI-D-15-0356.1

*Meteonorm Software V.7.3*. (2018). https://meteonorm.com/

Moazami, A., Nik, V., Carlucci, S., Energy, S. G.-A., & 2019, U. (2019). Impacts of future weather data typology on building energy performance–Investigating long-term patterns of climate change and extreme weather conditions. *Elsevier*. https://www.sciencedirect.com/science/article/pii/S0306261919300868?casa_token=zWxXdutGiy8AAAAA:o_b3WZfx9tYj8PLiANQah2TvY4edviud6mbmXLqwPIjerik2jJ9St6zhJMkeERsUYRI1tkjRERI

Nik, V. M., & Sasic Kalagasidis, A. (2013). Impact study of the climate change on the energy performance of the building stock in Stockholm considering four climate uncertainties. *Building and Environment*. https://doi.org/10.1016/j.buildenv.2012.11.005

Olsson, J., Berggren, K., Olofsson, M., & Viklander, M. (2009). Applying climate model precipitation scenarios for urban hydrological assessment: A case study in Kalmar City, Sweden. *Atmospheric Research*, *92*(3), 364–375. https://doi.org/10.1016/J.ATMOSRES.2009.01.015

Overbye, T., Vittal, V., Energy, I. D.-I. P. &, & 2012, undefined. (2013). Engineering resilient cyber-physical systems. *Documents.Pserc.Wisc.Edu*.

A Dictionary of Environment and Conservation, Oxford (2007). https://doi.org/10.1093/ACREF/9780198609957.001.0001

Pachauri, R., & Reisinger, A. (2008). *Climate change 2007. Synthesis report. Contribution of Working Groups I, II and III to the fourth assessment report*. https://www.osti.gov/etdeweb/biblio/944235

Peacock, A. D., Jenkins, D. P., & Kane, D. (2010). Investigating the potential of overheating in UK dwellings as a consequence of extant climate change. *Energy Policy*, *38*(7), 3277–3288. https://doi.org/10.1016/j.enpol.2010.01.021

Pérez-Andreu, V., Aparicio-Fernández, C., Martínez-Ibernón, A., & Vivancos, J. L. (2018). Impact of climate change on heating and cooling energy demand in a residential building in a Mediterranean climate. *Energy*. https://doi.org/10.1016/j.energy.2018.09.015

Puy, A., Piano, S. lo, Saltelli, A., & Levin, S. A. (2022). sensobol: {An} {R} {Package} to {Compute} {Variance}-{Based} {Sensitivity} {Indices}. *Journal of Statistical Software*, *102*, 1–37. https://doi.org/10.18637/jss.v102.i05

Radhi, H., Sharples, S., Taleb, H., & Fahmy, M. (2017). Will cool roofs improve the thermal performance of our built environment? A study assessing roof systems in Bahrain. *Energy and Buildings*, *135*, 324–337. https://doi.org/10.1016/J.ENBUILD.2016.11.048

Ramon, D., Allacker, K., van Lipzig, N. P. M., de Troyer, F., & Wouters, H. (2019). Future Weather Data for Dynamic Building Energy Simulations: Overview of Available Data and Presentation of Newly Derived Data for Belgium. *Energy, Environment, and Sustainability*, 111–138. https://doi.org/10.1007/978-981-13-3284-5_6

Remund, J., & Bern, D. D. (2010). *Aerosol optical depth and Linke turbidity climatology Description for final report of IEA SHC Task 36 Client: IEA SHC Task 36 Editing*.

Remund, J., & Kunz, S. (1997). *METEONORM: Global Meteorological Database for Solar Energy and Applied Climatology*. Meteotest.

Remund, J., Müller, S. C., Schilter, C., & Rihm, B. (2010). The use of Meteonorm weather generator for climate change studies. *Ui.Adsabs.Harvard.Edu*. https://ui.adsabs.harvard.edu/abs/2010ems.confE.417R/abstract

Remund, J., Wald, L., Lefevre, M., Ranchin, T., & Page, J. (2003). Worldwide Linke turbidity information. *Proceedings of ISES Solar World Congress, 16-19 June, GÄteborg, Sweden*, 16–19. http://aeronet.gsfc.nasa.gov/

Ridley, B., Boland, J., & Lauret, P. (2010). Modelling of diffuse solar fraction with multiple predictors. *Renewable Energy*, *35*(2), 478–483. https://doi.org/10.1016/J.RENENE.2009.07.018

Rissim, J., & Hallie, K. (2013). *Low-Emissivity Windows" case studies on the Governments role in energy technology innovation*.

Rodrigues, E., & Fernandes, M. S. (2020). Overheating risk in Mediterranean residential buildings: Comparison of current and future climate scenarios. *Applied Energy*. https://doi.org/10.1016/j.apenergy.2019.114110

Rubin, M., Powles, R., & von Rottkay, K. (1999). Models for the angle-dependent optical properties of coated glazing materials. *Solar Energy*, *66*(4), 267–276. https://doi.org/10.1016/S0038-092X(99)00029-8

Saltelli, A., Annoni, P., Azzini, I., Campolongo, F., Ratto, M., & Tarantola, S. (2010). Variance based sensitivity analysis of model output. {Design} and estimator for the total sensitivity index. *Computer Physics Communications*, *181*(2), 259–270. https://doi.org/10.1016/j.cpc.2009.09.018

Saltelli, A., Ratto, M., Andres, T., Campolongo, F., Cariboni, J., Gatelli, D., Saisana, M., & Tarantola, S. (2008). *Global {Sensitivity} {Analysis}: {The} {Primer}*. John Wiley \& Sons.

Saltelli, A., Tarantola, S., Campolongo, F., & Ratto, M. (2004). *Sensitivity {Analysis} in {Practice}: {A} {Guide} to {Assessing} {Scientific} {Models}*. John Wiley \& Sons.

Santamouris, M., Sfakianaki, A., & Pavlou, K. (2010). On the efficiency of night ventilation techniques applied to residential buildings. *Energy and Buildings*, *42*(8), 1309–1313. https://doi.org/10.1016/J.ENBUILD.2010.02.024

Schaefer, C., Bräuer, G., & Szczyrbowski, J. (1997). Low emissivity coatings on architectural glass. *Surface and Coatings Technology*, *93*(1), 37–45. https://doi.org/10.1016/S0257-8972(97)00034-0

Shen, J., Copertaro, B., Sangelantoni, L., Zhang, X., Suo, H., & Guan, X. (2020). An early-stage analysis of climate-adaptive designs for multi-family buildings

under future climate scenario: Case studies in Rome, Italy and Stockholm, Sweden. *Journal of Building Engineering*, *27*, 100972. https://doi.org/10.1016/J.JOBE.2019.100972

Shen, P. (2017). Impacts of climate change on U.S. building energy use by using downscaled hourly future weather data. *Energy and Buildings*. https://doi.org/10.1016/j.enbuild.2016.09.028

Shen, P., & Lukes, J. R. (2015). Impact of global warming on performance of ground source heat pumps in US climate zones. *Energy Conversion and Management*. https://doi.org/10.1016/j.enconman.2015.06.027

Skea, J., & Ekins, P. (2009). *Min: UKERC energy 2050 project*. https://scholar.google.com/scholar_lookup?title=Energy 2050 Project&author=UK Energy Research Center (UKERC)&publication_year=2009

Soares, P. M. M., Cardoso, R. M., Miranda, P. M., Medeiros, J., Soares, P. M. M., Pedro, •, Miranda, M. A., de Medeiros, J., Belo-Pereira, M., Fátima, •, & Santo, E.-. (2012). WRF high resolution dynamical downscaling of ERA-Interim for Portugal. *Springer*, *39*(9–10), 2497–2522. https://doi.org/10.1007/s00382-012-1315-2

Sobol′, I. M. (2001). Global sensitivity indices for nonlinear mathematical models and their {Monte} {Carlo} estimates. *Mathematics and Computers in Simulation*, *55*(1), 271–280. https://doi.org/10.1016/S0378-4754(00)00270-6

*Statistical Downscaling | Regional Climate Model Evaluation System-California institute of technology*. (n.d.). Retrieved July 12, 2022, from https://rcmes.jpl.nasa.gov/content/statistical-downscaling#quantile

Summa, S., Tarabelli, L., Ulpiani, G., & Di Perna, C. (2020). Impact of climate change on the energy and comfort performance of nzeb: A case study in Italy. *Climate*. https://doi.org/10.3390/cli8110125

Sun, K., Specian, M., & Hong, T. (2020). Nexus of thermal resilience and energy efficiency in buildings: A case study of a nursing home. *Building and Environment*, *177*. https://doi.org/10.1016/j.buildenv.2020.106842

Symon, C. (2013). *Climate change: Action, trends and implications for business*. The IPCC's Fifth Assessment Report.

Tabatabaei Sameni, S. M., Gaterell, M., Montazami, A., & Ahmed, A. (2015). Overheating investigation in UK social housing flats built to the Passivhaus standard. *Building and Environment*, *92*, 222–235. https://doi.org/10.1016/j.buildenv.2015.03.030

*The Italian national organization for standardization, UNI/TS 11300-1: 2014– Energy performance of buildings Part 1: Evaluation of energy need for space heating and cooling (in Italian). UNI: Milan, Italy, 2014.* (n.d.).

Torres-Quezada, J., Coch, H., & Isalgué, A. (2019). Assessment of the reflectivity and emissivity impact on light metal roofs thermal behaviour, in warm and humid climate. *Energy and Buildings*, *188–189*, 200–208. https://doi.org/10.1016/J.ENBUILD.2019.02.022

Troup, L., & Fannon, D. (2016). Morphing Climate Data to Simulate Building Energy Consumption. *ASHRAE and IBPSA-USA SimBuild 2016 Building Performance Modeling Conference*.

UN-Habitat. (2017). How Resilient is Your City? . https://unhabitat.org/how-resilient-is-your-city.

UNI. (2016). *UNI 10349-1:2016 Heating and cooling of buildings-Climatic data-Part 1: Monthly means for evaluation of energy need for space heating and cooling and methods for splitting global solar irradiance into the direct and diffuse parts and to calculate the sola*. http://store.uni.com/catalogo/uni-10349-1-2016 (2016).

Uppala, S. M., Kållberg, P. W., Simmons, A. J., Andrae, U., da Costa Bechtold, V., Fiorino, M., Gibson, J. K., Haseler, J., Hernandez, A., Kelly, G. A., Li, X., Onogi, K., Saarinen, S., Sokka, N., Allan, R. P., Andersson, E., Arpe, K., Balmaseda, M. A., Beljaars, A. C. M., … Woollen, J. (2005). The ERA-40 re-analysis. *Quarterly Journal of the Royal Meteorological Society*, *131*(612), 2961–3012. https://doi.org/10.1256/QJ.04.176

EnergyPlus Version 9.6.0 Documentation/Auxiliary Programs. Chapter 2, (2021).

van der linden, P., & Mitchell, J. E. (2009). *Climate Change and its Impacts: Summary of Research and Results from the ENSEMBLES Project*.

Vrac, M., & Friederichs, P. (2015). Multivariate—intervariable, spatial, and temporal—bias correction. *Climate*. https://journals.ametsoc.org/view/journals/clim/28/1/jcli-d-14-00059.1.xml?tab_body=abstract-display

Vurro, G., Santamaria, V., Chiarantoni, C., & Fiorito, F. (2022). Climate Change Impact on Energy Poverty and Energy Efficiency in the Public Housing Building Stock of Bari, Italy. *Climate 2022, Vol. 10, Page 55*, *10*(4), 55. https://doi.org/10.3390/CLI10040055

Wan, K., Li, D., Pan, W., & Energy, J. L.-A. (2012). Impact of climate change on building energy use in different climate zones and mitigation and adaptation implications. *Elsevier*.

Wang, X., Chen, D., & Ren, Z. (2010). Assessment of climate change impact on residential building heating and cooling energy requirement in Australia. *Building and Environment*, *45*(7), 1663–1682. https://doi.org/10.1016/j.buildenv.2010.01.022

*WeatherShift*. (2020). Retrieved December 2, 2020, from http://www.weather-shift.com

World Research Climate Program (WRCP). *Coordinated Downscaling Experiment—European Domain*. Retrieved December 2, 2020, from https://www.eurocordex.net

Zachariadis, T., & Hadjinicolaou, P. (2014). The effect of climate change on electricity needs - A case study from Mediterranean Europe. *Energy*. https://doi.org/10.1016/j.energy.2014.09.001

Zhang, C., Kazanci, O., Levinson, R., … P. H.-E. and, & 2021, U. (2021). Resilient cooling strategies–A critical review and qualitative assessment. *Elsevier*. https://www.sciencedirect.com/science/article/pii/S037877882100596X

Zhang, X., Lau, S. K., Lau, S. S. Y., & Zhao, Y. (2018). Photovoltaic integrated shading devices (PVSDs): A review. *Solar Energy*, *170*, 947–968. https://doi.org/10.1016/J.SOLENER.2018.05.067

Zuo, J., Pullen, S., Palmer, J., Bennetts, H., Chileshe, N., & Ma, T. (2015). Impacts of heat waves and corresponding measures: A review. In *Journal of Cleaner Production*. https://doi.org/10.1016/j.jclepro.2014.12.078